The use of FLP-mediated recombination for the functional analysis of an effector gene family in the biotrophic smut fungus *Ustilago maydis*

Dissertation

zur Erlangung des Doktorgrades
der Naturwissenschaften
(Dr. rer. nat.)

dem
Fachbereich Biologie
der Philipps-Universität Marburg
vorgelegt von

Yuliya Khrunyk
aus Lviv, Ukraine

Marburg/Lahn, 2010

Vom Fachbereich Biologie

der Philipps-Universität Marburg als Dissertation

angenommen am: _____

Erstgutachterin: Frau Prof. Dr. Regine Kahmann

Zweitgutachter: Herr Prof. Dr. Michael Bölker

Tag der mündlichen Prüfung:_____

Die Untersuchungen zur vorliegenden Arbeit wurden von Anfang Oktober 2006 bis Februar 2010 unter der Betreuung von Frau Prof. Dr. Regine Kahmann in Marburg am Max-Planck-Institut für terrestrische Mikrobiologie in der Abteilung Organismische Interaktionen durchgeführt.

Declaration

I hereby declare that the dissertation entitled “The use of FLP-mediated recombination for the functional analysis of an effector gene family in the biotrophic smut fungus *Ustilago maydis*” submitted to the Department of Biology, Philipps-Universität Marburg, is the original and independent work carried out by me under the guidance of the PhD committee, and the dissertation is not formed previously on the basis of any award of Degree, Diploma or other similar titles.

_____ _____

(Date and Place) (Yuliya Khrunyk)

Parts of this work are presented in the following submitted article: **Khrunyk, Y., Münch, K., Schipper, K., Lupas, A. N., Kahmann, R.** (2010) The use of FLP-mediated recombination for the functional analysis of an effector gene family in the biotrophic smut fungus *Ustilago maydis*. *New Phytol*.
In press.

Table of contents

Abstract

Ustilago maydis, a dimorphic hemibasidiomycete fungus, is the causative agent of corn smut disease and has become one of the models for the study of biotrophic interactions. The establishment of biotrophic growth critically depends on secreted effector molecules. Among the novel secreted *U. maydis* effectors some are encoded by gene families which may have redundant functions. Due to the limited number of selectable markers it was not possible to perform sequential gene deletions when this thesis was started, i.e. the functional analysis of effector gene families was not possible. To solve this problem I have established an inducible FLP-mediated marker recycling system in *U. maydis*. It consists of three main steps: i) the generation of a deletion mutant in which the selectable marker introduced is flanked by directly oriented FRT (FLP recombination targets) sites, ii) the introduction of an inducible FLP gene on an autonomously replicating plasmid and iii) the induction of FLP expression and the subsequent screening for the loss of the selectable marker as well as the FLP donor plasmid. To eliminate possible inter- and intramolecular recombination events between identical FRT sites left in the genome after excision, FRT sequences with different point mutations in the core region were employed.

The FLP-mediated selectable marker removal technique was successfully applied to delete a family of 11 effector genes (*eff1*) using five sequential rounds of recombination. All Eff1 proteins have the same architecture, consisting of an N-terminal signal sequence, a central region predicted to be natively unstructured, and a conserved C-terminal domain, which presumably represents the only folded part of these proteins. I showed that expression of all 11 genes is specifically upregulated during the biotrophic phase. Strains carrying deletions of 9 or all 11 genes displayed a significant reduction in virulence and this phenotype could be partially complemented by the introduction of different members from the gene family, demonstrating redundancy. The combined deletion analysis and complementation studies conducted for members of the *eff1* family has revealed that three of the 11 *eff1* genes contribute most significantly to virulence, while all the other members of this gene family contribute to virulence only weakly.

Der dimorphe Hemibasidiomycet *Ustilago maydis*, Erreger des Maisbeulenbrandes, ist ein Modellorganismus für die Untersuchung biotropher Interaktionen. Die Sekretion von Effektorproteinen ist eine zwingende Voraussetzung für biotrophes Wachstum. Einige der neuen von *U. maydis* sekretierten Effektoren werden von Genfamilien kodiert, welche möglicherweise redundante Funktionen erfüllen. Bedingt durch die begrenzte Anzahl verfügbarer Selektionsmarker war es bei Beginn dieser Arbeit nicht möglich, sequenzielle Gendeletionen vorzunehmen. Somit war zu diesem Zeitpunkt die funktionelle Analyse dieser Genfamilien nicht möglich. In dieser Arbeit wurde ein induzierbares, FLP-vermitteltes System zur Wiederverwertung von Selektionsmarkern etabliert. Das System beruht auf drei wesentlichen Schritten: Erstens, der Herstellung einer Deletionsmutante in welcher der eingeführte Selektionsmarker von gleichgerichteten FLP-Erkennungsstellen, sogenannten FRT-Sequenzen, flankiert wird. Zweitens, der Einbringung eines für FLP kodierenden Gens unter der Kontrolle eines induzierbaren Promoters, welches auf einem autonom replizierenden Plasmid vorliegt. Drittens, der Induktion der Expression von FLP und die subsequente Überprüfung auf Verlust des Selektionsmarkes und Verlust des FLP-Donorplasmids. Um inter- und intramolekulare Rekombination zwischen nach der Entfernung des Selektionsmarkers im Genom verbliebenen identischen FRT-Sequenzen auszuschließen, wurden FRT-Sequenzen mit unterschiedlichen Punktmutationen in der Kernsequenz verwendet.

Die FLP-vermittelte Technik zur Entfernung von Selektionsmarkern wurde erfolgreich verwendet um eine Genfamilie aus elf Effektorgenen (*eff1*) in fünf aufeinanderfolgenden Rekombinationen zu deletieren. Alle Eff1-Proteine haben einen vergleichbaren Aufbau. Eine N-terminale Signalsequenz ist gefolgt von einem weitgehend unstrukturierten Bereich, an den sich die konservierte C-terminale Domäne anschließt - voraussichtlich der einzige gefaltete Bereich dieser Proteine. Es konnte gezeigt werden, dass die Expression aller elf Gene während der biotrophen Phase spezifisch hochreguliert wird. Stämme mit Deletionen von neun oder allen elf Genen zeigten einen signifikanten Rückgang der Virulenz. Dieser Phänotyp konnte durch Einbringung verschiedener Gene dieser Genfamilie teilweise komplementiert werden, woraus sich ableiten lässt, dass die entsprechenden Gene redundant sind. Die vorliegenden Untersuchungen zur Deletion und Komplementierung von Mitgliedern der *eff1*-Genfamilie belegen, dass drei der elf *eff1*-

Gene entscheidend zu der Virulenz von *U. maydis* beitragen, während der Einfluss der restlichen Genfamilie vernachlässigbar ist.

Glossary

A280	absorbance at 280 nm
aa	amino acid
Amp	Ampicillin
bp	base pair
BSA	Bovine serum albumin
Cbx^R	carboxin resistance
cDNA	single-stranded complementary DNA
CM	complete medium
C-terminal	carboxyl-terminal
dH_2O	distilled water
DMSO	dimethylsulfoxide
dpi	days post infection
EDTA	ethylendiamintetraacetic acid
eGFP	enhanced green fluorescent protein
FLP	FLP Recombinase
FRT	FLP recombination target
h	hour
hph	hygromycin phosphotransferase gene
Hyg^R	hygromycin resistance
IPTG	isopropyl β-D-1-thiogalaktopyranoside
ip	iron sulphur subunit of the succinate dehydrogenase locus
kb	kilobase
min	minutes
M	molar
MOPS	3-[N-morpholino] propanesulfonic acid
mRNA	messenger ribonucleic acid
NLS	nuclear localization sequence
N-terminal	amino-terminal
OD600	optical density at 600 nm
ORF	open reading frame
PCR	polymerase chain reaction
PD	potato-dextrose
PEG	polyethylene glycol
SDS	sodium dodecyl sulfate
sec	second
rpm	rotations per minute
Tm	melting temperature
U	unit (enzyme activity)
UV	ultraviolet light
v/v	volume per volume
WGA	wheat germ agglutinin
wt	wild type
w/v	weight per volume
Δ	deletion

1. Introduction

1.1 Plant-microbe interactions

1.1.1 Key players in plant-microbe interactions

Plants and their associated pathogens such as fungi, bacteria, nematodes, viruses and oomycetes, have coevolved for many millions of years (Stukenbrock & McDonald, 2009). Since plants cannot move to escape such biotic stresses, they have evolved sophisticated mechanisms to perceive these attacks and initiate efficient innate immune responses (Dangl & Jones, 2001). Constitutive plant defensive layers against pathogen attack include waxy cuticular layers, rigid cell walls, anti-microbial enzymes and secondary metabolites (Nürnberger *et al.*, 2004). If a pathogen, however, overcomes such preformed barriers it may be sensed by membrane-resident pattern recognition receptors (PRRs) and initiate pathogen-associated molecular pattern (PAMP)-triggered immunity (Nürnberger *et al.*, 2004; Bent & Mackey, 2007; Shen *et al.*, 2007; Boller & He, 2009). PAMP-triggered innate immune responses attenuate pathogen growth and contribute to basal defense; they are initiated by a large variety of conserved microbe-associated molecules, referred to as "general elicitors". For example, via a PRR known as flagellin sensitive 2 receptor-like kinase (FLS2) plants perceive a 22 amino acid region of the conserved N-terminal part of bacterial flagellin (Zipfel, 2008; Boller & Felix, 2009). Main fungal and oomycete PAMPs are chitin and β-glucan, for which PRRs have been also revealed (Kaku *et al.*, 2006; Miya *et al.*, 2007). Different intracellular responses associated with PAMP-triggered immunity include rapid ion fluxes across the plasma membrane, MAP kinase activation, production of reactive oxygen species (ROS), rapid changes in gene expression, as well as cell wall reinforcement (Zipfel, 2008). Following from the "zigzag" model of plant-microbe coevolution proposed by Jones & Dangl (2006) reduced PAMP-mediated defense might result from successful host defense suppression by pathogen effectors (Chisholm *et al.*, 2006; Jones & Dangl, 2006). Alternatively, effectors can induce effector triggered immunity (ETI) in plants with cognate resistance R proteins. R proteins represent a second, mainly intracellular, immune receptor class having the capacity to directly or indirectly detect isolate-specific pathogen effectors, encoded by avirulence (*Avr*) genes (Chisholm *et al.*, 2006). ETI often leads to suicide of the infected cells which is called hypersensitive response (HR) (Keen, 1990; Heath, 2000; Greenberg & Yao, 2004). Such R-Avr type of interactions for the first time was

introduced by Flor (1942) in the gene-for-gene hypothesis. According to this classical model pathogen *Avr* gene products contribute to pathogen virulence on plants lacking the cognate *R* genes (Flor, 1942). *Avr* gene products belong to a large repertoire of pathogen-secreted proteins termed effectors, to emphasize their presumed intrinsic virulence function (van der Hoorn & Kamoun, 2008). Effectors are often secreted novel proteins that are expressed specifically during plant infection but not in artificial culture media (Ellis *et al.*, 2009). The *R* genes identified so far encode only five protein classes, the largest of which comprises "nucleotide-binding site plus leucine-rich repeat" (NB-LRR) proteins (Baker *et al.*, 1997; Jones & Dangl, 2006; Bent & Mackey, 2007; Takken & Tameling, 2009).

1.1.2 Interactions between pathogen effectors and plant R proteins

It is now well accepted that due to secretion of an arsenal of effectors filamentous pathogens such as fungi and oomycetes are intimately associated with their host plants and are sophisticated manipulators of plant cells (Oliva *et al.*, 2010). An example of R-effector interactions was shown in the barley/powdery mildew pathosystem, where the intracellular mildew A (MLA) R protein localized to the nucleus upon recognition of the AVRA10 effector of *Blumeria graminis*, interfering with WRKY transcription factors and then indirectly derepressing PAMP-triggered basal defence (Shen *et al.*, 2007). Another example for an R-effector interplay was demonstrated for *Pto* from tomato, which encodes a Ser/Thr kinase conferring resistance to *Pseudomonas syringae* strains carrying the *avrPto* effector gene. Intriguingly, although Pto functions through phosphorylation signal transduction, triggered by direct AvrPto-Pto interaction, it additionally requires the NB-LRR Prf R protein (Salmeron *et al.*, 1996; Tang *et al.*, 1996). Therefore, Prf is an R protein that "guards" Pto while monitoring its interdiction by AvrPto, and then triggers defence response. According to the "Guard model" that is based on such indirect perception mechanisms of effectors by R proteins, an interaction complex of an effector with its target (guardee) is recognized by the cognate R protein, which is then activated to initiate disease resistance (Dangl & Jones, 2001). Detailed genetic and biochemical studies on the interactions between effectors and R proteins paved the way for the establishment of a novel so-called "Decoy model" (van der Hoorn & Kamoun, 2008). The basis for this was the recent demonstration that the AvrPto-Pto complex suppresses the function of the PAMP-triggered immunity receptor-like kinases FLS2 and EFR (elongation factor

Tu receptor) (Xing *et al.*, 2007; Xiang *et al.*, 2008). It has been speculated that such functional mimicry mechanism evolved by plants during the evolutionary arms race, i.e. Pto probably plays the role of a decoy that leads to detection of pathogen effectors via R proteins (van der Hoorn & Kamoun, 2008). Surprisingly, some effectors are not species-specific, as was recently reported for Avr4 and Ecp2 (Stergiopoulos *et al.*, 2010). Both of them are functional homologs in the tomato pathogen *Cladosporium fulvum* and *Mycosphaerella fijiensis*, the agent of causal black Sigatoka disease of banana. Occurrence of such "core" effectors could facilitate virulence on distantly related host species (Stergiopoulos *et al.*, 2010).

Secretion of effector molecules most likely follows a sequential order adapted to overcome the layered plant defence responses (Göhre & Robatzek, 2008). In oomycetes such as *Phytophthora* species, effectors contain RXLR-dEER motif in their N-terminal parts, a motif which is involved in translocation into host cells (Birch *et al.*, 2006; Tyler *et al.*, 2006; Birch *et al.*, 2008). The RXLR sequence is similar to the Pexel motif, a host-cell-targeting signal required for translocation of proteins from *Plasmodium* species into the cytoplasm of host cells. This has led to the hypothesis that RXLR functions as an ancient general signal mediating trafficking into host cells (Hiller *et al.*, 2004; Marti *et al.*, 2004; Kamoun, 2006). Dou *et al.* reported, that all three *Plasmodium* host targeting domains could functionally replace the N-terminus of *Phytophthora sojae* Avr1b effector (Dou *et al.*, 2008). In the oomycete effectors the N-terminal domain of contains the signal peptide and conserved RXLR motif, i.e. the domains for secretion and targeting, while the remaining C-terminal domain harbors the effector activity and operates inside plant cells (Kamoun, 2007). The RXLR motif has not been detected in fungal effectors (Oliva *et al.*, 2010). Moreover, so far no functional signal for host uptake of fungal effectors has been identified (Birch *et al.*, 2008; Oliva *et al.*, 2010). Although the uptake mechanism is not yet known several fungal effectors were shown to function inside the host cell. For example, Avr-Pita effector from *Magnaporthe oryzae* was demonstrated to interact with cognate Pi-ta resistance protein inside the host plant cell (Jia *et al.*, 2000; Orbach *et al.*, 2000). In *Uromyces fabae*, Uf-RTP1p effector was shown to localize inside infected plant cells as was detected by immunofluorescence and electron microscopy (Kemen *et al.*, 2005).

1.1.3 Significance of effector gene families in plant-microbe interactions

Although in some cases R-effector interaction determines pathogen success or failure, the interplay between host and pathogen is usually much more complex and involves numerous genes in both partners (Stukenbrock & McDonald, 2009). Indeed, "molecular struggles" during the evolutionary arms race result in positive selection for variation of residues at the interaction surface between R proteins and effectors (Misas-Villamil & van der Hoorn, 2008). To circumvent ETI triggered by plant resistance R proteins pathogens modify their effectors or acquire novel ones, which leads to an evolutionary arms race between PAMP and ETI receptors in plants and effectors in pathogens (Göhre & Robatzek, 2008). Notably, in *Phytophthora infestans*, RXLR effector genes often reside in a genomic environment that is gene-sparse and repeat-rich. The mobile elements contributing to the dynamic nature of these repetitive regions may enable recombination events resulting in the higher rates of gene gain and gene loss observed for these effectors (Haas *et al.*, 2009). Due to gene duplications and functional redundancy caused by the arms race many effectors are individually dispensable. Indeed, functional redundancy of effector genes may foster rapid evolution of the pathogen to overcome host resistance by allowing effector genes to become inactivated without compromising parasite fitness (Birch *et al.*, 2008; Kvitko *et al.*, 2009).

For example it was demonstrated in *Pseudomonas syringae* that certain combinatorial deletions of 20 effector genes revealed that some disruptions decreased growth in its host *Nicotiana benthamiana* only in combination with other deletions suggesting a redundancy-based structure in the effector repertoire (Kvitko *et al.*, 2009). In another plant pathogen, *Ralstonia solanacearum*, deletion of all seven genes encoding GALA proteins is necessary to promote disease indicating that there is a functional redundancy between these effectors (Angot *et al.*, 2006; Birch *et al.*, 2009). Many effectors of fungal plant pathogens also seem to work in concert, and their individual contribution to virulence is often minor, as their disruption has no apparent effect on fitness or virulence (Stergiopoulos & de Wit, 2009). A prominent example is an extensive AVR_{k1} gene family consisting of 260 paralogs, which contribute to the establishment of haustoria in *Blumeria graminis* (Sacristan *et al.*, 2009). Most probably, these effectors were under diversifying selection and have coevolved with LINE-1 retrotransposons (Sacristan *et al.*, 2009). Additionally, in *Botrytis* species,

positive selection of several amino acid residues was demonstrated for homologs of NEP1 effector, which induces necrosis and leads to an increase of ethylene levels in its host (Staats *et al.*, 2007). Effectors can also have more than one activity as is possibly the case for the Avr4 and Ecp6 *C. fulvum*. These proteins both bind to chitin and thus could potentially protect the fungus against plant chitinases. At the same time they could suppress plant defense responses by scavenging chitin fragments released from fungal cell walls in the apoplast during infection (Bolton *et al.*, 2008; de Jonge & Thomma, 2009).

1.2 *Ustilago maydis* as a model for plant-microbe interactions

Ustilago maydis, a dimorphic hemibasidiomycete fungus, is the causative agent of corn smut disease and has become one of the models for the study of biotrophic interactions (Kahmann *et al.*, 2000). It belongs to the subphylum Ustilaginomycotina, which includes 1,500 species of true smut fungi and yeasts, most of which cause systemic infections of angiosperm hosts (James *et al.*, 2006). In nature, pathogenic development of the fungus is initiated after two compatible, yeast-like sporidia fuse on maize surface and form the infectious filamentous dikaryon (Banuett & Herskowitz, 2002; Perez-Martin *et al.*, 2006). On the leaf surface, the dikaryon develops non-melanized appressoria that directly penetrate the host tissue and establish a biotrophic interaction (Brefort *et al.*, 2009). During penetration, fungal hyphae become incased in the host plasma membrane and this persists during the early infection stages (Doehlemann *et al.*, 2009). At later stages, fungal hyphae accumulate in mesophyll tissue and are found mostly in apoplastic cavities that arise in the developing tumors (Fig. 1) (Snetselaar & Mims, 1993). There plant cells enlarge, undergo mitotic divisions and the hyphal aggregates differentiate into black-pigmented sexual teliospores. In contrast to other smut fungi *U. maydis* produces prominent symptoms on all aerial parts of its host plant, maize, which can be scored already one week after infection of three-leaf stage maize seedling (Brefort *et al.*, 2009). Figure 2 provides a scheme of the life cycle of *U. maydis*.

After we entered the post-sequencing era for *U. maydis* in 2006 (Kämper *et al.*, 2006), the scientific challenge is now the elucidation of the function of all effector genes. In *U. maydis*, identification of an effector involves generation of a mutant strain with a non-functional version of a gene by targeted gene deletion and assaying the ability of

the mutant to cause maize infection symptoms. An *ab initio* bioinformatical screen for potential effector candidates was based on two criteria: the protein should carry an N-terminal secretion signal sequence and the predicted product should be novel i.e. should not match database entries. Mueller *et al.* have revealed that in *U. maydis* 426 genes code for putatively secreted proteins, and of these, 272 code for either *U. maydis*-specific proteins or conserved proteins without recognized InterPro domains (Mueller *et al.*, 2008).

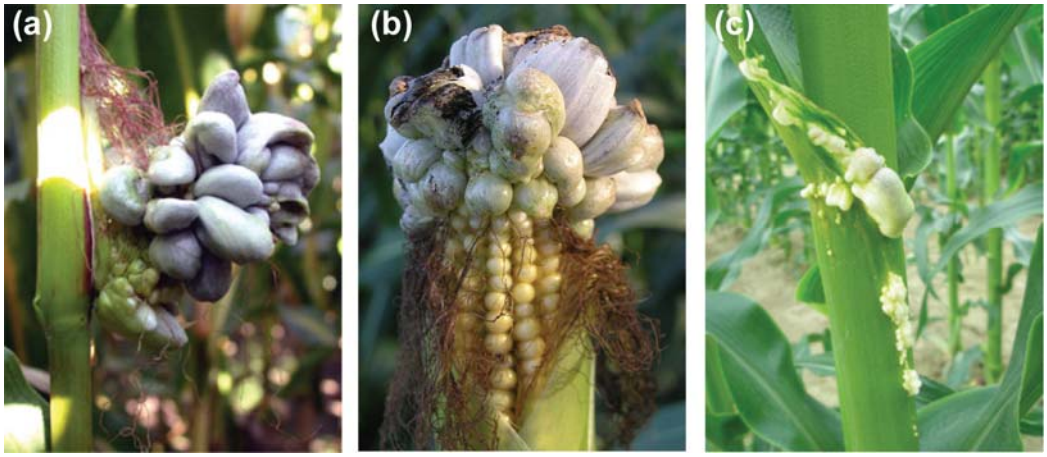

Fig. 1. Maize tumors induced by *U. maydis*. a) and b) tumors on corn ear; c) tumors on leaf.

Many of these potential effectors are encoded by gene clusters and the respective genes are induced in infected tissue during biotrophic growth. Deletions of several effector clusters result in dramatic effects on virulence (Kämper *et al.*, 2006). Interestingly, even single gene deletion mutants of an effector termed *pep1* and *stp1*, respectively, are completely blocked in biotrophic development (Doehlemann *et al.*, 2009; Schipper, 2009). Intriguingly, since disease progression requires response to maize organ-specific properties *U. maydis* most likely modifies effector deployment to redirect development of a specific organ primordium (Skibbe *et al.*, 2010). Presumably, the fungus interacts differently with vegetative and reproductive organs, possibly by expressing different genes in specific plant parts (Walbot & Skibbe, 2010).

Among the novel secreted *U. maydis* effectors some are encoded by gene families (Kämper *et al.*, 2006). One such family is an 11 gene effector family (designated *eff1*) originally described as three gene family by Kämper *et al*. (2006).

.

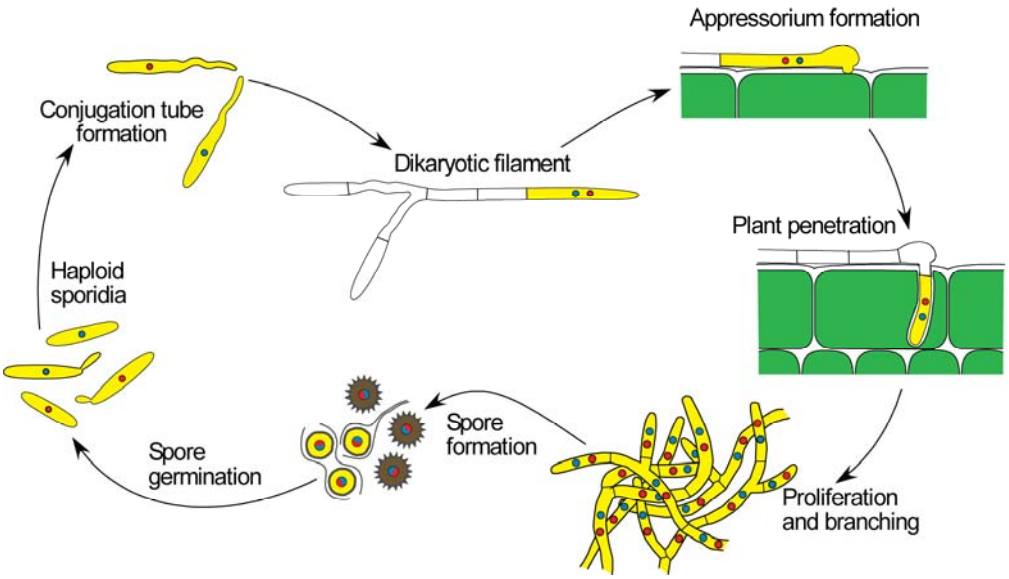

Fig. 2. Modified scheme of life cycle of *U. maydis* published by Kämper *et al*. (2006).

To shed light on the function of secreted proteins, which are encoded by gene families, generation of multiple gene deletion mutants is necessary. Although tools like a PCR-based system for the generation of gene replacement mutants in *U. maydis* is in place only a limited number of dominant drug-resistance markers such as hygromycin (Wang *et al.*, 1988), carboxin (Keon *et al.*, 1991), phleomycin and nourseothricin (Gold *et al.*, 1994) have been developed. Because the generation of deletion mutants is complicated by the need of two compatible wild type strains the solopathogenic strain SG200, which is a haploid strain engineered to harbor hybrid mating type loci, is frequently used (Kämper *et al.*, 2006). However, since SG200 strain is already phleomycin resistant, and the link between phenotype and deletion of a particular gene needs to be established by complementation, this reduces the number of available dominant markers further. To avoid these limitations, the development of new genetic tools is needed. Such obstacles can be overcome by recycling of the

resistance marker, which can be achieved via site-specific recombination (Bucholtz, 2008; Birling *et al.*, 2009).

1.3 FLP-mediated marker recycling

Site-specific recombination systems that have been shown to be functional in eukaryotes include i) Cre-lox from *Escherichia coli* phage P1, where the Cre (control of recombination) protein recognizes lox (locus of x-over) sites (Hoess *et al.*, 1990); ii) FLP-FRT from the 2 µm plasmid of *Saccharomyces cerevisiae* where the FLP recombinase acts on the FLP recognition target, FRT sites (Vetter *et al.*, 1983; Gronostajski & Sadowski, 1985; Senecoff *et al.*, 1985; Chen & Rice, 2003); iii) a mutant Gin protein (G inversion) and the gix sites from bacteriophage Mu (Kahmann *et al.*, 1985); iiii) as well as R-RS from *Zygosaccharomyces rouxii*, where R and RS are the recombinase and recombinase targets, respectively (Matsuzaki *et al.*, 1990). Currently, FLP and Cre recombinases are the primary candidates for applications in genetic studies of higher eukaryotes (Bischof & Basler, 2008). Both FLP and Cre belong to the tyrosine family of recombinases. The hallmark of tyrosine recombinase is defined by four strongly conserved active-site residues in the catalytic domain. These residues consist of an arginine-histidine-arginine triad, and a tyrosine nucleophile that covalently binds the DNA upon cleavage of the phosphodiester backbone (Nunes-Düby *et al.*, 1998). Tyrosine recombinases exchange DNA strands one pair at a time, and thus the reaction proceeds via an intermediate which is similar to the Holliday junction in homologous recombination (Holliday, 1964; Chen & Rice, 2003). These site-specific recombinases catalyze efficient inversion and excision events depending on the relative orientation of their recombination targets (Fig. 3) (Babineau *et al.*, 1985). FLP-mediated excision of the intervening DNA segment flanked by two FRT sites in a direct orientation leaves one recombination site behind. If the selectable marker is placed on the intervening DNA segment this allows generation of unmarked gene disruptions and recycling of the selectable marker (Wirth *et al.*, 2007). To date, such marker recycling systems have been successfully established in different organisms, such as *S. cerevisiae* (Storici *et al.*, 1999), *Candida albicans* (Morschhauser *et al.*, 1999; Wirsching *et al.*, 2000), *Aspergillus nidulans* (Forment *et al.*, 2006), *Cryptococcus neoformans* (Patel *et al.*, 2010), maize (Kerbach *et al.*, 2005), turfgrass (Hu *et al.*, 2006), rice (Radhakrishnan & Srivastava, 2005), aspen (Fladung & Becker, 2010), and mouse (Branda & Dymecki, 2004; Hacking,

2008; Wu *et al.*, 2008; Birling *et al.*, 2009) and bacteria (Schweizer, 2003). In addition, a protocol for removal of antibiotic resistance cassettes was established in human embryonic stem cells (Davis *et al.*, 2008). A scheme for FLP-mediated marker recycling in shown in Fig. 4. The 45 kDa FLP recombinase is the best characterized eukaryotic member of tyrosine recombinases. A minimal fully functional FRT site is 34 bp long and consists of an 8 bp asymmetric spacer (core region) that defines the orientation of the FRT site, flanked by two 13 bp palindromic sequences that constitute the binding sites for FLP (Chen & Rice, 2003). The spacer determines the direction of the recognition sites and therefore the type of FLP-mediated reaction. Since FLP mediated recombination does not require any accessory host proteins which has contributed to its wide use in heterologous systems. Another advantage of the FLP/FRT system is that FLP exhibits optimal activity at 30 °C (Buchholz *et al.*, 1996), which is a temperature at which *U. maydis* can be cultivated under laboratory conditions.

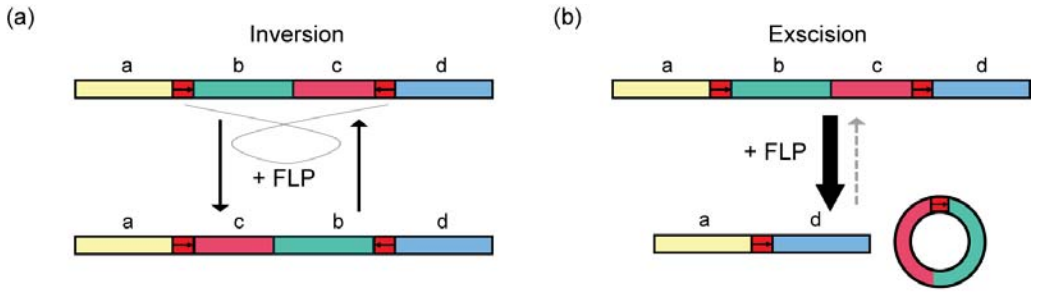

Fig. 3. Reactions catalyzed by FLP. FRT sites are depicted as arrowed red boxes. DNA fragments are highlighted in different colors and marked as a, b, c, and d respectively. Depending on the relative orientation of the FRT sites with respect to each other, FLP-mediated recombination leads to different outcomes. a) FLP will cause the inversion of the sequence between two FRT sites oriented in an opposite direction relative to each other. The inversion event occurs in a repeated fashion as long as the recombinase is present and active in the system. b) FLP will case the excision of the sequence between two FRT sites placed in the same direction.

A limitation encountered when using site-specific recombinases to recycle selectable marker is that every deletion event leaves one recognition sequence, a “scar”, behind. Such residual sequences can be sites of chromosomal rearrangements upon subsequent exposure to the recombinase (Hare & Chua, 2002). However, this can be

circumvented by introducing FRT sites with different point mutations in the core region (Storici *et al.*, 1999; Barrett *et al.*, 2008). Indeed, as was reported by Andrews *et al.* (1986), the sequence within the core region of an FRT site may vary yet remains functional as long as the second recombination site also carries this variation. An FRT site containing a point mutation within the core region is, however, unable to recombine with a wild-type FRT site (Andrews *et al.*, 1986). Studies of Whiteson & Rice (2008) have provided evidence that several mutant FRT sites that bind FLP well are cleaved poorly, suggesting that sequence requirements for optimal binding and catalysis are not identical (Whiteson & Rice, 2008).

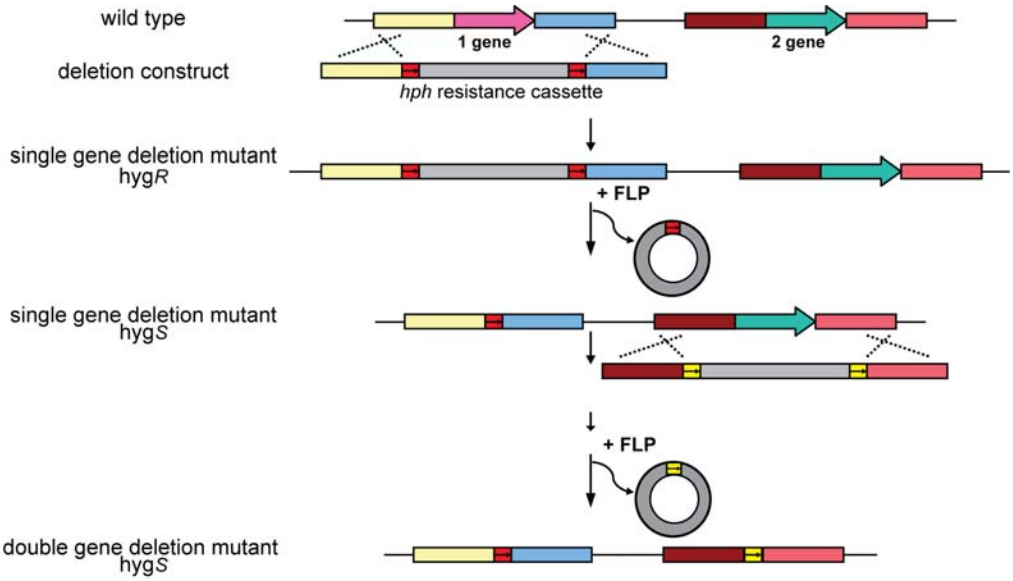

Fig. 4. Scheme of multiple gene deletions via FLP-mediated recycling of hygromycin resistance (*hph*) cassette. Grey boxes represent *hph* cassette. Flanking regions of the first target gene are shown in yellow and blue while of the second gene to be disrupted by brown and light-red. After each gene deletion FLP activity can be induced and *hph* cassette flanked by FRT sequences will be excised as a circularized molecule leaving one FRT site, "scar", behind. Then the strain becomes hygromycin-sensitive and the same *hph* resistance marker can be reused for another gene disruption in the same strain. To eliminate possible intra- and/or intermolecular recombinations caused by FRT scars for each round of gene deletion FRTs with different mutations were used. FRTs are highlighted as red and yellow arrowed boxes.

1.4 Aim of this study

In the *U. maydis* genome several effector proteins are encoded by gene families suggesting a redundant function. Due to the limited number of resistance markers these effector gene families have not yet been functionally analyzed. To facilitate functional analysis of the effector gene families the first focus of this study was the establishment of the FLP/FRT system in *U. maydis*. The inducible FLP-mediated marker recycling can be used as a tool for generation of multiple gene deletion mutants. The second aim of this thesis was to study the expression of all 11 genes of the *eff1* gene family coding for secreted proteins with an unknown function followed by deleting all 11 genes using the FLP/FRT system. The fourth goal was to get more insights on the role of Eff1 proteins during the biotrophic stage of the *U. maydis* growth by using microscopic analysis and lipid binding assays.

2. Results

2.1 Establishment of the FLP-mediated marker recycling in *U. maydis*

2.1.1 Design of an arabinose-inducible FLP expression system for U. maydis

In general it is difficult to express heterologous proteins in *Ustilago maydis* due to premature transcription termination (Ladendorf *et al*., 2003; Zarnack *et al*., 2006). Among factors which could play a role for heterologous gene expression is a codon bias (Kane, 1995). Codon bias can lead to premature termination of translation, misincorporation of amino acids, or frameshift mutations (Calderone *et al.*, 1996). Therefore, I designed a codon-optimized FLP gene according to a contest-dependent dicodon usage preferred by *U. maydis*. Compared to FLP from *S. cerevisiae*, the optimised FLP sequence contained 384 silent base mutations that modified 316 of 423 codons (Fig. 5). This increased the G+C content from 37% to 60%. The synthetic FLP gene was assembled from oligonucleotides using the strategy described by Stemmer (Stemmer *et al.*, 1995) and (Hale & Thompson, 1998). To test FLP expression I generated strain SG200FLP, in which FLP recombinase is integrated in single copy in the *ip* locus (Loubradou *et al.*, 2001) of *U. maydis* strain SG200 under the control of arabinose inducible *crg1* promoter. By northern blot analysis FLP recombinase gene expression could be visualized 1 h after shift to complete medium containing arabinose (CM-ara) as sole carbon source (Fig. 6a). To assess FLP activity *in vivo* the self-replicating recombination reporter plasmid pIF1 was introduced into SG200FLP and into SG200 as control. In pIF1 *lacZ´* is disrupted by a cassette in which FRT sites flank a constitutively expressed *egfp* gene under the control of *po2tef* promoter. FLP-mediated recombination should excise the *egfp* cassette and leave a plasmid in which the *lacZ´* gene is restored (Fig. 6b). After growth in CM-glu medium SG200pIF1 and SG200FLPpIF1 strains were grown in CM-ara medium for up to 16 hours. Starting at 8 h a decrease of relative fluorescence units was observed in the SG200FLPpIF1 grown in the CM-ara medium indicative of excision of reporter *egfp* gene (Fig. 6d). Neither in the control strain SG200pIF1 nor in SG200FLPpIF1 grown in CM-glu medium could such a decrease in relative fluorescence be observed (Fig. 6d). After an induction period of 16 hrs DNA was prepared and introduced into DH5α by electroporation. Of 953 transformants with DNA isolated from SG200pIF1 all were white on X-Gal plates while of 1078 transformants with DNA isolated from SG200FLPpIF1 659 were light blue (Fig. 6c) indicative of partial restoration of the

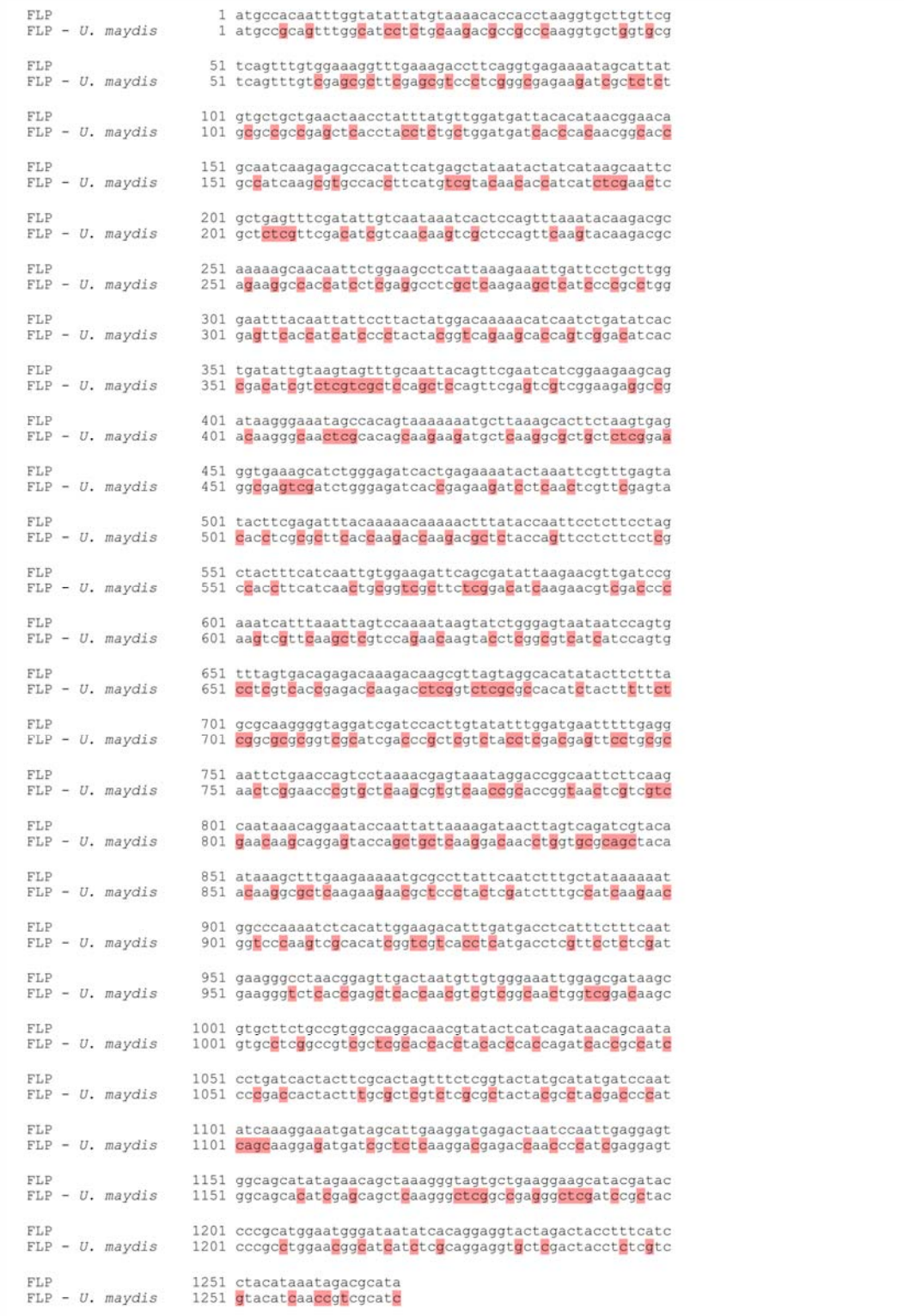

Fig. 5. Nucleotide sequence of the codon-optimized FLP recombinase. Codon-optimized (FLP – *U. maydis*) and FLP recombinase from the 2 micron plasmid of *S. cerevisiae* (FLP) are compared. Sequence differences are highlighted in pink color.

lacZ´ gene. In three independent experiments the average frequency of lacZ´ restoration was 67.8 ± 15.5 % while restoration of *lacZ´* could not be observed after transforming DNA from SG200pIF1 into DH5α. When FLP activity was not induced 1,8 % of the transformants showed a light blue phenotype indicating leaking of the *crg1* promoter.

Restriction analysis revealed that the plasmids isolated from these light blue colonies were reduced in size by 2.0 kb, indicative of excision (Fig. 7). The precise site-specific FLP-mediated excision event was verified by sequencing the junctions in 5 of the plasmids using primers pIF1fw and pI. This illustrated efficient FLP-mediated excision when FRT sites are located on an autonomously replicating plasmid.

2.1.2 FLP-mediated excision of an hph cassette from U. maydis genome

Next, I tested the efficiency of FLP-mediated excision from the genome. On a statistical basis, a 34 base pairs (bp) consensus FRT site is not expected to be found in the genome. However, illegitimate recombination events caused by Cre action via cryptic loxP sites (which are also 34 bp long) were reported to occur in yeast and some mammalian genomes (Schmidt *et al.*, 2000; Loonstra *et al.*, 2001; Silver *&* Livingston, 2001). A BLAST search of the *U. maydis* genome excluded the possibility of cryptic FRT targets being present. Figure 9 shows schematically the pHwtFRT plasmid harbouring an FRT-bordered *hph* cassette used in this study to generate gene deletion constructs.

Um01796 was disrupted in SG200FLP via homologous recombination employing the *hph* cassette flanked by wild type FRT sites from pHwtFRT (Fig. 8a). The resulting strain SG200FPLΔ01796$^{FRT/FRT}$ was grown in CM-glu liquid medium to an OD600 = 0.7 and shifted to CM-ara liquid medium to induce FLP expression. Genomic DNA was isolated at different time points after induction of FLP expression. By PCR analysis with um01796LBfw and um01796RBrv primers (see Materials and Methods, Table 4) the appearance of the 2 kb excision product could be demonstrated already after an induction period of 2 hours and the intensity of this band increased with increased induction time (Fig. 8b).

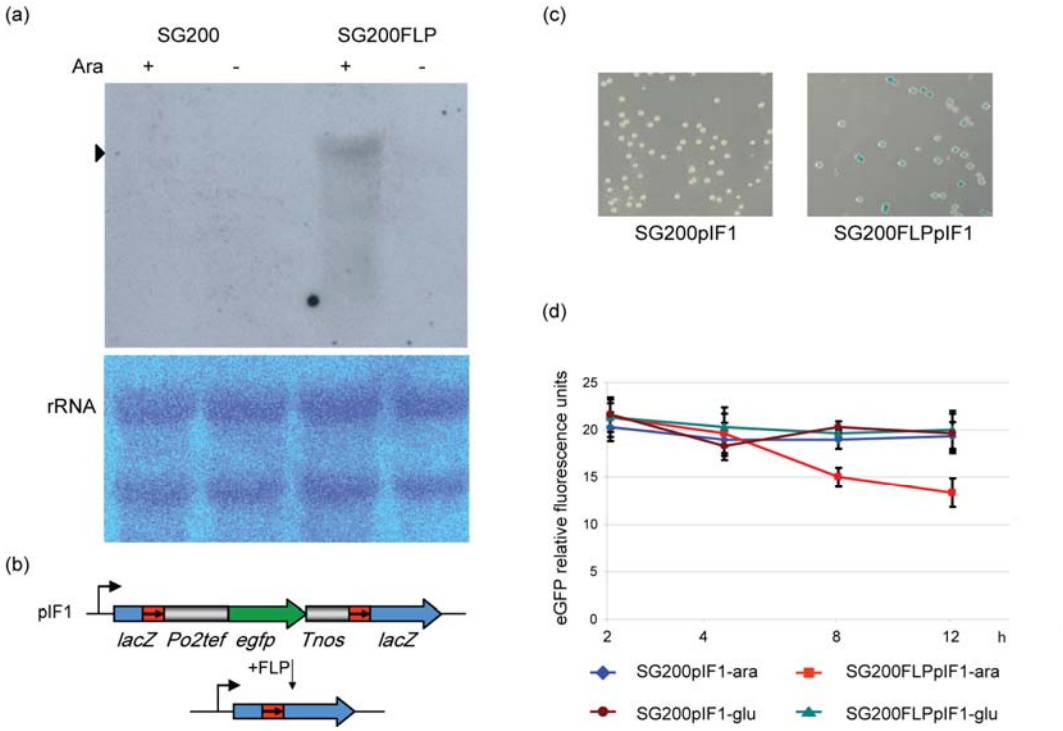

Fig. 6. Establishment of the FLP/FRT system in *U. maydis*. a) SG200 and SG200FLP were grown in CM-glu and then shifted to either CM-glu (-) or CM-ara (+) medium for 1 h. Total RNA was prepared and subjected to northern blot analysis using a 1.3 kb PCR product of FLP gene as probe (Methods S2). FLP mRNA is marked with an arrow. Methylene blue rRNA loading control of samples is shown below. b) Scheme of the recombination reporter plasmid pIF1. *Egfp* is inserted in the *lacZ´* gene and is flanked by directly repeated FRT sites (red bars with arrows). *Egfp* expression is controlled by the constitutive *Po2tef* promoter and the *nos* terminator (upper panel). FLP-mediated recombination excises *egfp* leaving one FRT site. This site is in frame with the open reading frame of *lacZ´* (lower panel). c) 16 hrs after the shift of SG200pIF1 and SG200FLPpIF1 to CM-ara medium DNA was prepared, transformed into DH5α and transformants were plated on YT-XGal plates. All transformants with DNA recovered from SG200pIF1 yielded white colonies (left) while about two thirds of the transformants with DNA from SG200FLPpIF1 yielded blue colonies (right). d) SG200FLPpIF1 and SG200pIF1 were either grown in CM-glu or shifted to CM-ara for the indicated time. Relative eGFP fluorescence/OD600 was determined in triplicate experiments. Average values are shown and standard errors are indicated for SG200FLPpIF1 shifted to CM-ara (red) and CM-glu (dark red) and SG200pIF1 shifted to CM-ara (blue) and CM-glu (green).

Since the low level of basal expression of FLP in SG200FLP could cause premature excision of the resistance cassette and prevent the identification of the desired transformants we have also generated a self-replicating FLP-expressing plasmid pFLPexpC conferring carboxin resistance (Fig. 9).

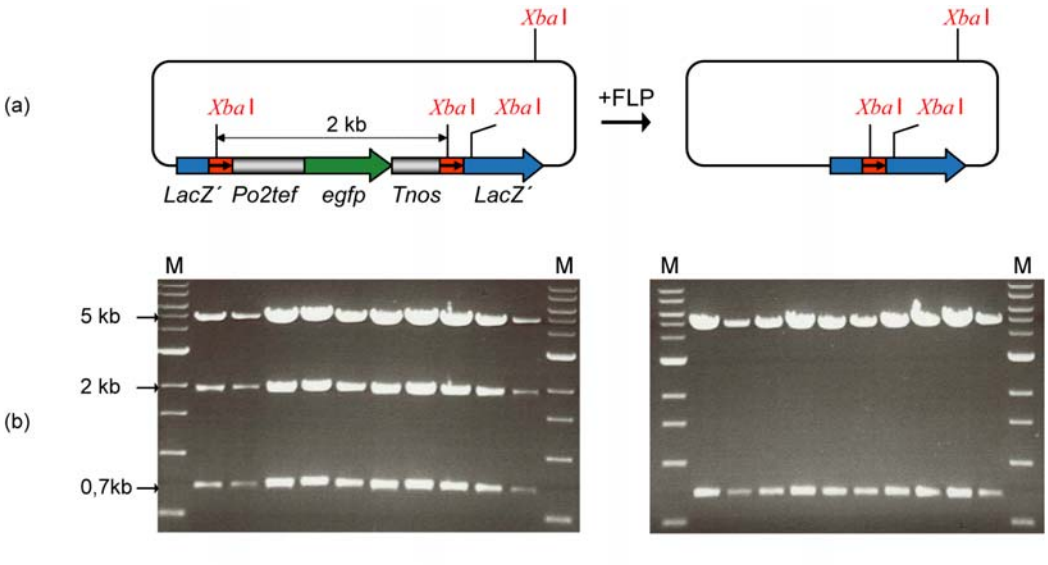

Fig. 7. FLP-mediated excision assay. a) Schematic representation of the recombination test plasmid pIF1 and its derivative after FLP-mediated pop-out of the FRT-flanked fragment. FRT sites are indicated in red and their orientation is given by the arrow. The *laz´* gene is indicated in blue, the *egfp* gene flanked by the constitutive *Po2tef* promoter and *Tnos* terminator is indicated in green and grey, respectively. Diagnostic *Xba*I restriction sites are indicated. Digestion of pIF1 with *Xba*I results in four fragments of 5.0, 2.0, 0.7 and 0.055 kb (not visible on these gels). *Xba*I digestion of pIF1 after FLP-mediated excision results in two fragments of 5.0 and 0.7 kb. b) DH5α was transformed with DNA from SG200FLPpIF1, incubated for 16 h in CM-ara and plated on X-gal plates. Left panel: *Xba*I restriction analysis of ten plasmids isolated from white colonies. Right panel: *Xba*I restriction analysis of ten plasmids isolated from light blue colonies. M = 1 kb ladder.

This plasmid was introduced into SG200Δ01796$^{FRT/FRT}$. FLP expression was then induced by shift to CM-ara medium, and colonies that had lost the hygromycin cassette as well as the FLP donor plasmid were subsequently identified (see Materials and Methods for details). In three independent experiments an excision frequency of 65.71 ± 4.34% could be determined and of these cells 21.06 ± 2.58% were also carboxin sensitive, i.e. they had lost pFLPexpC. To verify the correct excision of *hph* cassette DNA was isolated from five hygromycin-sensitive and from four hygromycin-resistant colonies and analysed by PCR (Fig. 10 a, b). There was a perfect correlation between the presence of the excision product and hygromycin sensitivity. Additionally, correct excision of the FRT-flanked DNA segment was analyzed by Southern blotting (Fig. 10 c, d). These results demonstrate that it will be feasible to screen for FLP-mediated excision and loss of the FLP donor plasmid simultaneously and for the subsequent experiments this procedure was applied.

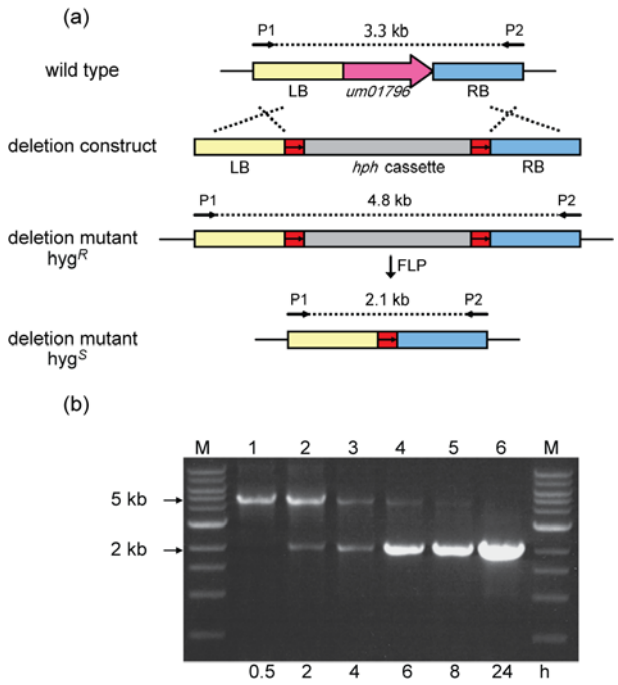

Fig. 8. Time course and efficiency of FLP-mediated excision of the *hph* cassette from a genomic location. a) Scheme of the events leading to deletion of *um01796* and subsequent FLP-mediated excision. FRT sites are indicated as red boxes and their orientation is given by arrows. In the first step the deletion construct for gene *um01796* is integrated in the genomic locus by homologous recombination (dotted crosses) yielding a hygromycin resistant transformant. After induction of FLP expression the hygromycin resistance cassette is excised leaving one FRT site in the genome. PCR primers used for verification are indicated together with the length of the amplified fragments. b) SG2000FLPΔ1796$^{FRT/FRT}$ was grown in CM-glu medium and shifted to CM-ara medium for 24 h. Samples were taken at the indicated times and DNA was prepared. Using PCR with primers P1 and P2 excision was monitored. The 4.8 kb fragment corresponds to the non-excised cassette, the 2.1 kb fragment indicates the post-excision product.

2.1.3 One step FLP-mediated excision of the hph cassette and the FLP coding sequence

The generation of successive deletion mutants was very time consuming due to repeated introduction of the FLP expressing pFLPexpC once a gene had been deleted, FLP induction and then screening for the loss of the plasmid. Therefore, I modified the system in such a way that in future experiments the FLP gene could be introduced into the genome together with the *hph* cassette.

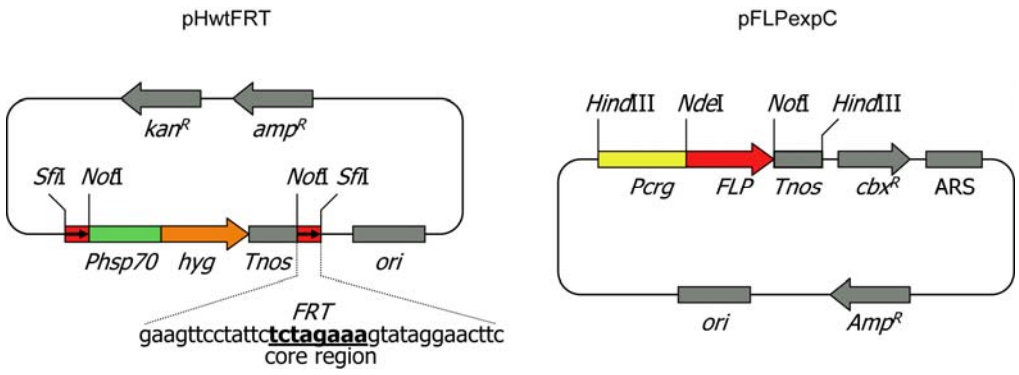

Fig. 9. Schematic representation of plasmids used in recombination assays. Schematic representation of plasmids used in recombination assays. pHwtFRT is an *E. coli* plasmid that serves as the source of the *hph* cassette flanked by FRT sites (red boxes, orientation is indicated by arrows) used for generating deletion constructs. The bacterial gene for hygromycin-phosphotransferase (*hph*) is under control of the *U. maydis hsp70* promoter (*Phsp70* in green); termination is facilitated by the *Agrobacterium tumefaciens nos* terminator (*Tnos* in grey). *Not*1 and *Sfi*I sites are indicated. For selection in *E. coli* this plasmid harbors a kanamycin as well as an ampicillin resistance gene. pFLPexpC is the FLP expressing self replicating plasmid for maintenance in *U. maydis*. It harbors the synthetic FLP gene (red) under control of the arabinose-inducible *Pcrg1* promoter (yellow) and carries a *cbx* resistance gene for selection in *U. maydis*.

To demonstrate its utility I disrupted *um01796* in SG200 by introducing pYUIF-FRTm2 (Fig. 11). Then FLP activity in the resulting mutant strain $\Delta 01796^{FRTm2/FRTm2}$::pYUIFm2 was induced for 16 hrs by shift to CM-ara medium. After inducing FLP, 34 ± 9 % of the resulting single colonies were hygromycin sensitive. PCR analysis revealed that in these colonies the *hph* as well as the FLP gene had been lost (Fig. 11). This illustrates that the experimental speed in future studies can be significantly increased. The drawback of this protocol is a large size of the deletion cassette (8 kb) which reduces cloning efficiency of the ligation product into the TOPO vector (see Materials & Methods). The large size is mostly due to the *crg1* promoter, which is 3.6 kb long. However, integration of FLP under 2 kb nitrate-inducible *nar* promoter resulted in a high excision frequency already in non-induced cells (data not shown), presumably because this promoter is less efficiently regulated by ammonium.

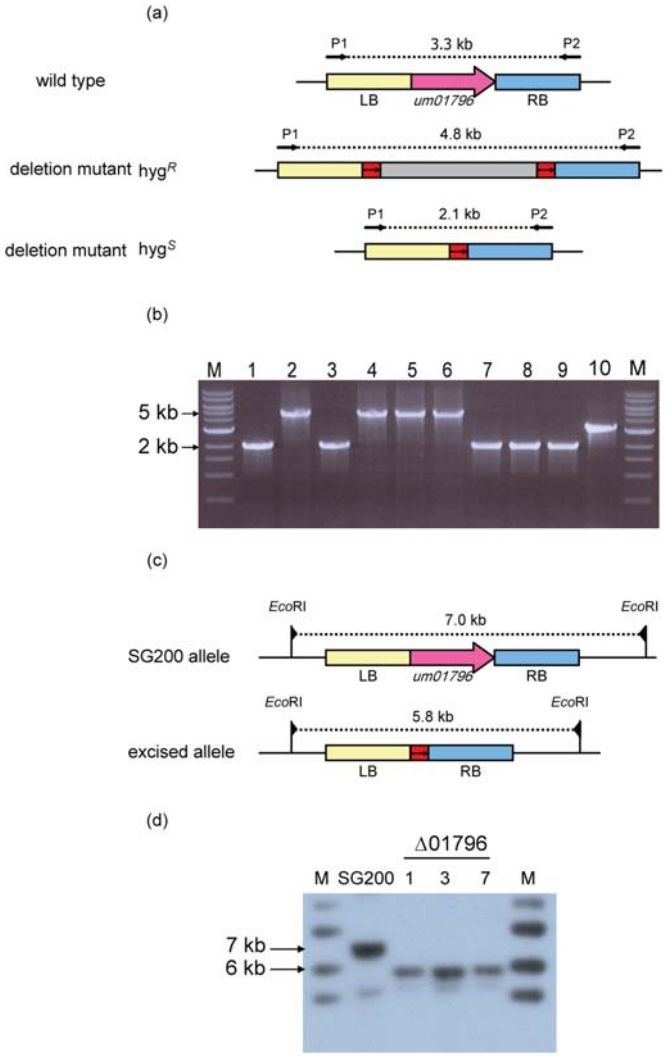

Fig. 10. Time course and efficiency of FLP-mediated excision of the *hph* cassette from a genomic location. a) Schematic representation of sizes of PCR amplification products obtained with P1 and P2 primer pair from wild type, *hyg* resistant mutant SG200Δ01796$^{FRT/FRT}$ as well as *hyg* sensitive mutant SG200Δ01796^{FRT} DNA templates. FRT sites are indicated as red boxes and their orientation is given by arrows. After introduction of pFlpexpC and induction of FLP the hygromycin resistance cassette is excised leaving one FRT site in the genome. PCR primers used for verification are indicated together with the length of the amplified fragments. b) SG200Δ01796$^{FRT/FRT}$pFlpexpC was grown in CM-ara medium for 16 hrs and then plated on CM. DNA was prepared from nine single colonies (lanes 1-9) and analyzed by PCR using primers P1 and P2. Hygromycin-resistant colonies contained the non-excised cassette (4.8 kb) while all hygromycin-sensitive colonies had excised the cassette (2.1 kb). SG200 yields a 3.3 kb PCR product (lane 10). M = 1 kb ladder. c) Schematic representation of SG200 allele and excised allele. FRT site is shown as red arrowed box. The *EcoR*I restriction sites and sizes of the hybridization fragments are indicated. d) Southern blot analysis of FLP-mediated *hph*-cassette excision event in Δum01796pFlpexpC mutants after PCR screen. Genomic DNA from clones #1, #3, and #7 was used. Genomic DNA was isolated 18 h after incubation of cells in YEPSL medium, digested with *EcoR*I restriction enzyme, and Southern blot analysis was performed utilizing the knock-out construct as a probe.

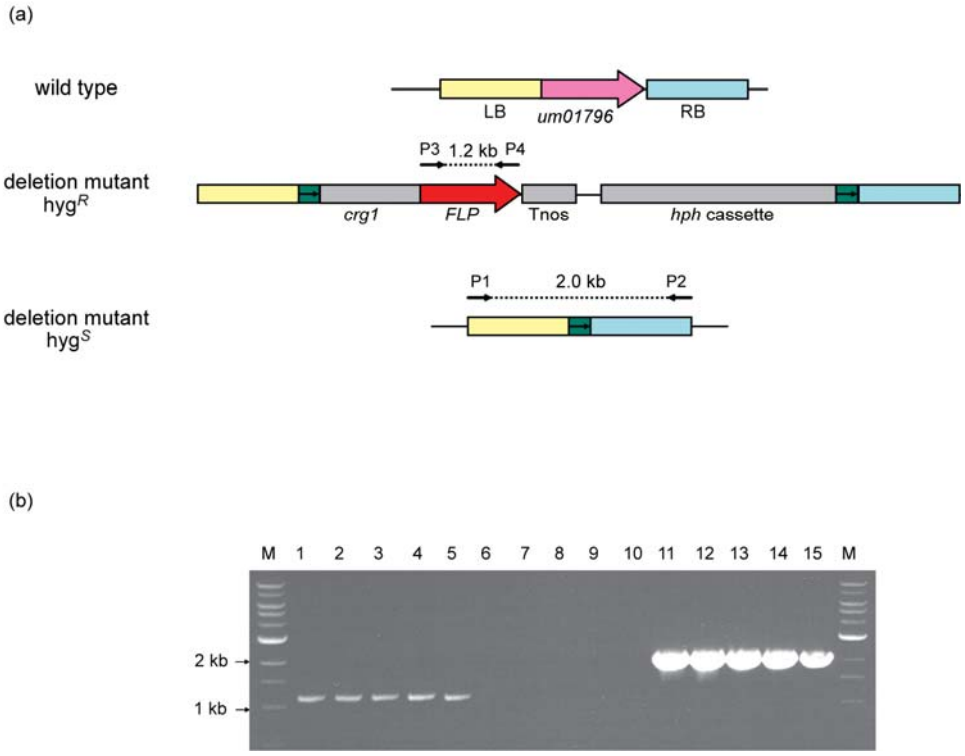

Fig. 11. Screen for FLP-mediated recombination leading to excision of the *hph* cassette as well as the FLP gene. (a) Scheme for deleting *um01796* (top line) and replacing it with a cassette harboring FRTm2 sites (green), the *crg1*-inducible FLP gene (red with regulatory elements shown in grey) and the *hph* cassette (in grey) (middle line). The border fragments flanking *um01796* are indicated in yellow (left border, LB) and light blue (right border, RB). After induction of FLP a hygromycin sensitive deletion mutant is generated that lacks the FLP gene (lower line). P1 (um01796LBfw), P2 (um01796RBrv), P3 (a+4) and P4 (c-9) indicate primers used for diagnostic amplifications. (b) SG200Δ01796::pYUIF-FRTm2 was grown in CM-ara for 16 hrs and plated for single colonies on PD plates and replica plated on hyg plates. 5 hygromycin resistant (lanes 1-5) and 5 hygromycin sensitive (lanes 4-10) colonies were identified, DNA was prepared and amplified with primers P3 and P4 to visualize the presence or absence of the FLP gene. In addition, the DNA from the five hygromycin sensitive colonies was amplified with primers P1 and P2 to visualize the expected post-excision band of 2.0 kb (lanes 11 – 15). M = 1 kb ladder.

2.1.4 Recombination assay on core-mutated FRT sequences

When multiple gene deletions are performed by FLP-mediated recombination multiple FRT sequences are left in the genome that can cause genomic instability in the presence of FLP (Hare & Chua, 2002). To minimize the chance for chromosome rearrangements caused by intra- and intermolecular recombination between identical

FRT sites left in the genome four mutant FRT sequences were designed (Fig. 12) each with a different point mutation in the core region (see Materials and Methods).

GAAGTTCCTATTC**TCTAGAAA**GTATAGGAACTTC	**FRT**
GAAGTTCCTATTC**TCGAGAAA**GTATAGGAACTTC	**FRTm1**
GAAGTTCCTATTC**TCAAGAAA**GTATAGGAACTTC	**FRTm2**
GAAGTTCCTATTC**TCCAGAAA**GTATAGGAACTTC	**FRTm3**
GAAGTTCCTATTC**TCTGGAAA**GTATAGGAACTTC	**FRTm4**

Fig. 12. Sequences of FRT sites used in this study. Eight nucleotides of the FRT core region are underlined and indicated in bold. Point mutations introduced are marked in red.

Plasmids were generated in which the *hph* cassette is flanked by two direct copies of these mutated FRT sequences. pHwtFRT, pHFRTm1, pHFRTm2, pHFRTm3, pHFRTm4 were introduced into SG200FLP individually to disrupt gene *um11377.2*.

The efficiency of FLP-mediated recombination of the mutated FRT sites was assayed (see Materials & Methods). The assay was performed three times and in total about 200 cells were tested for the loss of resistance marker. Relative to recombination in pHwtFRT carrying wild type FRT sequences the mutated FRT sequences recombined 2-5 times less efficiently (Fig. 13).

2.1.5 Stability of strains harboring multiple FRT sequences

To assess the stability of strains carrying multiple integrations of FRT sites we used SG200Δ01796^{FRT}Δ11377.2$^{FRT/FRT}$ in which two wild type FRT sites are situated 0.43 Mb apart on chromosome 3. In parallel the four strains SG200Δ01796^{FRT}Δ11377.2$^{FRTm1/FRTm1}$, SG200Δ01796^{FRT}Δ11377.2$^{FRTm2/FRTm2}$ SG200Δ01796^{FRT}Δ11377.2$^{FRTm3/FRTm3}$ SG200Δ01796^{FRT}Δ11377.2$^{FRTm4/FRTm4}$ (see Materials and Methods, Table 3) that differ from SG200Δ01796^{FRT}Δ11377.2$^{FRT/FRT}$ only by the m1, m2, m3 or m4 mutation in the FRT sites (Fig. 14) residing in the *um11377.2* locus (prior to excision) were generated. After introducing pFLPexpC and inducing FLP expression (see Materials and Methods) DNA was isolated and

analyzed by PCR for deletion events between FRT sites in the *um01796* and the *um11377.2* locus using primer combinations shown in Fig. 14a.

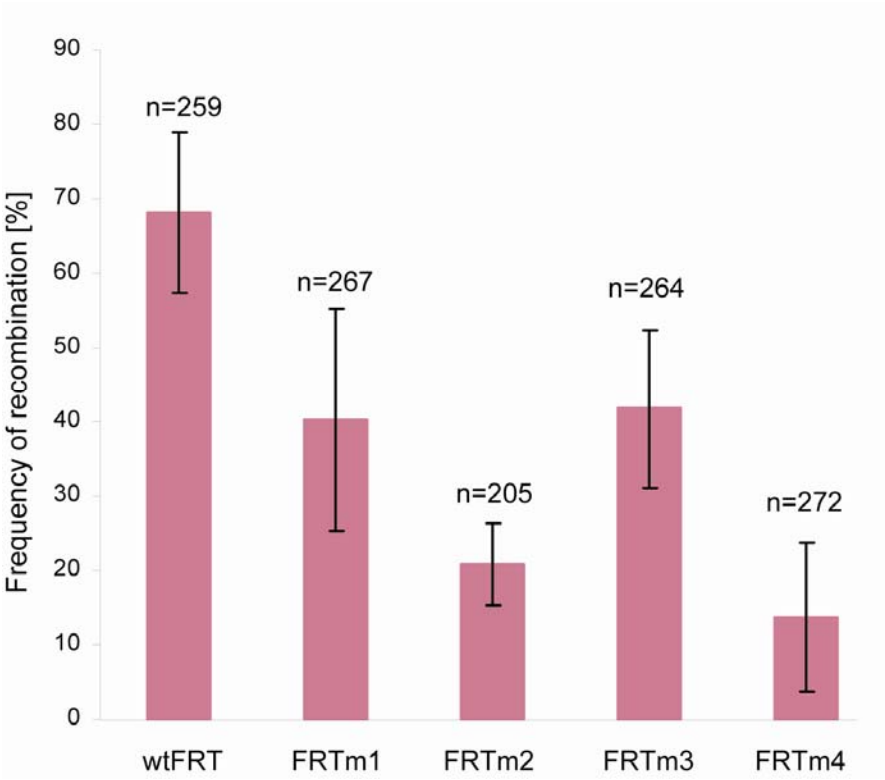

Fig. 13. FLP-mediated recombination in SG200FLPΔ11377.2 strains carrying *hph* cassettes flanked by direct copies of either wild type or mutant FRT sites. Recombination efficiency was calculated by determining the percentage of cells in which the *hph* cassette was excised after incubation for 24 h in CM-ara medium and plating on PD and hyg plates. N gives the total number of colonies screened in three independent experiments. Bars indicate standard error.

While recombination could be visualized between a wild type FRT site in the *um01796* locus and wild type FRT sites in the *um11377.2* locus in DNA isolated from SG200Δ01796^{FRT}Δ11377.2$^{FRT/FRT}$ such a 3.1 kb product was not amplified when strains harbored a wild type FRT site and any of the mutated FRT sites (Fig. 14). This illustrates that the introduced FRT mutations greatly reduce or abolish recombination with wild type FRT sites, which should consequently help to maintain strain integrity.

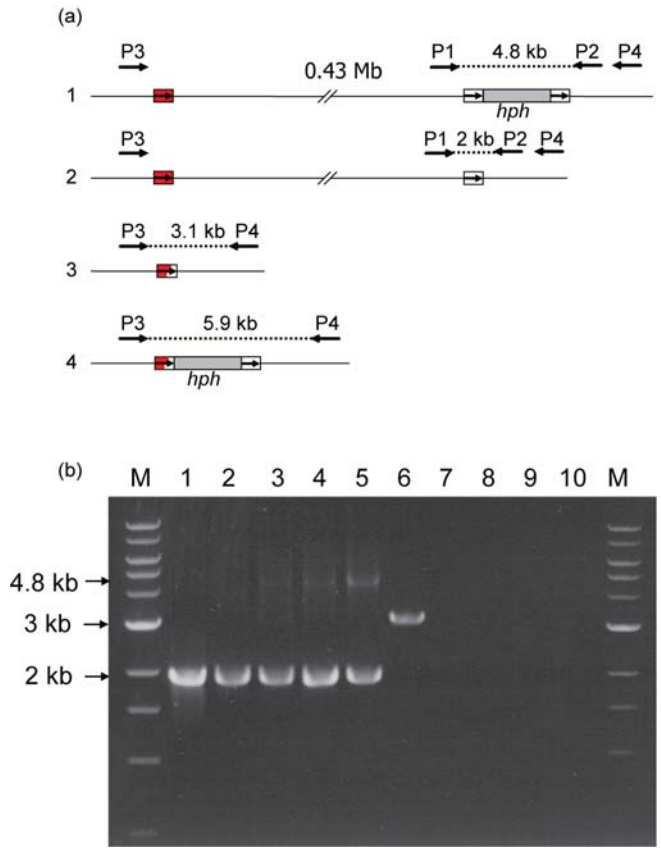

Fig. 14. Stability of SG200 strains carrying wild type and mutant FRT sites after induction of FLP gene expression. (a) Scheme for possible recombination events in SG200Δ01796^{FRT}Δ11377.2 derivatives carrying one wild type FRT site replacing *um01796* (indicated in red) plus two FRT wild type or mutant sites flanking the hygromycin resistance cassette that has replaced *um11377.2* (indicated in white). Arrows indicate the orientation of FRT sites. Primers P1 (um11377.2LBfw), P2 (um11377.2RBrv), P3(um01796LBfw) and P4 (um11377.2-FRTassay-rv) (see Table S1) which were used in PCR reactions to visualize possible excision events (lines 1 - 4) are indicated. (b) All strains were shifted to CM-ara medium for 16 hrs, total DNA was isolated and amplified using primer pair P1+P2 (lanes 1 - 5) and primers P3+P4 (lanes 6 - 10). Strains used are SG200Δ01796^{FRT}Δ11377.2$^{FRT/FRT}$ (lanes 1 and 6), SG200Δ01796^{FRT}Δ11377.2$^{FRTm1/FRTm1}$ (lanes 2 and 7), SG200Δ01796^{FRT}Δ11377.2$^{FRTm2/FRTm2}$ (lanes 3 and 8), SG200Δ01796^{FRT}Δ11377.2$^{FRTm3/FRTm3}$ (lanes 4 and 9), SG200Δ01796^{FRT}Δ11377.2$^{FRTm4/FRTm4}$ (lanes 5 and 10). M = 1 kb marker. The 4.8 kb band is characteristic for the unexcised *hph* cassette and its presence indicates the lower recombination efficiency of mutated FRT sites. The 3.1 kb fragment indicates recombination between the wild type FRT site and one of the FRT sites residing in the *um11377.2* locus. This band is visible only when in strain SG200Δ01796^{FRT}Δ11377.2$^{FRT/FRT}$ carrying three wild type FRT sites. The 5.9 kb fragment was never detected, presumably because excision of the *hph* cassette even in strain SG200Δ01796^{FRT}Δ11377.2$^{FRT/FRT}$ was much more efficient than recombination between the sites 0.43 Mb apart.

2.2 An 11 gene effector family in *U. maydis*

2.2.1 Bioinformatic analysis of eff1 genes

2.2.1.1 General characterization of eff1 family

U. maydis families 9 and 17 have been described to consist of four and three genes, respectively, encoding novel secreted proteins that are *U. maydis* specific (Kämper *et al.*, 2006). Our initial interest in these groups of secreted proteins was based on the finding that three members of these two gene families contain putative NLS sequences (Mueller *et al*., 2008). However, these putative NLS sequences occur at non-conserved locations, and are therefore not considered functionally relevant. Additionally, a more rigorous search for related genes using profile Hidden Markov Models (HMMs) revealed that these seven genes in family 9 and 17 are related and four additional paralogs exist in the genome. We designate this enlarged gene family as *eff1* family (Table 1). The *eff1* family comprises *um01796* and *um11377* on chromosome 3, the adjacent genes *um03313* and *um03314* on chromosome 8 and the seven genes, *um02135*, *um02136, um02137*, *um02138*, *um02139*, *um02140*, and *um02141*, clustered on chromosome 5.

According to MUMDB http://mips.helmholtz-muenchen.de/genre/proj/ustilago all encoded proteins except Um11377 contain putative N-terminal secretion signals and an analysis of the *um11377* gene region showed that sequence similarity to other Eff1 proteins extends well upstream of the predicted Um11377 start methionine and includes a putative signal sequence. This larger frame is however disrupted by a stop codon at position 64. We re-sequenced this gene from the sequenced *U. maydis* strain 521 and detected a sequencing error. The gene model has been corrected and the gene is now designated *um11377.2.* Additionally, based on sequence similarity between Um02139 and Um02140 (Fig. 15b) Met37 is strongly implied to be the true start codon of Um02140. The respective gene is now designated *um02140.2*. The *eff1* genes code for proteins ranging in size from 302 aa (Um02141) to 493 aa (Um02136) (Table 2). A complete alignment of all 11 Eff1 proteins employing the multiple sequence alignment program ClustalW (Thompson *et al.*, 1994) revealed several strictly conserved as well as some highly prevalent residues located in the C-terminal region (Fig. 15b). Um03313 and Um03314 display 60% amino acid identity, indicating that a recent duplication event has generated these adjacent genes.

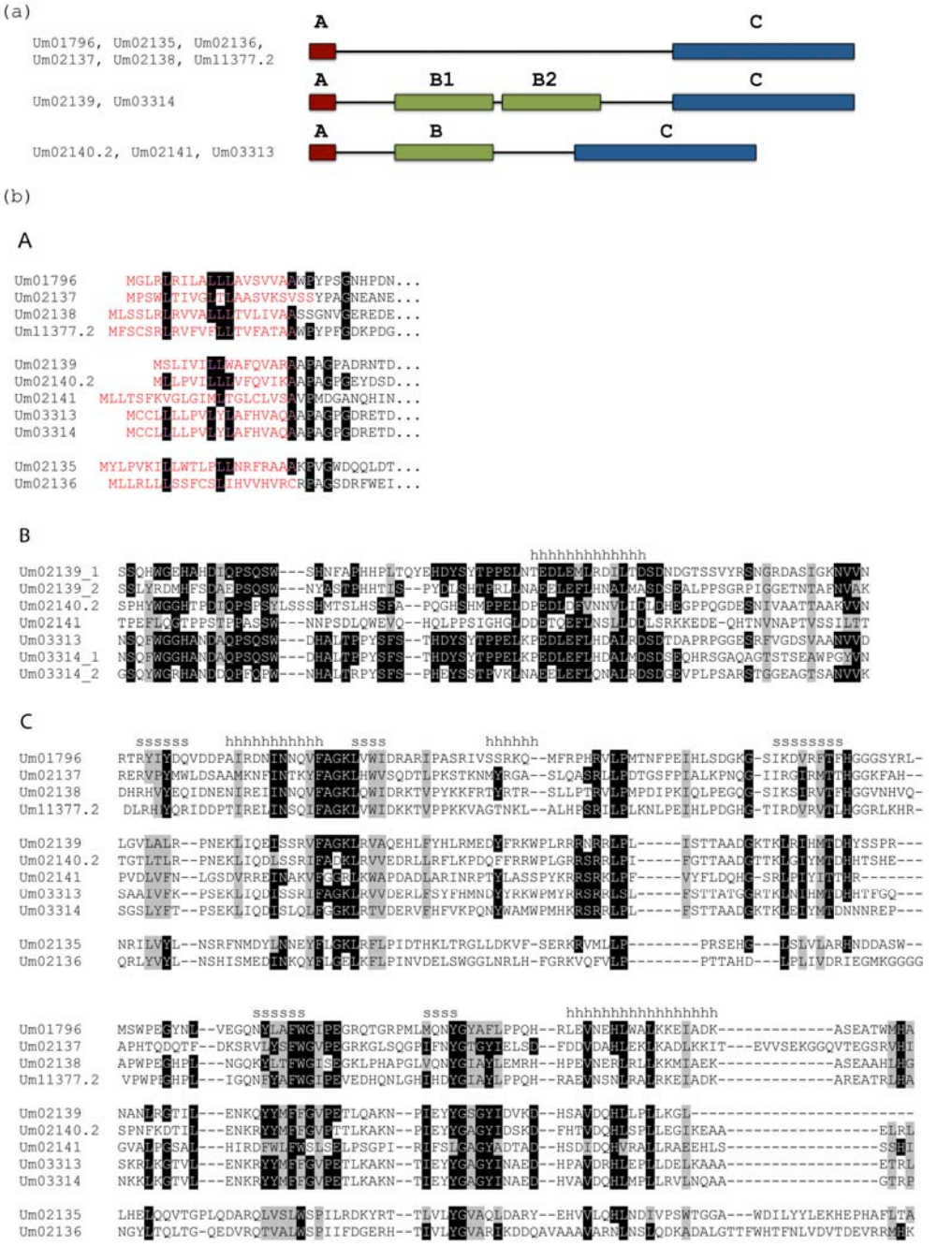

Fig. 15. Domains of Eff1 proteins. (a) On top the domain structure of Eff1 proteins is depicted schematically. (b) A) The proteins are defined by an N-terminal signal sequence colored red in the alignment; cleavage site consensus: A/x-[PS]-x-[GP]-x-G). B) In all Eff1 proteins, the central region is predicted to be unstructured and has very low secondary structure propensity. In subgroup II sequences (see Fig. 16), this region contains a conserved segment with an area of elevated helical propensity. This segment is duplicated in two of the proteins. C) The C-terminal conserved domain is the only part of the mature proteins that appears to have a folded structure (the predicted secondary structure is shown above the alignment; s - strand; h - helix).

Um01796 and Um02138 show an amino acid identity of 42.5 % and Um11377.2 shares 45 %identity with Um01796. Amino acid sequence conservation in all 11 proteins is most evident in the C-terminal domains (Fig. 15b). Using the program "PredictNLS" putative monopartite nuclear localization signals (NLS) were predicted for Um02137 (^{287}**KKRRRK**^{292}) and Um02139 (^{288}ESL**KR**T^{293}), and these are located in the conserved C-terminal domain of the respective proteins. A putative bipartite NLS sequence consisting of two stretches of basic amino acids (^{351}**KR**S**RR**^{355}) and (^{384}**KK**L**K**^{387}) was detected in Um03314.

Table 1. The *eff1* gene family

um gene number*	gene name	accession number
um01796	***eff1-1***	XP_757943
um11377.2	***eff1-2***	XP_758119
um03313	***eff1-3***	XP_759460
um03314	***eff1-4***	XP_759461
um02135	***eff1-5***	XP_758282
um02136	***eff1-6***	XP_758283
um02137	***eff1-7***	XP_758284
um02138	***eff1-8***	XP_758285
um02139	***eff1-9***	XP_758286
um02140.2	***eff1-10***	XP_758287
um02141	***eff1-11***	XP_758288

* MUMDB gene assignment http://mips.helmholtz-muenchen.de/genre/proj/ustilago

An alignment of eleven Eff1 proteins was analyzed by neighbor joining and parsimony with statistical confidence measured by bootstrap analysis. With a bootstrap support 100% in distant analysis both sets of phylogenetic analyses revealed that the family has split up into three groups consisting of subgroup I (Um02138, Um01796, Um11377.2, Um02137), subgroup II (Um03314, Um03313, Um02139, Um02140.2, Um02141) and subgroup III (Um02135 and Um02136) (Fig. 16). Relationships of some individual proteins in these groups could not be strongly resolved due to the very high similarity between closely related sequences.

2.2.1.2 Eff1 paralogs revealed in S. relianum

To gain insights into the putative function of family Eff1 proteins, all eleven amino acid sequences as well as identified motifs alone were used to screen the nonredundant National Center for Biotechnology Information (NCBI) protein database. Significantly, a BLASTp search against (NCBI) revealed no other proteins

sharing any of four discovered motifs. However, homology search in a close relative of *U. maydis*, *Sporisorium relianum* (G. Mannhaupt and R. Kahmann, personal communication), was able to detect ten homologous genes of family *Eff1*. Figure 22 shows a phylogenetic tree obtained from alignment of Eff1 proteins together with their paralogs from *S. relianum* genome.

Table 2. General characterization of Eff1 family proteins

Gene	Length, aa	Identity over the total length, %	Chromosomal location	Predicted size of signal peptide	Comments
um01796	430	100,0	Resides on chromosome 3	19	
um02138	447	42	Resides on chromosome 5	21	
um11377.2	385	41	Resides on chromosome 3 at a distance 0.43 Mb from *um01796* towards 3´ end of the chromosome	21	
um02137	487	24	Resides on chromosome 5	21	contains NLS
um03314	447	22	Resides on chromosome 8	19	contains NLS
um02139	450	21	Resides on chromosome 5	16	contains NLS
um03313	363	21	Resides on chromosome 8	19	
um02136	493	20	Resides on chromosome 5	21	
um02135	462	19	Resides on chromosome 5	22	
um02140.2	377	18	Resides on chromosome 5	24	
um02141	302	18	Resides on chromosome 5	22	

An alignment of all these proteins was analyzed by neighbor joining as well as parsimony with statistical confidence measured by bootstrap analysis. Relationships of individual proteins within two groups could not be strongly resolved due to the very high similarity among closely related sequences (Fig. 17). The composite tree reveals a number of interesting relationships (Fig. 17). Um02135 and Um02136 in contrast to other proteins in Eff1 family have no close orthologues in the genome of *S. relianum*. Subgroup III and subgroup II proteins have three and one orthologs in *S.*

relianum, respectively (Fig. 17, b, c). High values of bootstrap support suggest that the relationship within the two groups is a result of true phylogenetic signal.

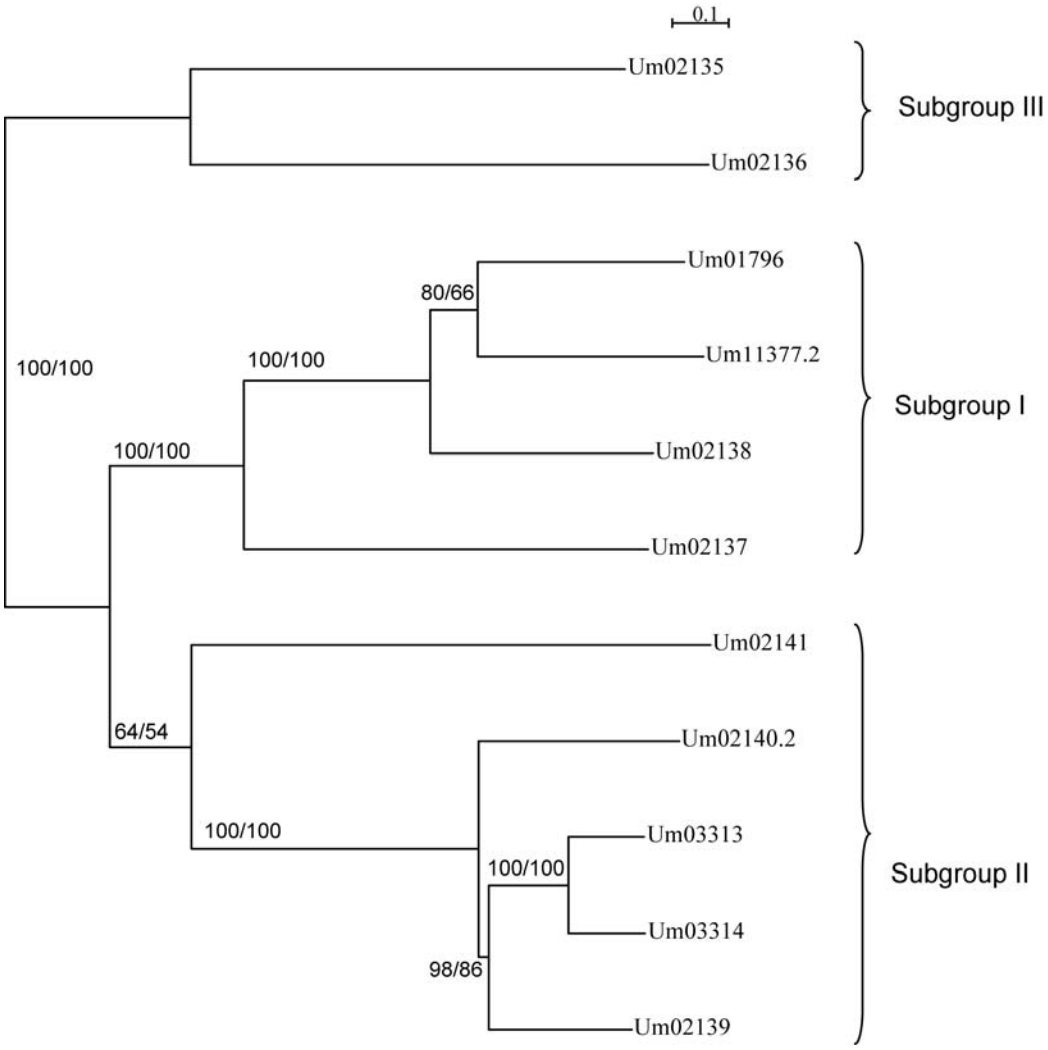

Fig. 16. Phylogenetic analysis of Eff1 proteins reveals subgroups. Amino acid sequences of full-length proteins were aligned using ClustalW program. The tree shown was derived by neighbor-joining distance analysis of eleven proteins using SeaView software (version 4.2.3). Bootstrap values (based on hundred bootstraps) are indicated above the nodes, with the number on the left for the neighbor joining and on the right for parsimony.

In *S. relianum*, eight of the ten proteins related to the Eff1 proteins contain a signal sequence. However, only one member of S. relianum family, Sr13382, contains putative NLS sequence.

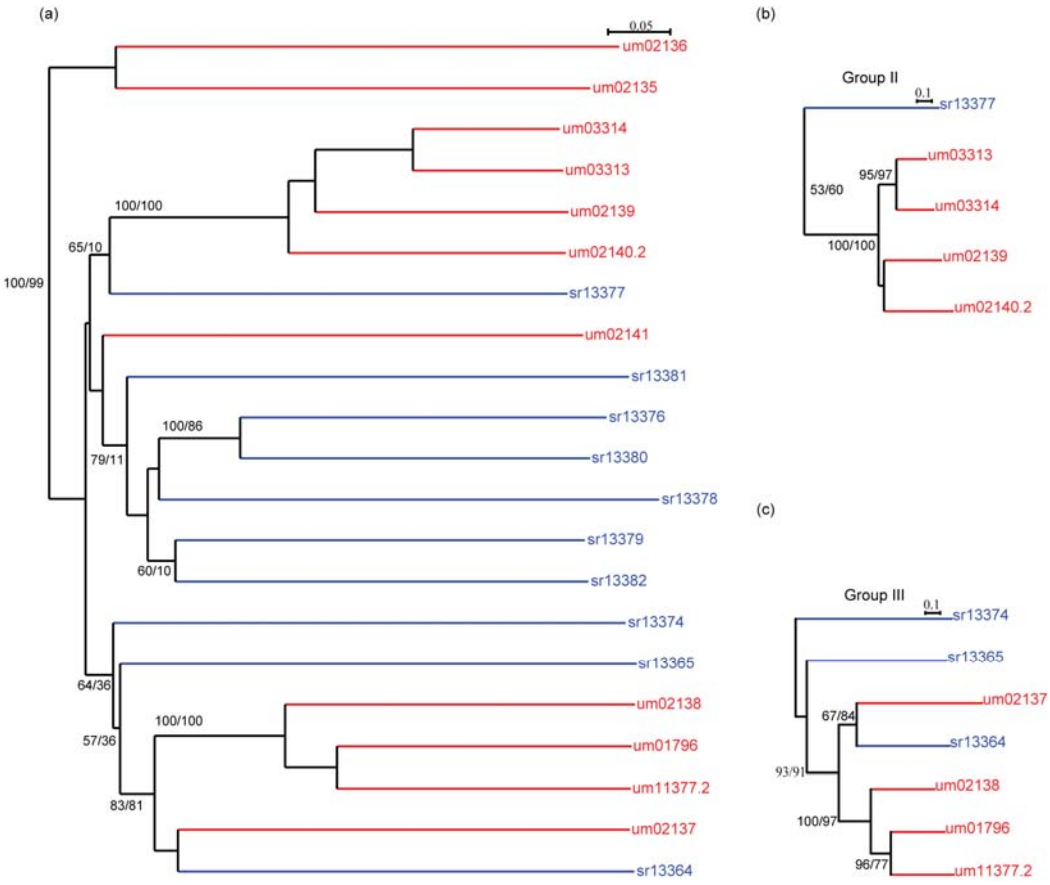

Fig. 17. Phylogenetic analysis of Eff1 proteins and their orthologs in *S. relianum*. a) The phylogenetic tree shown was derived by neighbor-joining distance analysis of eleven *U. maydis* Eff1 proteins as well as their ten orthologs in *S. relianum* using SeaView software (version 4.2.3). Bootstrap values (based on hundred bootstraps) are indicated above the nodes, with the number on the left for the neighbor joining and on the right for parsimony. Amino acid sequences of full-length proteins were aligned using ClustalW program. b), c) Relationships among sequences within two groups were further refined. *U. maydis* and *S. relianum* branches are highlighted with red and blue color, respectively.

2.2.2 Expression pattern of the family eff1 effector genes

The expression patterns of all members of the *eff1* family was analyzed by quantitative Real-Time-PCR during different stages of fungal development. Gene expression levels were quantified in reference to the constitutively expressed peptidyl-prolyl *cis-trans* isomerase gene *ppi1* (accession number EAK84904). During axenic growth of SG200 in YEPSL expression of the 11 *eff1* genes could not be detected. 24 hours after plant infection, a time point when *U. maydis* has developed appressoria and has begun to invade the host tissue (Mendoza-Mendoza *et al.*, 2009), expression of seven genes could be demonstrated (Fig. 18). At this time point the *um02141*

transcript was about 1000-fold up-regulated compared to the *ppi1* expression level. Over the next seven days of biotrophic growth expression levels of *um02141* decreased by 2-3 fold (Fig. 18). *um01796*, *um03313*, and *um02139* showed maximum transcript levels at 5 days post infection, while *um11377.2* and *um02140.2* demonstrated the highest expression levels at 3 days post infection. For *um02137* and *um02138* there was a continuous increase in expression over the period from 1 to 8 days post infection. Except for *um02129*, which was at most 5 fold upregulated, all other genes were at least 50- fold up-regulated at one of the chosen time points (Fig. 18). This illustrates that all members of this gene family are specifically expressed during the biotrophic phase and thus qualify to be called effectors. Accordingly, they were renamed *eff1-1* to *eff1-11* (Table 1).

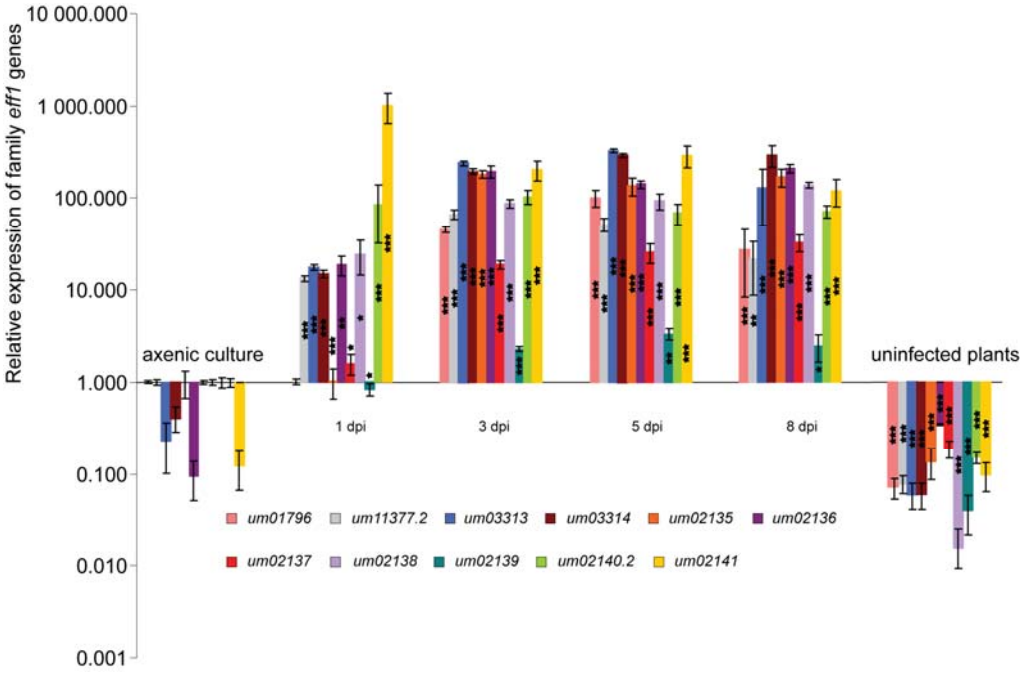

Fig. 18. Expression analysis of the family *eff1* genes by quantitative Real-Time-PCR. RNA was prepared from SG200 grown saprophytically in YEPSL liquid medium as well as from maize seedlings 1, 3, 5, and 8 days post infection. Expression levels of the *eff1* family genes was standardized relative to the constitutively transcribed *ppi* gene. Three biological replicates with two technical replicates each were conducted. Standard deviations are indicated. P-values calculated by Student´s t-test are shown as asterisks. Asterisks indicate significant differences relative to expression values in axenic culture. *, ** and *** represent P-values < 0.05, 0.01 and 0.001, respectively. Expression of the *eff1* genes was also tested in uninfected plant material (depicted on the right) and in this case P-values were calculated relative to expression values in infected plant material 5 days post infection (see Materials and Methods). The color code for individual genes is shown below.

2.2.3 The generation of mutants lacking members of eff1 gene family

To generate mutants lacking either all or different combinations of the genes constituting the *eff1* gene family we followed the scheme depicted in Fig. 19a using five successive rounds of FLP-mediated recombination (see Methods and Methods). This allowed us to generate strains SG200eff1Δ1, SG200eff1Δ1,2, SG200eff1Δ1,2,3,4, SG200eff1Δ1,2,3,4,7,8,9,10 and SG200eff1Δ1-11 (see Methods and Methods). In addition another five strains carrying different combinations of *eff1*

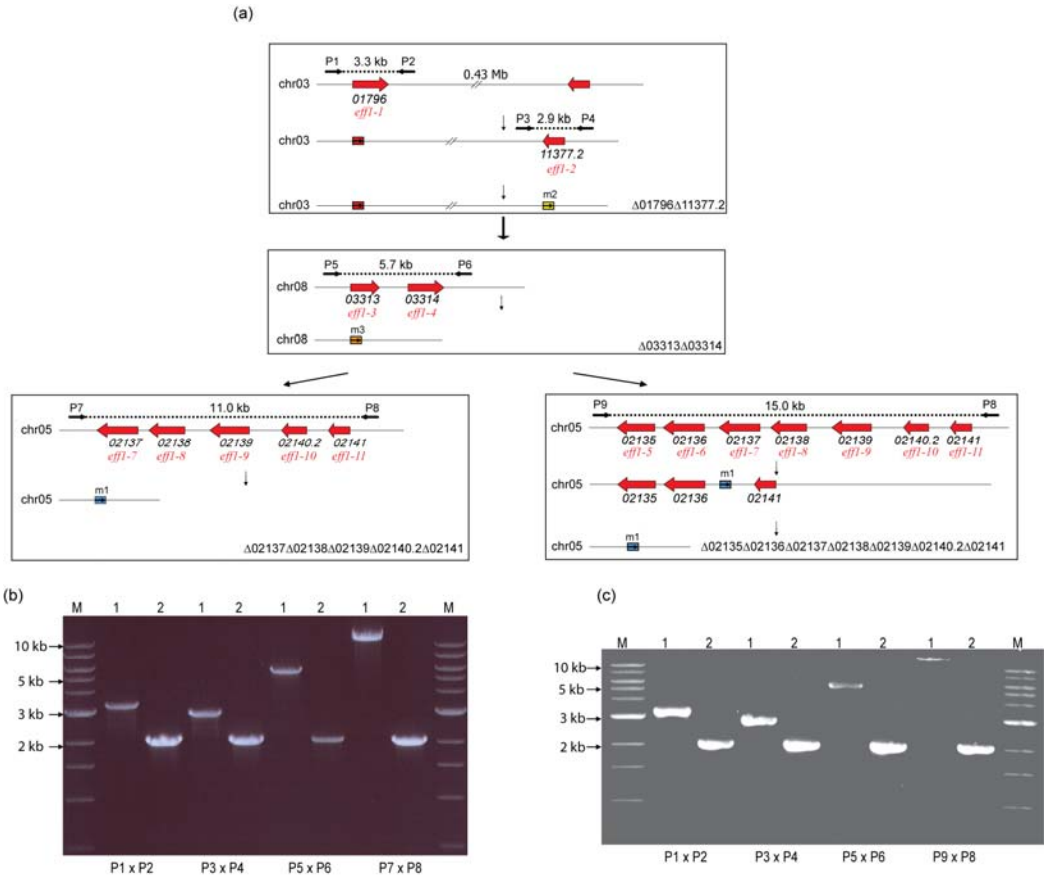

Fig. 19. Strategy for the construction of *eff1* deletion strains and their verification. a) The arrangement of family *eff1* genes on chromosomes 3, 8 and 5 is shown in the upper part of each panel. Below intermediate as well as the final structure of the respective chromosomes are shown. Wild type and mutant FRT sites remaining after excision are indicated in color. The binding sites of diagnostic primers and sizes of PCR fragments are indicated. b), c) Verification of all deletions in SG200eff1Δ1,2,3,4,7,8,9,10,11 and SG200eff1Δ1-11 respectively. DNA was prepared from SG200, SG200eff1Δ1,2,3,4,7,8,9,10,11, and SG200eff1Δ1-11 and diagnostic fragments were amplified from SG200 DNA (lanes 1) and SG200eff1Δ1,2,3,4,7,8,9,10,11 (lanes 2) in b) and SG200eff1Δ11 (lanes 2) in c; primer pairs used are indicated below. M = 1 kb ladder.

gene deletions were generated. These are strains SG200eff1Δ3,4, SG200eff1Δ1,8, SG200eff1Δ1,3,4,8, SG200eff1Δ1,2,7,8,9,10 and SG200eff1Δ1,2,3,4,7,8,9,10,11 (see Methods and Methods). In both SG200eff1Δ1,2,3,4,7,8,9,10,11 and SG200eff1Δ1-11 disruptions of all 11 genes was verified by PCR using primers that bind to the left and right borders of the segments which were deleted (Fig. 19).

2.2.4. Phenotypic analysis of eff1 mutants

To test the phenotype of mutants in which different combinations of *eff1* genes were deleted the mutant strains were grown on various stress media (sorbitol, sodium chloride, calcofluor, Congo red and H_2O_2). In no case could significant differences in growth between SG200 and mutants be observed (Fig. 20). In addition, all mutants developed vigorous filaments on CM-charcoal plates that was comparable to SG200 (Fig. 20). Next, the 10 strains carrying different deletion combinations of family *eff1* genes (see Materials and Methods) were tested for pathogenicity. It had been shown previously that virulence can be lost completely when a single effector gene, in this case *pep1*, is deleted in SG200 (Doehlemann *et al*., 2009). Compared to SG200 infections, significantly reduced virulence was observed when 9 or all 11 *eff1* genes were deleted (Fig. 21). In comparison to symptoms caused by SG200 two effects were seen with SG200eff1Δ1-11: on the one hand, the number of plants showing symptoms decreased from >95 %, to about 50 % and secondly, the symptom severity was reduced. In comparison, the symptoms (ligula swellings and small tumors) observed after infection with SG200eff1Δ1-11 and SG200eff1Δ1,2,3,4,7,8,9,10,11 were also significantly different, suggesting that the two genes from group III, *eff1-5* and *eff1-6* (Fig. 16) also contribute weakly to the phenotype of the 11 gene deletion strain. Compared to SG200eff1Δ1,2,3,4,7,8,9,10,11, SG200eff1Δ1,2,3,4,7,8,9,10 showed more large tumors and dead plants, suggesting that *eff1-11* is an important gene for tumor formation. SG200eff1Δ1,2 induced more chlorosis and less tumors, but no reduction in plants showing symptoms (still almost 100%). Thus, *eff1-1* and *eff1-2* are important for tumor formation and they explain the elevated amount of chlorosis in all strains where they are deleted. SG200eff1Δ1,2,3,4 and SG200eff1Δ3,4 were similar in type of symptoms, but they showed differences in the number of plants with symptoms, which was reduced in SG200eff1Δ1,2,3,4.

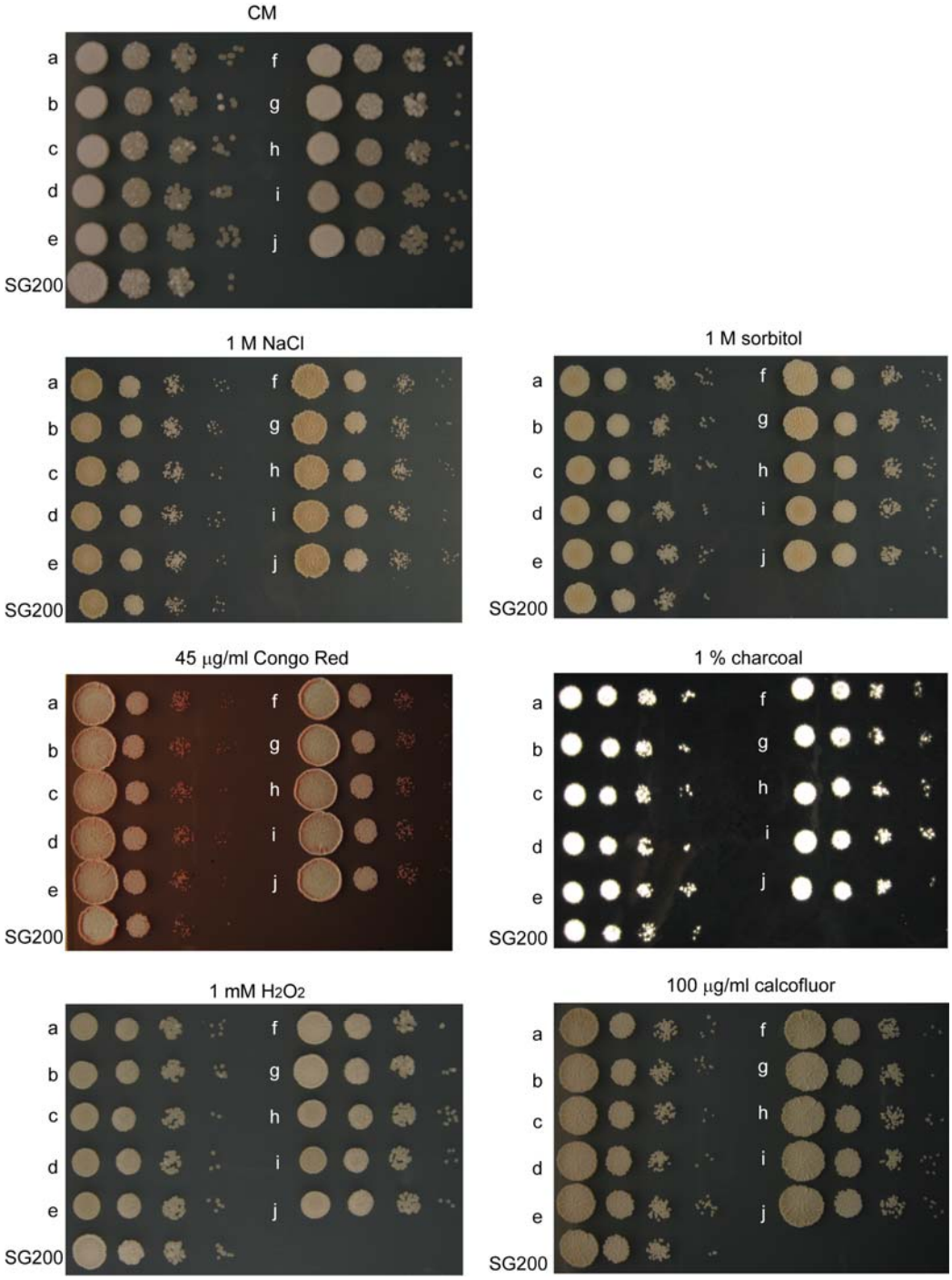

Fig. 20. Growth of SG200 and SG200eff1 mutant strains on different stress media. Drops (5 µl) of serial dilutions of SG200 and *eff1* gene deletion strains were spotted on PD medium supplemented with calcofluor white, sodium chloride, hydrogen peroxide, Congo red, sorbitol, and charcoal at the concentrations indicated.
a: SG200eff1Δ1,2,3,4; b: SG200eff1Δ3,4; c: SG200eff1Δ1,8; d: SG200eff1Δ1,2; e: SG200eff1Δ1; f: SG200eff1Δ1-11; g: SG200eff1Δ1,2,3,4,7,8,9,10,11; h: SG200eff1Δ1,2,3,4,7,8,9,10; i: SG200eff1Δ1,2,7,8,9,10; j: SG200eff1Δ1,3,4,8.

This shows again that *eff1-* and *eff1-2* positively contribute to virulence. Since SG200eff1Δ1,2,7,8,9,10 induced comparable symptoms to SG200eff1Δ1,2, there is no clear contribution of *eff1-7*, *eff1-8*, *eff1-9*, and *eff1-10* to virulence. SG200eff1Δ1,2,3,4,7,8,9,10 showed significantly decreased tumor symptoms compared to SG200eff1Δ1,2,7,8,9,10 (Fig. 21), suggesting a contribution of *eff1-3* and *eff1-4* to virulence. This conclusion was reinforced by the attenuated virulence seen after infection with SG200eff1Δ3,4 (Fig. 21).

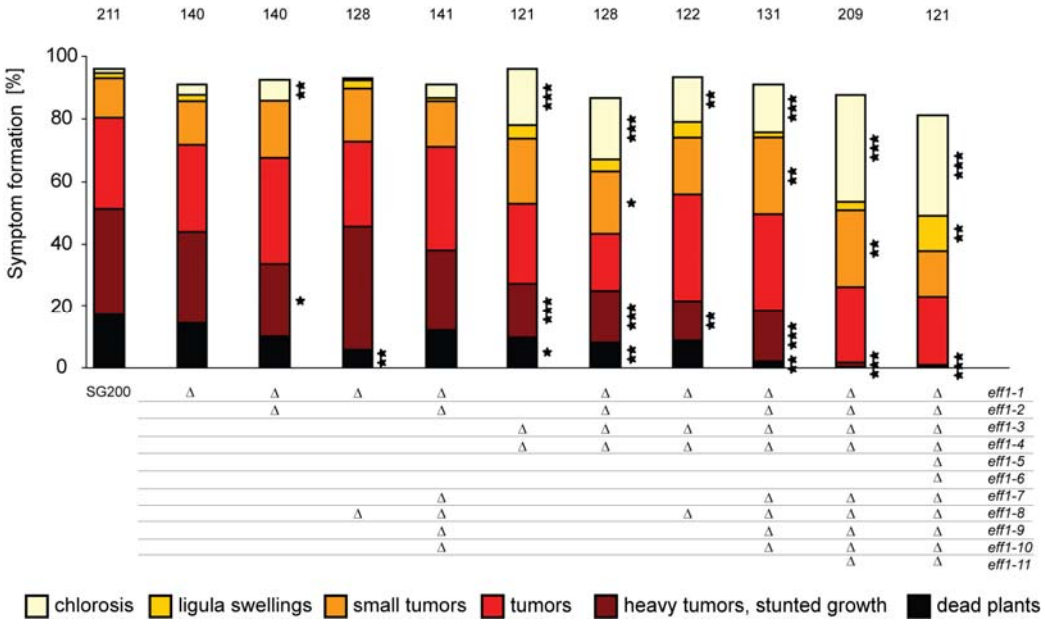

Fig. 21. Disease symptoms caused by SG200 and SG200 carrying different combinations of *eff1* gene deletions. For each strain three independent infections were performed and the total number of infected plants is given above each column. Symptoms were scored 14 days after infection and average scores from the three experiments are shown. To facilitate comparisons, the 11 *eff1* genes are listed on the right and their absence in individual strains is indicated by Δ. The color code for disease rating is given below. P-values are shown as asterisks. *, ** and *** represent P-values of < 0.05, 0.01 and 0.001, respectively, relative to symptoms caused by SG200.

To assess the contribution of individual *eff1* genes to the virulence phenotype several complementation strains were generated in which individual *eff1* effector genes were re-introduced into SG200eff1Δ1,2,3,4,7,8,9,10,11. Two strains carrying single copy integrations of *eff1-1* or eff1-8, respectively, were generated. Both strains showed

statistically relevant elevated virulence compared to the strain carrying nine *eff1* gene deletions with *eff1-1* showing stronger complementation than *eff1-8* (Fig. 22).

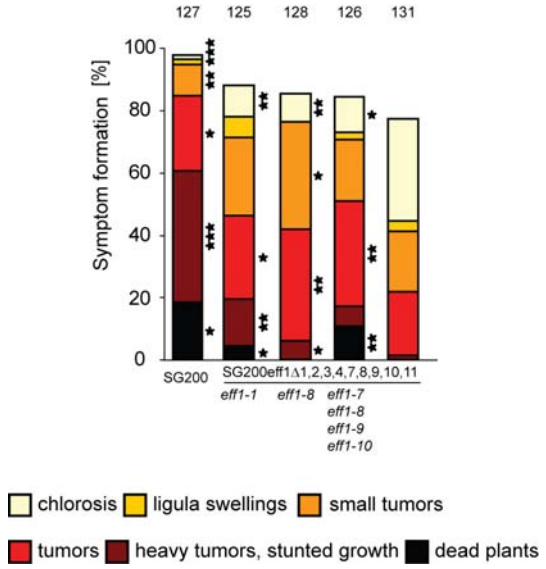

Fig. 22. Complementation of SG200eff1Δ1,2,3,4,7,8,9,10,11 with different *eff1* genes. Disease symptoms caused by SG200, SG200eff1Δ1,2,3,4,7,8,9,10,11 and three different complementation strains are shown. Genes reintroduced in SG200eff1Δ1,2,3,4,7,8,9,10,11 are listed below. The color code for disease rating is given below. P-values are shown. *, ** and *** represent P-values of < 0.05, 0.01 and 0.001, respectively, relative to symptoms caused by SG200eff1Δ1,2,3,4,7,8,9,10,11.

Additionally, a SG200eff1Δ1,2,3,4,7,8,9,10,11 strain was generated in which the four genes *eff1-7*, *eff1-8*, *eff1-9* and *eff1-10* were introduced in single copy, and this strain also showed statistically relevant increased virulence compared to the nine gene deletion strain (Fig. 22). Since the severely reduced virulence of the nine gene deletion mutant could be partially restored by complementation with all genes tested we assume functional redundancy within the *eff1* gene family.

Next, we performed confocal microscopy to visualize early infection-related development of SG200 and SG200eff1Δ1−11 strain 60 h after infection. To visualize hyphae, they were stained by WGA-AF488, plant structures were stained with propidium iodide. Confocal microscopy (in collaboration with Kerstin Schipper) revealed that the SG200eff1Δ1−11 mutant had colonized the plant tissue. With respect to With respect to development of branched hyphae no significant differences could

be observed compared to SG200 (Fig. 23). This indicates that at this stage there was no specific arrest of fungal development (Fig. 23).

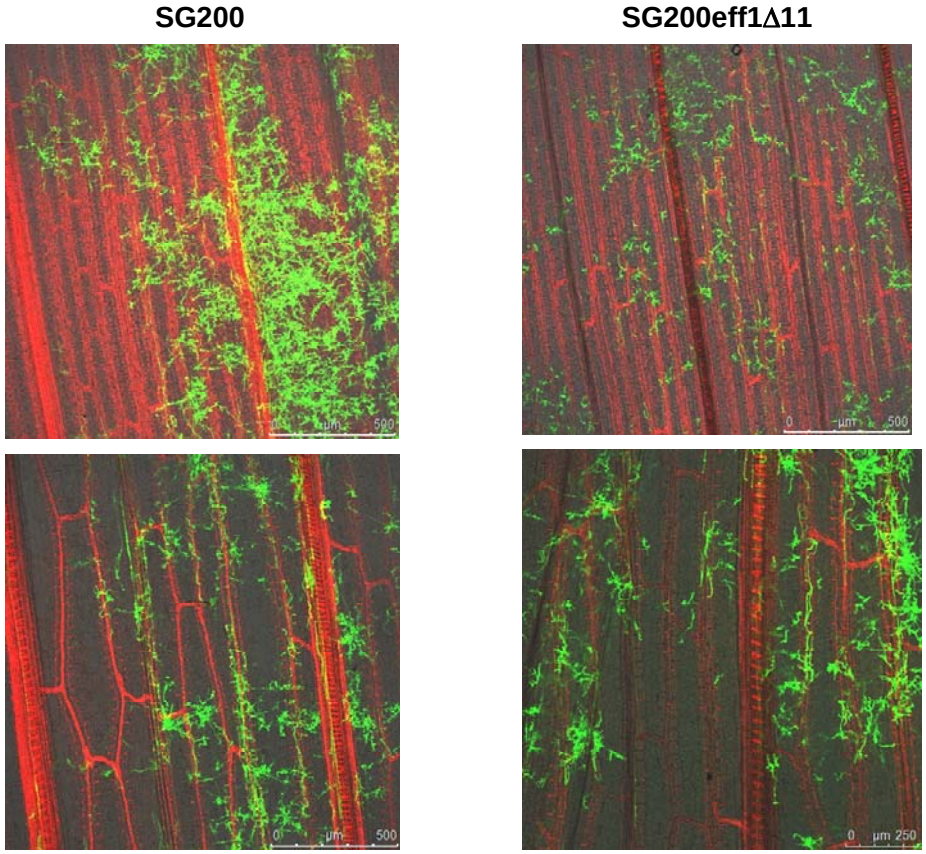

Fig. 23 Microscopic analysis of early infection-related development of *U. maydis* 11 gene deletion mutant SG200eff1Δ1−11. Pathogenic development of SG200 and SG200eff1Δ1−11 mutant were analyzed 60 h after infection. Confocal projections show fungal hyphae stained with WGA-AF488 (green) and plant cells stained with propidium-iodide (red). No significant difference could be visualized between colonization of the plant host by SG200 and mutant strain. The photos were made by Kerstin Schipper.

2.2.5 Eff1 nine gene deletion mutant affects plant hormone levels

Diseased plants often show phenotypes consistent with hormone perturbations (Grant & Jones, 2009). SA signalling and jasmonic acid (JA) can compromise each other (Koornneef & Pieterse, 2008). Because the balance between JA and SA can determine whether the plant succumbs to infection, selection favors pathogens that can affect this balance in their favour (Grant & Jones, 2009). Indeed, Doehlemann *et al*. revealed that after *U. maydis* infection, significant induction of 9 genes, annotated to be involved in JA biosynthesis and signalling, was detected already 24 hours past

infection (hpi) and high expression levels of host genes were maintained at later stages (Doehlemann *et al.*, 2008).

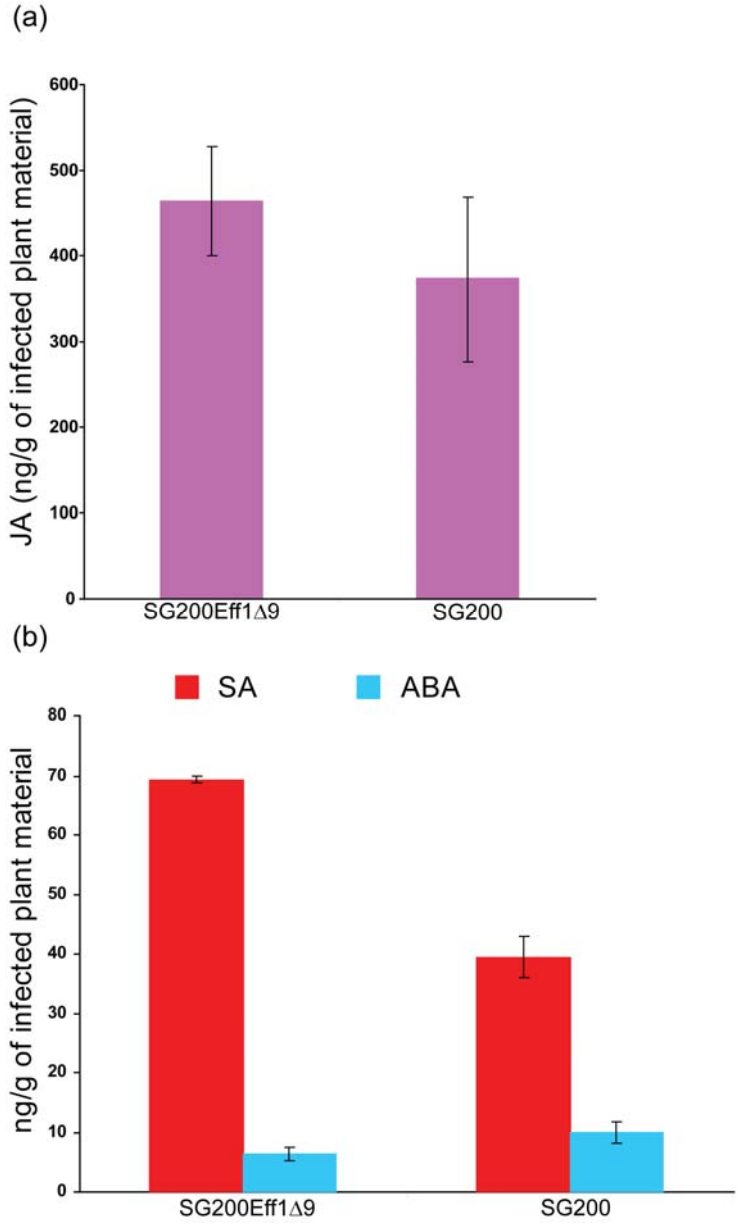

Fig. 24 Concentrations of plant hormones in plants infected by SG200eff1Δ1,2,3,4,7,8,9,10,11 (SG200eff1Δ9) and SG200. Bars indicate standard deviations. Leaf tissue was taken from plants 5 dpi. For each measurement, five biological replicates were used. a) Levels of jasmonic acid (JA). b) Levels of salicylic acid (SA) and abscisic acid (ABA).

To gain more insight of the plant responses induced by *eff1* genes, we tested levels of plant hormones in maize leaves infected by SG200eff1Δ1,2,3,4,7,8,9,10,11 (Table 3, see Materials and Methods) in comparison to SG200 (collaboration with Jinsong Wu). Concentrations of plant hormones, particularly JA, SA, and abscisic acid (ABA) were analyzed in infected leaf tissue five days past infection (dpi). Infection of maize with SG200eff1Δ9 resulted in 77% increase of SA levels indicating a "non-biotrophic" character of plant-mutant interaction (Fig. 24b). Additionally, in leaf tissue infected with SG200eff1Δ9 the level of ABA was slightly decreased (Fig. 24b). While the level of JA, however, was in the range of variation for both SG200- and SG200eff1Δ9-infected plants (Fig. 24a). Taken together, these data suggest that the mutant is affected in establishing a biotrophic interaction.

2.2.6. Lipid binding affinity and root uptake assays of the Um02137-GFP fusion protein

Recent work of Kale *et al*. showed that in order to translocate effectors into host cells, RXLR-like motifs in fungal effectors, such as AvrL567 from *Melampsora lini*, Avr2 from *Fusarium oxysporum* f. sp. *lycopersici*, and AvrLm6 from *Leptosphaeria maculans* bind to host cell surface phosphatidylinositol-3-phosphate (PtdIns-(3)-P) (Kale *et al.*, 2010). Indeed, phosphorylated derivatives of phosphatidylinositol (PI), collectively called phosphoinositides, play a fundamental part in controlling membrane–cytosol interfaces. Through interactions mediated by their headgroups phosphoinositides mediate regulation of membrane traffic, the cytoskeleton, nuclear events and the permeability and transport functions of membranes (Di Paolo & De Camilli, 2006). The possibility that *eff1* family effectors might enter plant cell via the same mechanism was explored using protein-lipid overlay (PLO) assays. Since Um02137 has an NLS sequence and contains the highest number of putative N-terminal RXLR-like motifs of two types (based on the consensus sequences derived from Tyler´s lab, B. Tyler, personal communication), we have chosen this effector as a primary candidate to test lipid binding.

The PLO assay enables the identification of the lipid ligands with which lipid binding proteins interact and provides qualitative information on the relative affinity with which a protein binds to a lipid. GST- and His-tagged Um02137-GFP fusion protein

was expressed in *E. coli* and purified by Ni^{2+}-NTA chromatography (see Materials & Methods). Purified GFP alone was used as a negative control (Fig. 25 c).

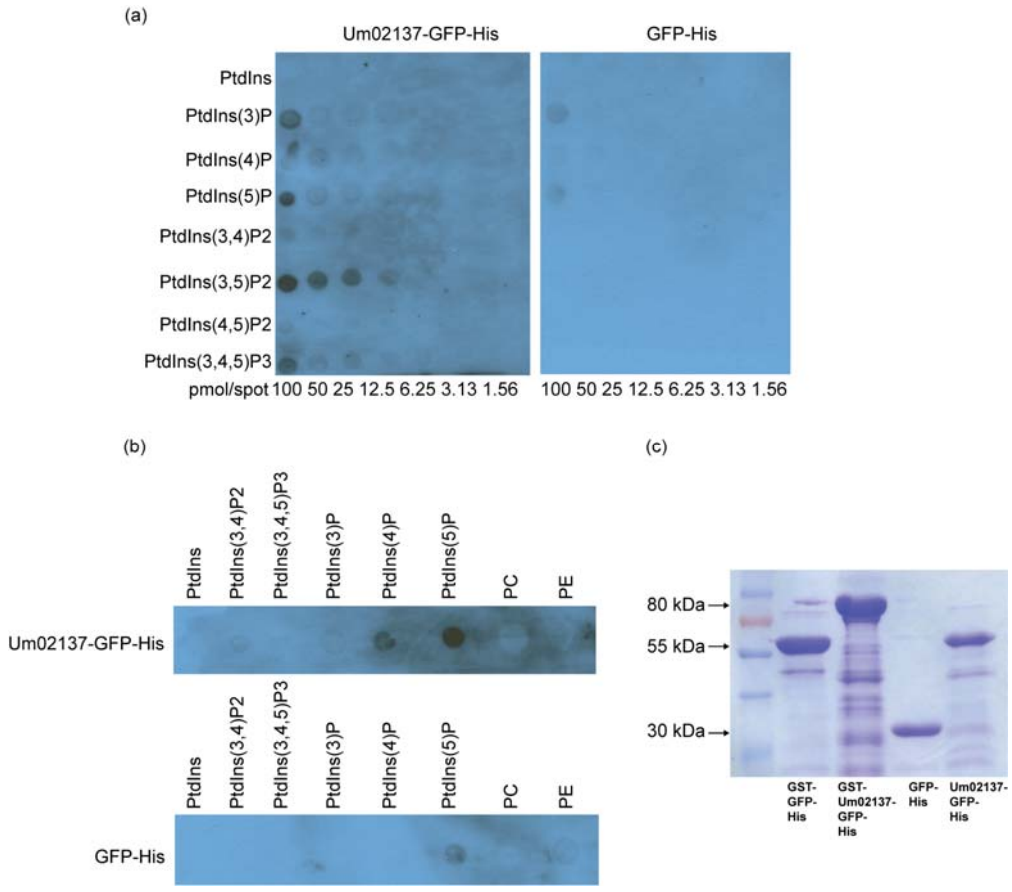

Fig. 25. Interactions of Um02137-GFP-His with lipids using the protein-lipid overlay (PLO) assay. The ability of GFP Um02137-His protein to bind various phospholipids was analyzed. Purified GFP served as negative control. Proteins were expressed in *E. coli* and purified by Ni^{2+}-NTA chromatography. PtdIns = phosphatidylinositol; PtdIns(3)P = phosphatidylinositol-3-phosphate; PtdIns(4)P = phosphatidylinositol-4-phosphate; PtdIns(5)P = phosphatidylinositol-5-phosphate; PtdIns(3,4)P2 = phosphatidylinositol-3,4-biphosphate; PtdIns(3,5)P2 = phosphatidylinositol-3,5-biphosphate; PtdIns(4,5)P2 = phosphatidylinositol-4,5-biphosphate; PtdIns(3,4,5)P3 = phosphatidylinositol-3,4,5-triphosphate; PC = phosphytidylcholine; PE = phosphatidylethanolamine. a) Serial dilutions (100, 50, 25, 12.5, 6.25, 3.13, 1.56 pmol) of the indicated phosphoinositides were immobilized on nitrocellulose membranes, which were then incubated with the indicated proteins. The membranes were washed and the proteins bound to the membrane by virtue of their interaction with lipid were detected using an antibody that recognizes the His tag. This PLO assay shows binding of the Um02137-GFP-His to different amounts (in pmol/spot) of the lipids, revealing specific affinity of Um02137-GFP-His to PtdIns(3,5)P2 and PtdIns(5)P. b) 1 µl of eight lipids (100 pmol) was spotted onto nitrocellulose membrane. This assay shows specific binding of Um02137-His to PtdIns(5)P and a weaker binding to PtdIns(4)P. c) Coomassie-stained SDS gel of GST-Um02137-GFP-His and GST-GFP-His proteins as well as Um02137-GFP-His and GFP-His proteins after removal of GST moiety by thrombin treatment.

To establish whether Um02137 has lipid-binding activity six phosphoinositides were tested, as well as phosphytidylcholine and phosphatidylethanolamine. Phosphoinositides were spotted onto a nitrocellulose membrane and incubated with 30µg of purified Um02137-GFP-His recombinant protein. Bound Um02137-GFP-His was then detected with His antibody and one spot yielded a signal, which corresponded to phophytidylinositol-5-phosphate (PtdIns-5-P). A weaker binding was shown also to phophytidylinositol-4-phosphate (PtdIns-4-P) (Fig. 25b). Experiments with serially diluted phosphoinositides further confirmed the specificity of the Um02137 binding to PtdIns-5-P, and additionally revealed a highly specific binding to phosphatidylinositol-3,5-biphosphate (PtdIns(3,5)P2) (Fig. 25a). Using such prespotted nitrocellulose arrays weak binding of Um02137 to phosphatidylinositol-3-phosphate (PtdIns(3)P) and phosphatidylinositol-3,4,5-triphosphate (PtdIns(3,4,5)P3) was also observed as well as weak non-specific binding of Um02137-GFP-His to PtdIns(3)P and PtdIns-5-P (Fig. 25a).

For the *P. sojae* Avr1b effector a root uptake assay was developed to demonstrate plant cell entry of, was described by Dou *et al*. (Dou *et al.*, 2008). Indeed, incubation of root tips of soybean seedlings for 12 h in a solution containing purified fusion protein Avr1b-GFP allowed to detect uptake of Avr1b-GFP up to 10 cell layers deep (Dou *et al.*, 2008). To perform such an assay root tips of soybean seedlings were incubated with the purified Um02137-GFP-His fusion protein for 12 h, washed for 2 h in water, and then observed by confocal microscopy to localize the GFP (Fig. 26a). As shown in Fig. 26, GFP accumulated inside many of the root cells, while GFP alone did not produce any fluorescence (Fig. 26b). In some cells Um02137-GFP is localized to the nuclei, indicating that the protein is located inside of plant cells and that the cells are alive (Fig. 26c).

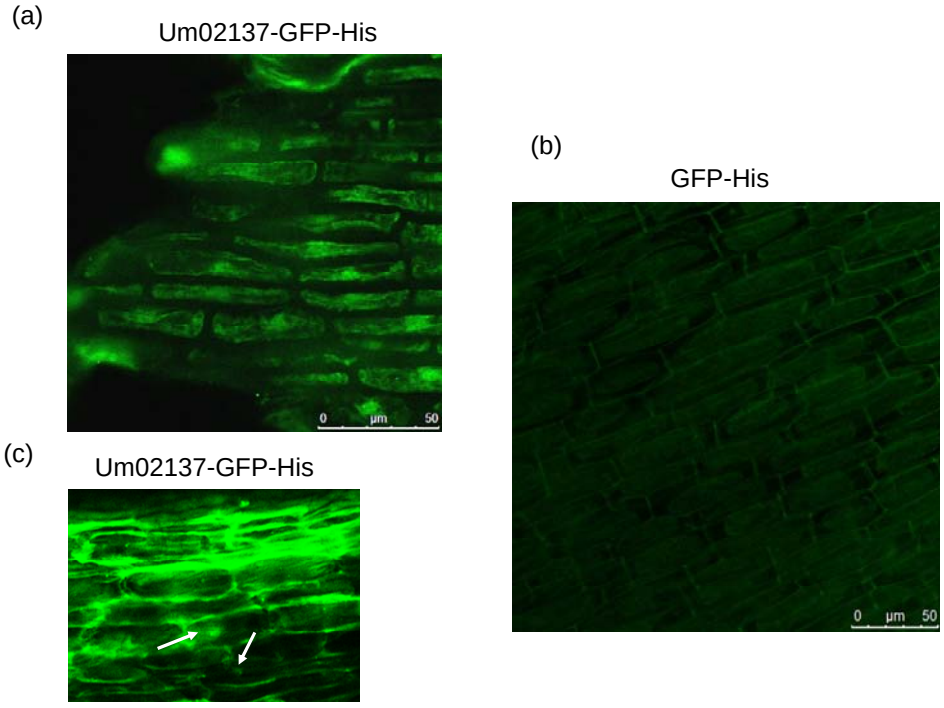

Fig. 26 Entry of Um02137-GFP-His fusion protein into soybean root cells. GFP-His was used as negative control. Proteins were expressed in *E. coli* and purified by Ni^{2+}-NTA chromatography. Root tips 1 cm long were completely submerged in protein solution (5 mg/mL) for 12 hr, then washed for 2 hr. Arrows indicate fluorescent plant cell nuclei. Fluorescent images of the Um02137-GFP-His (a, c) and GFP-His (b).

3. Discussion

In this thesis the FLP-mediated recombination system was successfully established in *U. maydis* and subsequently used to delete a gene family consisting of 11 effector genes in 5 consecutive recombination rounds. Deletion mutants lacking more than eight genes were significantly reduced in virulence.

3.1 Features of the FLP-recombination system in *U. maydis*

3.1.1 Efficiency of the FLP-mediated recombination in U. maydis

In this thesis, we provide several direct lines of evidence demonstrating that FLP recombinase from the 2 micron plasmid of *Saccharomyces cerevisiae* stably or transiently expressed in *U. maydis* efficiently catalyzes site-specific excision of DNA segments. Since it was known that optimizing the codon usage can overcome failure or poor expression of heterologous genes in *U. maydis* (Zarnack *et al.*, 2006), expression was attempted in this study from a codon-optimized FLP gene. Indeed, although codon bias is not the only factor involved in protein expression, it has become increasingly obvious that codon biases can have a significant impact on the expression of heterologous proteins (Kane, 1995). Application of a context-dependent dicodon usage strategy was successful for all heterologous genes tested in *U. maydis* so far. Such examples include *Tc1* and *Mos1* from *Caenorhabditis elegans* and *Drosophila mauritiana*, respectively (Ladendorf, 2003), *tetR* repressor gene from *E. coli* (Zarnack *et al.*, 2006) as well as the activation domain of the herpes simplex virus *VP16* (M. Treutlein & J. Kämper, unpublished). Codon-optimization of the FLP gene has been applied to improve the efficiency of FLP-mediated recombination in several species. For example, Song and Niederweis adapted the FLP codon usage to that preferred by *Mycobacterium tuberculosis*; this increased the G/C content from 37% to 61% (Song & Niederweis, 2007). Expression of such a codon-optimized FLP increased the frequency of deletion of an FRT-*hph*-FRT cassette in *Mycobacterium smegmatis* by more than 100-fold (Song & Niederweis, 2007). Likewise, (Fladung *et al.*, 2009) demonstrated that by increasing the G/C content of FLP to 55%, it was possible to enhance FLP expression up to 22-fold in maize zygotic embryos.

Therefore, to guarantee expression of FLP in *U. maydis* a codon-optimized FLP gene was engineered *de novo* and placed under control of arabinose-inducible *crg1*

promoter. Similar to synthetic FLP generated for *M. tuberculosis* (Song & Niederweis, 2007), alterations of the FLP sequence for the expression in *U. maydis* led to an increase in G/C content from 37% in its native form to 60% in the synthetic version, somewhat above the average G/C content of 54% in *U. maydis* (http://www.broadinstitute.org/annotation/genome/ustilago_maydis.2/GenomeStats.html). Expression of the codon-optimized FLP mRNA could be visualized after an 1 h shift to complete medium containing 1 % arabinose. The *crg1* promoter proved to be sufficiently tight as without induction of FLP only 1.8% of the colonies had lost the FRT-flanked DNA segment.

FLP-mediated recombination was assayed via a genetic screen as well as by PCR. FLP efficiently catalyzed site-specific recombination on the extra-chromosomal target as well as between FRT sites located in the genome. The FLP gene could be either expressed transiently or after stable integration into the *ip* locus of the *U. maydis* genome. FLP-mediated recombination on the extrachromosomal target varied from 52% to 83%. Likewise, efficiency of FLP-mediated recombination of the FRT-flanked DNA segment in the genome ranged from 57% to 79% when FLP was expressed from the genomic locus and from 66% to 75% for transiently expressed FLP encoded by the self-replicating plasmid pFLPexpC. Such results are consistent with studies of O'Gorman *et al.*, who reported 70 - 80% genomic recombination events in mammalian cells transiently transformed with a FLP gene (O'Gorman *et al.*, 1991). A FLP-mediated recombination efficiency of nearly 100% was reported by Kondo *et al*. for mouse embryonic stem cells where FLP was delivered by an adenovirus vector (Kondo *et al.*, 2006). In contrast, FLP-mediated deletion of an FRT-*neo*-FRT cassette in maize cells under transient expression conditions for FLP was only 2-3% (Lyznik *et al.*, 1996). A dramatically low FLP-mediated excision efficiency of the FRT-flanked segment from the genome in *S. cerevisiae* was reported by Storici *et al*.: depending on the plasmid delivering FLP recombination frequency varied from 0.09% to 0.1% (Storici *et al.*, 1999).

3.1.2 FLP-mediated marker recycling in U. maydis

The multiple gene disruption system for *U. maydis* presented in this study allowed for effective and standardized generation of multiple gene disruptions by a simple repetitive procedure using a FRT-*hph*-FRT cassette for FLP-mediated removal of the

selectable *hph* marker. The scheme for the FLP-mediated marker recycling consisted of three main steps: i) the generation of a deletion mutant in which the selectable marker introduced is flanked by directly oriented FRT sites, ii) the introduction of an inducible FLP gene on an autonomously replicating plasmid and iii) the induction of FLP expression and the subsequent screening for the loss of the selectable marker as well as the FLP donor plasmid. The system was highly efficient and 21 ± 8 % of the single colonies grown up after 16 h induction of FLP from the autonomously replicating plasmid pFLPexpC had lost the chromosomal marker flanked by FRT sites as well as the FLP donor plasmid.

FLP-mediated excision of the FRT-*hph*-FRT resistance cassette leaves a "scar" containing an FRT site; the length of such "scar" is dependent on the source of the FRT sites, but is usually less than 90 bp (Schweizer, 2003). In this study, the length of an FRT "scar" is 65 bp. These "scars" could be problematic after subsequent expression of FLP and undesirable inter- and intramolecular recombination events between identical FRTs at different loci might result by FLP action (Datsenko & Wanner, 2000). From an extensive *in vitro* and *in vivo* characterization of FLP-mediated recombination it is known that DNA heterology between the core regions of two FRT sites abolishes their ability to recombine. However, mutations are tolerated within the FRT sequences as long as the two recombination sites harbor identical alterations in core regions (Andrews *et al.*, 1986; McLeod *et al.*, 1986; Senecoff *et al.*, 1988; Symington, 1997; Storici *et al.*, 1999). Therefore, to avoid possible chromosome rearrangements between FRT "scars" it is necessary to introduce point mutations into the FRT core regions. Based on these properties of FLP/FRT system I have designed four additional FRT sequences, each carrying a point mutation in the core region. If the wild-type FRT cassette is used in the first round of gene deletion, then the hyg resistance marker in the second round of allelic replacement should be flanked by two identical FRTs with different core region sequences. Respective allelic replacement vectors based on the *hph* resistance cassette were generated. For efficient application of the FLP-mediated marker recycling all FRT-*hph*-FRT cassettes were flanked by *Sfi*I restriction enzyme sites for compatibility with the gene replacement system developed previously for *U. maydis* (Brachmann *et al.*, 2004; Kämper, 2004). In our recombination assays on core-mutated FRT sequences to test the frequency of recombination within the mutated FRT pairs (as detected by loss of *hph* resistance)

we found frequencies from 14% to 42%, while the frequency for the wild-type FRT sites was 68%. Such frequencies are high enough to screen relatively small numbers of clones for the loss of *hph* resistance. For all such FRT sites it was demonstrated that they failed to recombine with wild type FRT sites while recombination could be detected in a strain where two identical FRT sites resided on the same chromosome but were 0.43 Mb apart. Apparently such a large distance did not prevent FLP-mediated recombination to occur. Indeed, several cases for FLP-mediated recombination on distantly located FRT sites have been described. For example, in *Pseudomonas aeruginosa,* FLP catalyzed the inversion of a 1.59 Mb fragment at high frequencies (83%) (Barekzi *et al.*, 2000). In *Salmonella enterica*, the FLP/FRT system was applied to delete a large genomic island of 43 kb in size (Doublet *et al.*, 2008).

For future use I have advanced the system in such a way that the inducible FLP gene can become an integral part of the cassette used to generate the deletion. A considerable advantage of using such cassette on the pYUIF-FRTm2 plasmid is that it alleviates the introduction of the plasmid harboring FLP after each round of recombination event. Given that when FLP expression was uninduced only 1.8% of FRT-flanked DNA segments were recombined, this frequency is low enough to verify gene disruption by Southern analysis without facing the problem of premature excision of the FRT-*hph*-FRT cassette by FLP recombinase. Following growth of strains in the medium containing arabinose to induce FLP expression, FLP catalyzes the excision of the FRT-flanked *hph* resistance cassette including its own coding sequence. This gene disruption system will significantly accelerate strain constructions in the future. Such autoexcision gene disruption cassettes were also tested for several other species. For example (Fladung *et al.*, 2009) designed a deletion construct for gene disruptions in hybrid aspen, which harbors FRT-flanked FLP gene together with *nptII* resistance marker under control of the heat-inducible *Gmhsp17.5-E* promoter from soybean FLP-mediated recombination efficiency using such construct was 65% in hybrid aspen. Likewise, (Reuss *et al.*, 2004) have generated a deletion cassette for *Candida albicans*, where in addition to the MPA resistance marker a *C. albicans*-adapted FLP gene was placed under control of the inducible *SAP2* promoter.

Taken together, the FLP-mediated gene disruption protocol described in this thesis has been applied to more than 20 strains, with the desired excision events observed in all that had lost the *hph* gene. None of the strains generated by several rounds of FLP-mediated recombination showed morphological defects and all of these strains developed vigorous filaments and were comparable to the progenitor strain with respect to growth under oxidative stress, cell wall stress, and osmotic stress. This makes it likely that such strains are stable and are unlikely to have acquired additional mutations, a prerequisite for assessing small virulence phenotypes of redundant genes. Thus, the FLP/FRT system is well suited for high frequency resistance marker excision in *U. maydis*. Considerable advantages, such as high accuracy and efficiency, make the FLP/FRT system an important tool in the genetic engineering of *U. maydis*. The use of FLP/FRT system could potentially be used for controlling gene expression in a temporal "off-on" manner. We expect that the establishment of the marker recycling system developed here will pave the way towards functional analysis of effector gene families as well as serving as a general tool to improve genetic manipulations in this fungus.

3.2. The *eff1* gene family in *U. maydis*

3.2.1 Characteristics of the eff1 gene family

In this thesis I have analyzed the impact of an *eff1* gene family coding for 11 secreted proteins with unknown function on virulence. All Eff1 proteins have the same architecture, consisting of an N-terminal signal sequence, a central region predicted to be natively unstructured, and a conserved C-terminal domain, which presumably represents the only folded part of these proteins (Fig. 15). We also note that in group II sequences, the central region predicted to be natively unstructured contains a conserved segment with an area of elevated helical propensity, which is duplicated in Um02139 and Um03314 (Fig. 15b). This region is quite abundant in negatively charged amino acids as well as polar hydrophilic amino acid residues, especially glutamine and serine (Fig. 15b). Database searches with the conserved C-terminal domain identified in this protein family (Fig. 15) did not produce any statistically significant matches. However, orthologs to the *eff1* genes were found in *Sporisorium reilianum*, the cause of head smut in maize (J. Schirawski, G. Mannhaupt and R. Kahmann, unpublished) and *Ustilago scitaminea*, the cause of sugarcane smut (G. Mannhaupt and R. Kahmann, unpublished) which makes it likely that this effector

family is smut specific and is not involved in determining host range. Notably, all ten *eff1* related genes identified in *S. relianum* reside in a cluster, which is syntenic with the *U. maydis eff1* large cluster on chromosome 5. Sequence comparisons between Eff1 proteins showed that the family forms three subgroups similar to the results of phylogenetic analysis (Fig. 27), group I comprising Um01796, Um11377.2, Um02137 and Um02138; group II Um02139, Um02140.2, Um02141, Um03313 and Um03314; and group III Um02135 and Um02136. Group III sequences are highly divergent, yet should be counted as true Eff1 homologs based on the following observations: (1) they make multiple, statistically significant connections to other Eff1 proteins in HMM comparisons (Fig. 27), (2) they are bidirectional best hits to the other Eff1 proteins in sequence searches by HMM, (3) they have the same domain structure as other Eff1 proteins (Fig. 27), and (4) they are located directly adjacent to the main cluster of Eff1 proteins on chromosome 5. Group III genes are not detected in *S. relianum* suggesting that this may be related to a species-specific evolutionary process. The fact that 9 of the 11 *eff1* genes reside in two clusters in the genome supports the assertion that they have originally arisen by a local gene duplication mechanism followed by rapid diversification and dispersion to other chromosomes. Given that Um03314 and Um02139 contain additional duplicated motifs in the N-terminal part separated by a conserved NDQTH amino acid stretch it is tempting to assume that duplication must have occurred in Um02139 and a duplicated copy of both Um02139 and Um02140 was translocated to chromosome 8 giving a rise to Um03313 and Um03314. The large *eff1* gene cluster on chromosome 5 is heterogeneous and contains genes from three different *eff1* groups (Fig. 30a).

Intriguingly, the two dispersed copies on chromosome 3 are closely related to each other as well as to the two adjacent genes *um02137* and *um02138* in the large cluster on chromosome 5. In addition, the two adjacent copies on chromosome 8 are closely related to each other and to the adjacent genes *um02139* and *um02140* in the large cluster on chromosome 5. It will be very interesting to analyze the number, distribution and groups of *eff1* effector genes in geographically distinct isolates of *U. maydis* as this might provide insights into the evolutionary fate of the clusters as well as the dispersed copies.

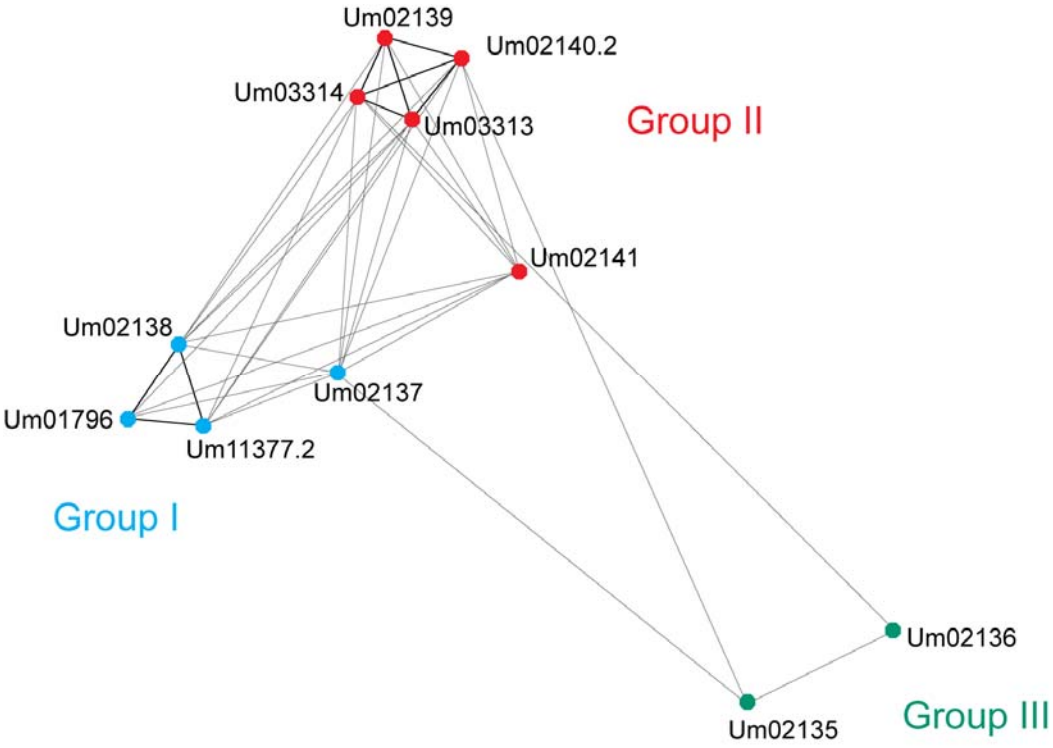

Fig. 27. Cluster map of Eff1 proteins (made by Prof. Dr. A. Lupas). Sequences were compared with BLAST, seeded randomly in space, and connected by forces proportional to the significance of their pairwise BLAST matches. The map was then equilibrated to convergence in a force-directed manner. BLAST matches at a P-value of 1.0 or better are shown as grey lines. Three groups of sequences are apparent, colored red, blue and green in the map. Group III is the most distant and looses connection to the other groups at a P-value cut-off of 1e-03. Groups I and II loose connection to each other at a cutoff of 1e-09. Eff1 proteins are labelled by their respective um numbers as well as by their *eff1* gene numbers.

Given that in *S. relianum* all ten *eff1* homologous genes reside in one cluster that is syntenic to the cluster on chromosome 5 of *U. maydis*, and is also heterogeneous and comprises orthologs of subgroups I and II, one could speculate that *U. maydis* and *S. relianum* evolved from a common ancestor and *um02135* and *um02136* appeared later following duplications and subsequent translocations in the large cluster on the chromosome 5 of *U. maydis*. Indeed, it has been hypothesized that duplications may confer a selective advantage since the duplicated locus would be more tolerant to deleterious mutations due to the functional redundancy created by the extra gene copy (James *et al.*, 2006). Thus, functional redundancy may foster rapid evolution of the

parasite to overcome host defense responses by allowing effector genes to become inactivated without compromising parasite fitness (Birch *et al.*, 2008; Kvitko *et al.*, 2009). On the other hand, duplications of an ancestral gene, followed by mutation could enable members of the gene family to take over new functions (Soanes *et al.*, 2008). For example, a large family of *Phytophthora infestans* RXLR effector genes show evidence of high rates of turnover: only 16 of the 563 genes were in 1:1:1 orthology relationships with genes in *Phytophthora sojae* and *Phytophthora ramorum* and many (88) are putative RXLR pseudogenes (Haas *et al.*, 2009). In *P. infestans*, fast-evolving effector gene families are localized to highly dynamic and expanded genomic regions (Haas *et al.*, 2009). Notably, some parasite effector genes are found in the proximity of transposable elements (TEs), which have been postulated to provide a mechanism for their expansion and movement within and among genomes (Sacristan & Garcia-Arenal, 2008). For example, in *Blumeria graminis*, the AVR_{k1} effector family has coevolved with a particular family of LINE-1 retrotransposons, named TE1a (Sacristan *et al.*, 2009). Examination of the flanking regions of *eff1* genes revealed no repetitive sequences. Indeed, the *U. maydis* genome is relatively devoid of transposable elements, in particular, no class II DNA elements or otherwise active endogenous elements could be found (Ladendorf, 2003; Kämper *et al.*, 2006). Sequencing of *U. maydis* genome showed that in contrast to most other fungi only 1.1% of the assembly consists of mostly non-functional, transposon-derived sequences (Kämper *et al.*, 2006). It may be possible that ectopical duplication of the heterogeneous cluster of *eff1* genes was mediated by previously active transposons which were lost during the evolution process. In this respect it will be very interesting to analyze the distribution of *eff1* family effectors in *U. hordei* which is rich in repetitive DNA. The annotation of its genome is currently in progress (R. Kahmann, personal communication).

3.2.2. Motifs in Eff1 family proteins

Comparisons based on alignments of all the Eff1 protein sequences using the ClustalW software and searches for conserved motifs employing the MEME program have revealed that the members of this family are highly divergent but show conserved motifs present in all or in only some alleles within the conserved C-terminal domain (Fig. 28).

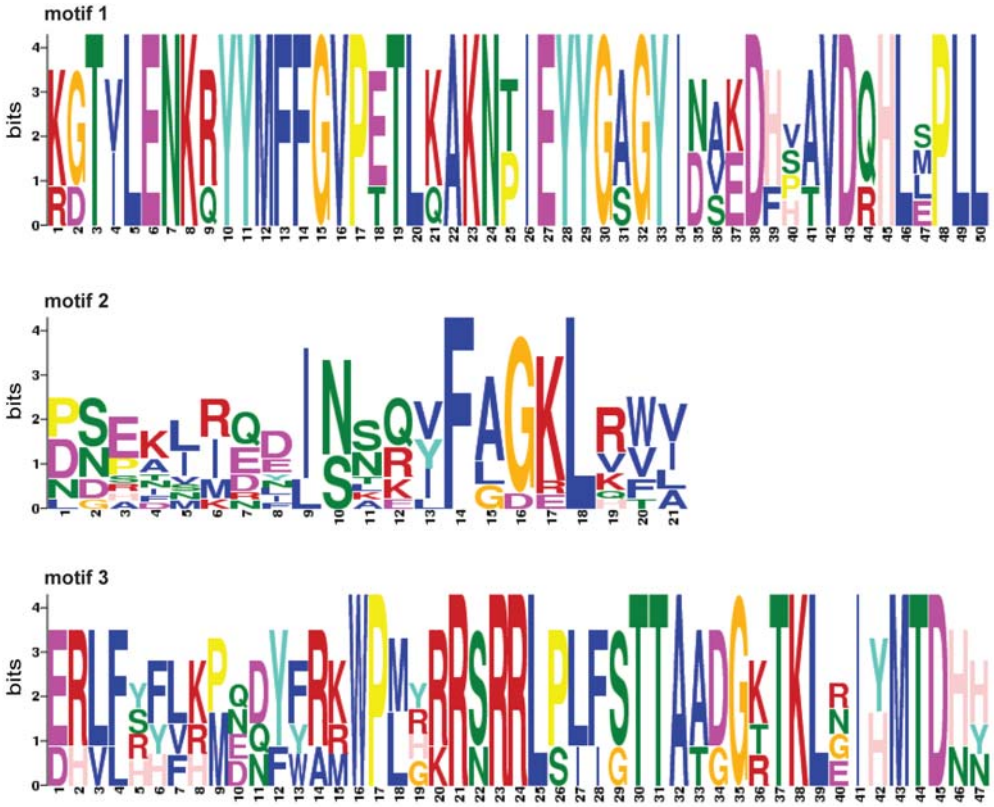

Fig. 28. Sequence logos of 3 motifs identified in Eff1 family proteins. Sequence logos were used to generate consensus sequence diagrams indicating the prevalence of amino acids at specific positions in each motif. Sequence logos were generated using a hidden markov model based program named multiple em for motif elucidation (MEME) version 4.3.0. All amino acid residues are shown according to the standard MEME color code: hydrophobic residues are blue (A, C, F, I, L, V, W, M); polar, non-charged, non-aliphatic residues are green (N, Q, S, T); acidic residues are shown in magenta (D, E); positively charged residues such as K and R are red, and H is shown in pink. G, P, and Y are drawn with orange, yellow, and turquoise, respectively. 4 bits correspond to 100 % conservation.

The presence of motif 2 in all 11 *eff1* genes most likely indicates that this motif adopts a defined structure that is sensitive to mutation. Motif 1 and motif 3 consist of strictly conserved as well as highly prevalent residues. For example, in motif 1 70% of amino acid residues (35 out of 50) are strictly conserved. Most noticeable is the strict conservation of tyrosine residues at positions 10, 11, 28, 29, and 33. Additionally, 51% of the conserved residues are hydrophobic amino acids. Sequence logo analysis of motif 3 revealed a frequent occurrence of well conserved positively charged amino acid residues, especially arginine with adjacent hydrophobic regions. Five strictly conserved positively charged amino acid residues are located at positions 20, 21, 23, 24 and 38 of the motif, respectively. Motif 2 has limited sequence conservation with notable exception of phenylalanine and leucine located at positions 14 and 18 (Fig.

28). In addition, motif 2 contains two strictly conserved hydrophobic residues at positions 15 and 16 together with a well conserved positively charged residue (mostly lysine) at position 17. This FAGKL-like motif is well conserved in all eleven protein sequences, which is also visible in the ClustalW schematic alignment data (Fig. 27b). It is also conserved within *S. reilianum* homologues of Eff1 proteins indicating that it most likely plays an important role in the function of *eff1* gene family members. There are also five sites in motif 2 where the chemical properties of the residues such as hydrophobicity, charge, and side chain structure are conserved. Motifs 1 and 3 are present only in subgroup II members of *eff1* gene family. Summarized data on relative location of MEME-based identified motifs is shown in Fig. 29.

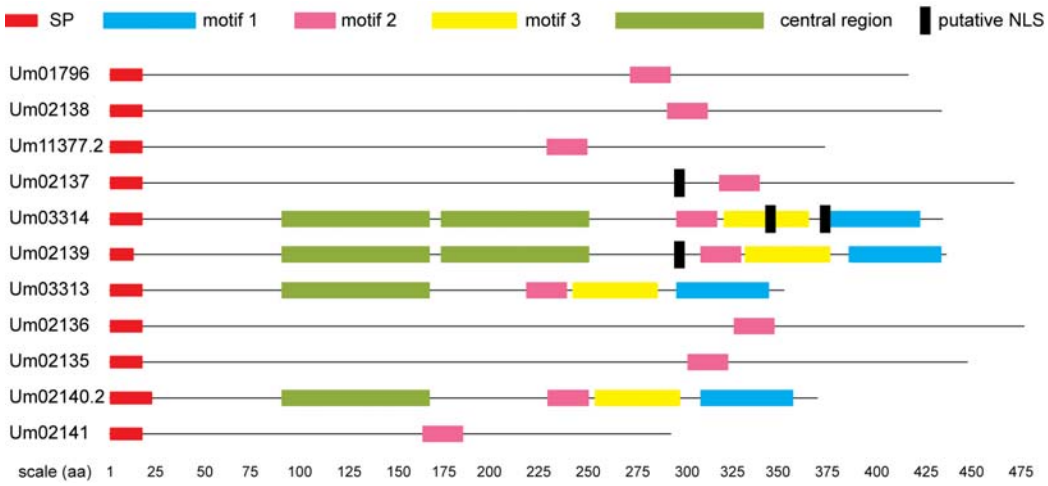

Fig. 29. Domain location of Eff1 family proteins. The relative positions of conserved motifs in Eff1 proteins are shown to scale. The motifs are highlighted in color following the scheme above. SP marks the signal peptide. Conserved central region (see Fig. 15) is shown in green. Putative NLS sequences are depicted in black.

Database searches with the three conserved motifs identified in this protein family (Fig. 28) did not produce any hits. Therefore, predictions on the function of Eff1 proteins remain highly speculative. At the same time the modular structure of the Eff1 proteins (Fig. 29) is somewhat reminiscent to the K, W and Y motifs found in the C-termini of a large percentage of *Phytophtora sojae* and *P. ramorum* RXLR-dEER effectors that have been assembled in the Avh superfamily (Dou *et al.*, 2008; Jiang *et al.*, 2008). In *P. sojae*, such C-terminal motifs are involved in interaction with cognate

resistance (R) genes and in suppression of host programmed cell death (Dou *et al.*, 2008).

3.2.3 Putative NLS sequences in Eff1 proteins

Based on the program "PredictNLS" analysis Um02137 and Um02139 contain putative monopartite nuclear localization signals (NLS), and these are located in conserved C-terminal domain of the respective proteins. A putative bipartite NLS sequence consisting of two stretches of basic amino acids was detected in Um03314 (Fig. 29). The presence of these putative NLS sequences could indicate that these proteins are translocated to plant cell and manipulate plant gene expression to ensure pathogenic development of *U. maydis*. Indeed, nucleocytoplasmic trafficking plays a key regulatory step in ETI and basal plant resistance. For example, Burch-Smith *et al.* (2007) demonstrated that the tobacco R protein N as well as its cognate Avr determinant p50 from TMV both co-localize to the plant nucleus. While the function of p50 protein is still not clear in the compatible interaction, its recognition by the TIR-domain of the N protein induces a strong HR response. Kanneganti *et al.* (2007) have shown that two effectors of *Phythphthora infestans*, Nuk6 and Nuk7, which carry monopartite NLS sequences, are transported to the nucleus of tobacco cells and this import requires two plant importin-α proteins, NbIMPα1 and NbIMPα2. Moreover, *Xanthomonas* AvrBs3 family effectors, which also harbor NLS sequences, were shown to enter the plant nucleus via interaction with importin-α protein and function as genuine plant transcription factors (Van den Ackerveken & Bonas, 1997; Kay *et al.*, 2007). In addition, several members of transcription activator-like (TAL) effector family in *Xanthomonas oryzae* were shown to localize to the nucleus of rice plant cell and induce expression of genes encoding transcription factor of bZIP transcription factor family and γ subunit of transcription factor TFIIA (Sugio *et al.*, 2007). Each TAL gene family effector harbors three NLS sequences (Sugio *et al.*, 2007). The loss of induction of these transcription factors was observed after plants were infected with *X. oryzae* strain carrying mutated all three NLS sequences of TAL effector PthXo1, which was demonstrated earlier to be crucial for causing bacterial blight of rice (Sugio *et al.*, 2007). Intriguingly, substitution of native NLS sequences in PthXo1 by NLS from SV40 has restored the induction of the above mentioned two plant transcription factors indicating that indeed NLS is necessary for TAL effector to

alter gene expression in its host (Sugio *et al.*, 2007). Taken together, it might be possible that Um02137, Um02139 and Um03314 are transported to the maize nucleus via an importin-mediated mechanism. Interestingly, V. Gründel and A. Djamej (unpublished) have observed nuclear localization of heterologously expressed Um02137, Um02139 and Um03314 proteins in *Nicotiana benthamiana* employing yellow fluorescent protein (YFP) fusions. Surprisingly, substitutions in two amino acid residues in the NLS by alanine did not abolish nuclear localization after expression in *N. benthamiana* (V. Gründel and A. Djamej, personal communication). This could indicate that there are additional NLS sequences in Um02137, Um02139 and Um03314, which could not be identified with the program Predict NLS mediating the entry of these proteins to the nucleus. Alternatively, nuclear import could be mediated by a plant protein that interacts with these effectors. Precedence for such a "backpack" scenarios give a few examples. In *S. reilianum*, according to Predict NLS analysis, only one Eff1 protein, Sr13382, contains a putative NLS sequence. Sr13382 is the closest homologue of Um02141. Based on these results it is highly unlikely that NLS sequences found in some Eff1 proteins are necessary for their function in these effectors. However, this does not exclude their function in the nucleus. In future experiments it will be necessary to demonstrate where these effectors reside after being secreted. If they accumulate in the nucleus one could fuse them with a NES tag and test if such alleles can compliment the eleven gene deletion phenotype.

3.2.4 Putative translocation motifs in Eff1 proteins

The RXLR-dEER motifs reside within about 120 amino acids from the N-terminus and are required for effector translocation to host cells (Whisson *et al.*, 2007; Dou *et al.*, 2008). Dou *et al* (2008) demonstrated that RXLR effectors of *P. sojae* are translocated to the plant cells in the absence of the pathogen. Integrity of the W and Y motifs was demonstrated to be required for suppression of programmed cell death in known Avr proteins, and several novel effectors containing these motifs showed activity in a cell death suppression assay as well (Dou *et al.*, 2008). Moreover, the Avh superfamily was also shown to contain a high proportion of pseudogenes (Jiang *et al.*, 2008). To test whether C-terminal motifs are indeed crucial for function a series of truncation and chimeric constructs of *eff1* gene family members may be generated. Complementation assays of *eff1* deletion mutants with such constructs should

contribute to our understanding of the motifs´ significance for successful virulence of *eff1* proteins.

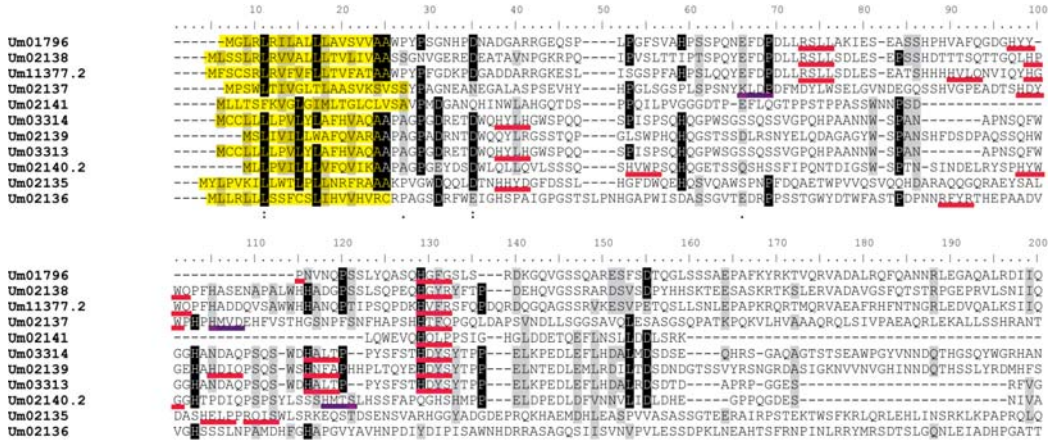

Fig. 30. Putative RXLR motifs of Eff1 proteins. Manual adjustment of ClustalW alignment was performed by BioEdit software. Identical amino acids are shaded in black. Similar amino acids are shaded in grey. Predicted signal peptide sequences are highlighted in yellow. Putative degenerate RXLR sequences are indicated following consensus sequences derived in the Tyler lab (B. Tyler, personal communication). R [K, H], X, L [M, I, F, Y, W], X (highlighted in red) or R [K, H], L[M], X, X (highlighted in purple).

The Eff1 proteins lack "classical" RXLR motifs found in the N-terminal domains of effector proteins from oomycetes that are translocated to plant cells (Kamoun & Goodwin, 2007; Ellis *et al.*, 2009; Tyler, 2009). Nevertheless, using a more degenerate RXLR motif search (B. Tyler, personal communication) revealed that all Eff1 proteins contain between one and four such degenerate motifs in their N-terminal domains (Fig. 30). Interestingly, histidine residues in the first position of the degenerate motifs are clearly overrepresented (71%) (Fig. 30). Given that eight Eff1 protein sequences carry putative RXLR motifs at conserved positions 129 – 132 in ClustalW alignment (Fig. 30) one could use these motifs as primary candidates to perform mutational analysis followed by complementation assays of the 11 gene deletion mutant. None of the Eff1 proteins contain LXLFLAK motif, which is present in effectors of another large family of oomycetes called Crinkler (CRN) proteins and may be also be involved in effector translocation to the plant cell (Kamoun, 2007). Further studies will reveal if the Eff1 effectors remain in the host-pathogen interface or enter plant cells by alternative, RXLR independent routes. Moreover, identification of interacting proteins and localization studies may give valuable hints concerning the function of the family members. Given the fact that the deletion mutant lacking all 11

eff1 genes has a strong virulence phenotype, functional studies can now be conducted. Of particular interest will be to analyze the effects of the deletion of the conserved C-terminal domain as well as deletions in the central domain. This could reveal whether these domains confer functions that can be separated, i.e. serve for targeting on the one hand and interaction with host proteins, on the other hand.

3.2.5 Expression of the eff1 gene family

Expression of all members of the eff1 gene family was strongly induced during biotrophic development. It is one of the few unifying features of filamentous pathogen effectors that the respective genes are upregulated during host colonization, either during penetration, in haustoria, or during later stages of pathogen development inside the plant tissue (Hahn *et al.*, 1997; Catanzariti *et al.*, 2006; Kämper *et al.*, 2006; Haas *et al.*, 2009; Oh *et al.*, 2009; Skibbe *et al.*, 2010). Real-Time-PCR analysis revealed a complex pattern of differential expression of individual genes. This could reflect that *eff1* genes respond to different physiological signals and are regulated at different time points. Skibbe *et al*. have proposed a two-phased model of pathogenic development of *U. maydis* (Skibbe *et al.*, 2010). First would be the establishment of compatibility, which most probably depends on universal pathogenicity factors to suppress plant defense responses during fungal penetration. Second, *U. maydis* might modify effector deployment to redirect physiology and development of a specific organ primordium during disease progression (Skibbe *et al.*, 2010). However, information on how this regulation could be connected to the different growth stages inside the host is scarce. In *U. maydis* the zinc finger protein Mzr1 has been defined as a transcriptional activator of *mig2-4* and *mig 2-5* effector genes during host colonization (Zheng *et al.*, 2008). However, Mrz1 regulates only two of the five *mig2* genes and is thus not a general regulator for effector genes. In addition, given the recent finding that several *U. maydis* effectors are expressed in a maize tissue-specific manner (Skibbe *et al.*, 2010) it is unlikely that such global effector regulatots exist at all. In *Fusarium oxysporum* a regulatory gene *SGE1* has recently been identified that was crucial for pathogenesis and affected the expression of the four tested *six* effector genes (Michielse *et al.*, 2009). It is unlikely, however, that SGE1 will turn out to be a dedicated regulator of effector genes as orthologs exist in all fungi, i.e. not only in plant pathogens (Michielse *et al.*, 2009). *U. maydis* has two genes related to SGE1 (*um06496* and *um05853*) (Michielse *et al.*, 2009) and it would be interesting to study

them functionally to elucidate if they are involved in regulating the *eff1* gene family or other effector genes.

3.2.6 Phenotypic analysis of eff1 mutant strains

None of the *eff1* mutants had a discernable phenotype on different stress media, which allows to exclude pleiotrophic effects. In addition, when filamentous growth was tested by spotting the cells on CM-charcoal plates all mutants developed vigorous filaments comparable to SG200. The analysis of deletion mutants demonstrated that several *eff1* deletion mutants were affected in virulence.

The combined deletion analysis and complementation studies conducted for members of the *eff1* family has revealed that genes *eff1-11*, *eff1-3*, and *eff1-4* contribute most significantly to virulence while all the other members of this gene family contribute to virulence only weakly (Figs. 21, 22). A highly decreased virulence observed after co-deletion of *eff1-11* is consistent with the finding that *eff1-11* is the most highly expressed *eff1* gene during biotrophic development. Since we have always deleted genes *eff1-3* and *eff1-4* simultaneously, we are presently unable to assess whether they both contribute to virulence. To further uncover the role of *eff1-3*, *eff1-4* and *eff1-11* in the pathogenicity of the fungus one could delete them in SG200 and perform infection studies with such single gene deletion mutants. Interestingly, the *eff1* genes with the strongest effect on virulence all belong to group II (Fig. 28). On the other hand, Eff1-4 is very similar to Eff1-9 with respect to domain structure, and nevertheless when this gene was co-deleted with three adjacent genes the effects on virulence were marginal. This could indicate that additional features that we do not yet recognize determine the strength of a given *eff1* gene. Alternatively, since *eff1-9* is the gene that shows the smallest increase in expression values during biotrophic growth, the differences in contribution to virulence could be attributed to these expression differences. This could be investigated by promoter-swap experiments.

Taken together, the deletion and complementation studies conducted make it highly likely that the different members of the *eff1* family have at least partially redundant functions. Since the observed complementation was in all cases partial it remains possible, that some sub-functualization in *eff1* genes (Conant & Wolfe, 2008) has occurred. In this respect it would be interesting to see whether the separate deletion of

the three different groups of *eff1* genes gives distinct phenotypic effects and whether these can than be complemented only by *eff1* genes from the same group or also by members of different groups. Such differences in virulence might become apparent when using different maize cultivars or when infecting different maize tissues like tassel, the cob or mature leaves (Skibbe *et al.*, 2010) rather than seedlings as used in this study.

3.2.7 Possible role of Eff1 effectors during biotrophic development

At present, the function of Eff1 proteins after secretion must remain highly speculative as the Eff1 effectors do not show any similarity to database entries. The members of this family are highly divergent but show conserved features. The central segment could represent a Eukaryotic Linear Motif, which binds specifically to a protein of the plant host and becomes partly ordered in the process. Using internet based algorithm (http://elm.eu.org/) all Eff1 proteins were checked for established Eukaryotic Linear Motifs (ELMs), however, no annotated ELM was detected. Although the C-terminal domain also lacks similarity to known domains as judged by HMM comparisons to the NCBI Conserved Domain Database (CDD), the fact that it is predicted to assume a folded conformation makes it the most likely domain conferring Eff1 protein activity. This is in line with results from oomycete effectors which revealed that functional domains reside in the C-terminus (Ellis *et al.*, 2009; Tyler, 2009). To shed light on the function of Eff1 family proteins it is necessary to perform localization studies, identifying interaction partners and establish the processes these effectors interfere with. Preliminary data of using Um02137-mCherry as well as Um02138- and Um01796-mCherry fusions showed the highest signal intensity at the intracellular hyphal tips, which suggests that these proteins are indeed secreted (data not shown). Since *U. maydis* hyphae are completely enclosed by the host plasma membrane during biotrophic development it was impossible to decide whether these protein fusions were localized to the apoplastic space or whether they were bound to the fungal cell wall or to the plant plasma membrane. In an attempt to discriminate between these possibilities I induced plasmolysis with mannitol to enlarge the space around infectious intracellular hyphae. Indeed, such an approach was successfully employed by Doehlemann *et al.* (2009) to show apoplastic localization of Pep1 effector in *U. maydis* (Doehlemann *et al.*, 2009). However, no mCherry signal could be detected in the apoplastic space, presumably due to the low

level expression of analyzed proteins (data not shown). Infection of maize with *eff1* deletion mutants including SG200eff1Δ1−11 did not cause necrosis. In strong contrast, leaves of maize infected with *pep1* deletion mutant displayed large necrotic areas 4 dpi (Doehlemann *et al.*, 2009). These data indicate that *eff1* gene deletion mutants are able to establish a compatible interaction with the host plant and do not elicit a hypersensitive response (HR). This data is in line with microscopic studies of SG200 and SG200eff1Δ1−11 revealing that there was no apparent morphological difference in biotrophic hyphae. Preliminary experiments indicate that the 11 gene deletion mutant does not elicit a hypersensitive response and is able to establish biotrophic growth (K. Schipper, Y. Khrunyk and R. Kahmann, unpublished). This is different from the phenotype of *pep1* effector mutants that are arrested during penetration and elicit strong defense responses (Doehlemann *et al.*, 2009). With the experiments conducted it was not possible to elucidate the stage at which SG200eff1Δ1−11 and wild-type strain differ during biotrophic development. In future experiments one should perform the microscopic analysis at different time points as well as carry out infections at the later stages of plant growth.

Given the fact that pathogens can enhance host susceptibility by manipulation of plant hormone and defense signaling (Grant & Jones, 2009), we analyzed levels of several plant hormones in the nine gene deletion mutants in comparison to SG200. We found that after infections with the SG200eff1Δ1,2,3,4,7,8,9,10,11 mutant a significantly increased level (77%) of salicylic acid (SA) in leaf material was observed at 5 dpi. This could indicate that the nine gene deletion mutant is less efficient in suppressing SA-mediated immunity than wild type. It is known that SA and jasmonic acid (JA) control resistance against pathogens with different infection strategies. While SA signaling primarily combats biotrophic pathogens and viruses, JA signaling protects plant against necrotrophic pathogens and insects (Glazebrook, 2005; Wang *et al.*, 2007). Necrotrophic pathogens induce SA-dependent cell death responses including expression of defense-related genes such as PR-1. Conversely, biotrophic pathogens activate primarily JA and ethylene responses during compatible interactions (Glazebrook, 2005; Wang *et al.*, 2007). Successful establishment of the biotrophic interaction of *U. maydis* with maize is accompanied by distinct transcriptional changes of plant hormone signaling genes (Doehlemann *et al.*, 2008). For example,

SA-dependent *PR-1* expression was undetectable during the early biotrophic phase of *U. maydis* infection, whereas activation of typical JA-responsive defense genes such as defensins and Bowman-Birk-like proteinase inhibitors was observed (Doehlemann *et al.*, 2008). Therefore, it is tempting to link the decreased virulence of the SG200eff1Δ1,2,3,4,7,8,9,10,11 mutant with the observed increase in SA levels as it indicates that *eff1* mutant could be unable to establish a fully functional biotrophic relationship. To test this in more detail one should analyze the transcriptional responses of maize when infected with this mutant.

3.2.8 Translocation of Eff1 effectors by RxLR-like motifs

Kale *et al.* demonstrated that effectors from three fungal pathogens, AvrL567 from *Melampsora lini*, AvrLm6 from *Leptosphaeria maculans*, Avr2 from *Fusarium oxysporum* f.sp. *lycopersici* can enter plant cells independently of the pathogen, and this translocation is mediated by RXLR-like motifs (Kale *et al.*, 2010). Interestingly, this cell entry is connected with binding phosphoinositides such as PtdIns(3)P (Kale *et al.*, 2010). Phosphoinositides are important components of the cell lipid pool, which function as intracellular and intercellular messengers in processes mediating plant growth and development, cytoskeletal rearrangements as well as signal transduction (Welti & Wang, 2004). In plants PtdIns(3)P, PtdIns(4)P, Ptdlns(5)P, Ptdlns(3,4)P2, Ptdlns(3,5)P2 and Ptdlns(4,5)P2 appear to be ubiquitous molecules (Drobak *et al.*, 1988; Munnik *et al.*, 1998); (Drobak *et al.*, 2005) except for Ptdlns(3,4,5)P3, which has so far only been reported in animal cells (Zhong & Ye, 2003; Drobak *et al.*, 2005).

Employing methods established in Tyler's lab we have performed a protein-lipid overlay (PLO) assay with Um02137-GFP-His purified from *E. coli*. Preliminary data demonstrated that Um02137 might bind to PtdIns(3,5)P2 and PtdIns(5)P. A weaker binding was observed with PtdIns(4)P. According to a degenerate RXLR consensus sequences provided by B. Tyler (B. Tyler, personal communication) Um02137 contains four potential RXLR-like motifs in the N-terminal part: KLDP, HDYW, HMVD, and HTFQ. Such PLO assays with modified Um02137-GFP-His proteins harboring mutated RXLR-like motifs would be necessary to verify if any of these domains are crucial for the observed binding affinity. All three phosphoinositides

shown to bind Um02137-GFP are ubiquitous for eukaryotic cells (Drobak *et al.*, 2005).

It is possible that during the biotrophic growth *U. maydis* effectors might employ these molecules as "receptors" to enter maize cells as has been hypothesized for PtdIns(3)P (Kale *et al.*, 2010). Preliminary results of root uptake assay with Um02137-GFP-His demonstrated GFP fluorescence in cytoplasm as well as in nuclei, which supports the hypothesis of Um02137 translocation into the plant cell in the absence of the pathogen. Our data is in line with findings showing pathogen-independent translocation into the plant cell of several oomycete effectors (Kale *et al.*, 2010).

Future experiments need to validate this finding for other members of the *eff1* gene family, combine this with a search for plant interacting proteins and demonstration that these interactors are relevant for the successful interaction of *U. maydis* with its host.

4 Materials and Methods

4.1 Materials and source of supplies

4.1.1 Chemicals

All chemicals used in this study were of research grade, and were obtained from Difco (Augsburg, Germany), Fluka (Buchs, Switzerland), Merck (Darmstadt, Germany), Riedel-de-Haën (Seelze, Germany), Roth (Karlsruhe, Germany) and Sigma-Aldrich (Deisenhofen, Germany).

4.1.2 Solutions and buffers

All standard solutions and buffers used in this study were prepared as described in Ausubel *et al*. (1987) and Sambrook *et al*. (1989). All additional specific solutions and buffers are listed in the corresponding method sections. All media, solutions and buffers were autoclaved for 5 min at 121 °C. Heat-sensitive solutions were filter-sterilized (pore size 0.2 µm; Merck, Darmstadt, Germany).

4.1.3 Enzymes

All restriction enzymes, *Taq* DNA polymerase, T4 DNA ligase, Antarctic Phosphatase were obtained from NEB (Frankfurt am Main, Germany). Phusion High-Fidelity DNA polymerase was obtained from Finnzymes (Frankfurt am Main, Germany). KOD Extreme Polymerase was obtained from Merck (Darmstadt, Germany).

4.1.4 Kits used in this study

The following kits were used in this study as described by the supplier: TOPO TA Cloning Kit (Invitrogen, Karlsruhe, Germany) was used to directly clone PCR products. QiaQuick PCR purification Kit (Qiagen, Hilden, Germany) was used to purify PCR products. QiaQuick Gel Extraction Kit (Qiagen, Hilden, Germany) was used to purify DNA fragments from agarose gels. QIAprep Spin MiniPrep Kit (Qiagen, Hilden, Germany) was used to isolate and purify plasmid DNA before sequencing. RNeasy Kit (Qiagen, Hilden, Germany) was used to purify total RNA to be used in Real-Time-PCR experiments. TURBO DNA-*free*TM (Ambion/Applied Biosystems, Darmstadt, Germany) was used for removal of DNA prior to first-strand

cDNA synthesis. SuperScript® III First-Strand Synthesis SuperMix (Invitrogen, Karlsruhe, Germany) was used for the first-strand cDNA synthesis. Platinum® SYBR® Green qPCR SuperMix-UDG (Invitrogen, Karlsruhe, Germany) was used for Real-Time-PCR. ECL Plus Western Blot detection reagent (GE Healthcare, München, Germany) was used for chemiluminescene detection.

4.2 Media

4.2.1 E. coli

For *E. coli* cultures, dYT liquid medium and YT solid medium were used (Ausubel *et al.*, 1987; Sambrook *et al.*, 1989). Ampicillin (Amp) and kanamycin (Kan) were added to a final concentration of 100 and 50 µg/ml, respectively. Liquid cultures were incubated at 37°C at 180 rpm. Solid media were incubated under aerobic condition at 37°C. For preparing frozen stocks exponentially growing cultures containing the appropriate antibiotic were mixed with dYT-glycerol at a 1:1 ratio and stored at -80°C.

dYT liquid medium	16 g Tryptone-Peptone (Difco) 10 g Yeast-Extract (Difco) 5 g NaCl Add dH_2O to 1 l and autoclave
YT solid medium	0.8 % (w/v) Tryptone-Peptone (Difco) 0.5 % (w/v) Yeast-Extract (Difco) 0.5 % (w/v) NaCl 1.3 % (w/v) Agar (Roth) Add dH_2O to 1 l and autoclave
dYT glycerol medium	16 g Tryptone-Peptone (Difco) 10 g Yeast-Extract (Difco) 5 g NaCl 800 ml (v/v) 87% Glycerin (f.c. 69.6%) Add dH_2O to 1 l and autoclave

4.2.2 U. maydis

U. maydis strains were grown on potato-dextrose-agar (Difco), CM-glu, CM-ara or YEPSL liquid media (Holliday, 1974; Molina & Kahmann, 2007) or the respective solid media containing 2 % agar in addition. To select transformants hygromycin B (Duchefa, Haarlem, Netherlands) and carboxin (Riedel de Haen, Seelze, Germany) were added to a final concentration of 200 µg/ml and 2 µg/ml, respectively. To prepare frozen stocks exponentially growing cultures were mixed with NSY-glycerol at a 1:1 ratio and stored at -80°C.

Potato-Dextrose-Agar (PD)	24 g Potato Dextrose Broth (Difco) 20 g Agar (Difco) Add dH_2O to 1 l and autoclave
YEPSL modified from Tsukuda *et al*., 1988	10 g Yeast-Extract (Difco) 10 g Bacto-Peptone (Difco) 10 g Sucrose Add dH_2O to 1 l and autoclave
Vitamin solution (Holliday, 1974)	100 mg Thiamin (Sigma) 50 mg Riboflavin (Sigma) 50 mg Pyridoxine (Sigma) 200 mg Calcium pantothenate (Sigma) 500 mg p-Aminobenzoic-acid (Sigma) 200 mg Nicotinic acid (Sigma) 200 mg Choline chloride (Sigma) 1000 mg myo-Inositol (Sigma I-5125) Add dH_2O up to 1 l and sterile filter
PD-Charcoal	24 g Potato Dextrose Broth (Difco) 10 g Charcoal (Sigma) 20 g Agar (Difco) Add dH_2O to 1 l and autoclave

CM medium (Holliday, 1974)

2.5 g Casamino acids (Difco)
1 g Yeast-Extract (Difco)
10 ml Vitamin solution (Holliday, 1974)
62.5 ml Salt solution (Holliday, 1974)
0.5 g DNA degr. Free Acid (Sigma)
1.5 g NH_4NO_3
Add dH_2O to 980 ml
Adjust pH to 7.0 (NaOH) and autoclave
2% (w/v) Glucose or Arabinose

Salt solution (Holliday, 1974)

16 g KH_2PO4
4 g Na_2SO4
8 g KCl
4 g $MgSO_4$ x$7H_2O$
1.32 g $CaCl_2$ x$2H_2O$
8 ml Trace elements
Add dH_2O up to 1 l and sterile filter

Trace element solution (Holliday, 1974)

60 mg H_3BO_3
140 mg $MnCl_2$ x$4H_2O$
400 mg $ZnCl_2$
40 mg $NaMoO_4$ x$2H_2O$
100 mg $FeCl_3$ x$6H_2O$
40 mg $CuSO_4$ x$5H_2O$
Add dH_2O up to 1 l and sterile filter

NM-MM medium

0.3% (w/v) KNO_3
6.25% (v/v) Salt solution (Holliday, 1974)
Adjust pH to 7.0 (NaOH), sterile filter
2% (w/v glucose)

AM-MM medium

0.3% (w/v) $(NH_4)_2SO_4$
6.25% (v/v) Salt solution (Holliday, 1974)
Adjust pH to 7.0 (NaOH), sterile filter
2% (w/v glucose)

Regeneration Agar (Schulz *et al*., 1990)	1.5 % (w/v) Agar (Difco) 1M Sorbitol (Sigma) in YEPSL (described above)
NSY glycerol medium	8 g Nutrient Broth (Difco) 1 g Yeast-Extract (Difco) 5 g Sucrose (Roth) 800 ml 87% Glycerol (f.c. 69.6%) Add dH_2O up to 1 l and autoclave

4.3 Microbiological and cell biology methods

4.3.1 E. coli strains

E. coli TOP10 (Invitrogen, Karlsruhe, Germany) (F- mcrA Δ(mrr-hsdRMS-mcrBC) Φ80lacZΔM15 ΔlacX74 deoR nupG recA1 araD139 Δ (ara-leu)7697 galU galK rpsL(Str^R) endA1 λ) which is a derivative of *E. coli* K12 was used for cloning purposes.

4.3.2 Maize variety (Zea mays)

For all pathogenicity assays the maize variety Early Golden Bantam (Old Seed Company, Madison Wisconsin, USA) was used.

4.3.3 U. maydis strains

All *U. maydis* strains used in this study are listed in Table 3. The solopathogenic *U. maydis* strain SG200 (*a1mfa2bE1bW2)* has been described (Kämper *et al.*, 2006).

To generate deletion mutants the single step method developed by Kämper (2004) was adopted. To delete the hygromycin resistance marker flanked by FRT sites strains were transformed with the FLP-expressing plasmid pFLPexpC. A carboxin-resistant colony was grown overnight in CM-ara medium and plated on PD to obtain single colonies. Colonies were replica-plated on PD plates and PD plates supplemented with hygromycin (PD-hyg). Colonies, which lost resistance to hygromycin were subsequently tested on PD plates supplemented with carboxin for the loss of pFLPexpC and analyzed by PCR to verify deletion events.

For integrations genes into the *ip* locus the strategy of Loubradou *et al.* (2001) was used. Plasmids pBScbx, pRU11, pNEBUH and p123 have been described (Keon *et al.*, 1991; Brachmann *et al.*, 2001; Weinzierl *et al.*, 2002; Aichinger *et al.*, 2003).

Table 3. *U. maydis* strains used and constructed for this study.

Name*	Resistance	Remarks
SG200	Phleo	(Kämper *et al*., 2006)
SG200FLP	Phleo Cbx	FLP insertion into *ip* locus
SG200FLPΔ01796$^{FRT/FRT}$	Phleo Hyg Cbx	FLP insertion into *ip* locus; 1 gene deletion
SG200FLPΔ11377.2$^{FRT/FRT}$	Phleo Hyg Cbx	FLP insertion into *ip* locus; 1 gene deletion
SG200FLPΔ11377.2$^{FRTm1/FRTm1}$	Phleo Hyg Cbx	FLP insertion into *ip* locus; 1 gene deletion
SG200FLPΔ11377.2$^{FRTm2/FRTm2}$	Phleo Hyg Cbx	FLP insertion into *ip* locus; 1 gene deletion
SG200FLPΔ11377.2$^{FRTm3/FRTm3}$	Phleo Hyg Cbx	FLP insertion into *ip* locus; 1 gene deletion
SG200FLPΔ11377.2$^{FRTm4/FRTm4}$	Phleo Hyg Cbx	FLP insertion into *ip* locus; 1 gene deletion
SG200Δ01796^{FRT} **SG200eff1Δ1**	Phleo	1 gene deletion
SG200Δ01796::pYUIF-FRTm2	Phleo Hyg	1 gene deletion; insertion of cassette harbouring FLP in *um01796* locus
SG200Δ01796^{FRT}Δ11377.2^{FRTm2} **SG200eff1Δ1,2**	Phleo	2 gene deletion
SG200Δ01796^{FRT}Δ11377.2$^{FRT/FRT}$	Phleo Hyg	2 gene deletion
SG200Δ01796^{FRT}Δ11377.2$^{FRTm1/FRTm1}$	Phleo Hyg	2 gene deletion
SG200Δ01796^{FRT}Δ11377.2$^{FRTm2/FRTm2}$	Phleo Hyg	2 gene deletion
SG200Δ01796^{FRT}Δ11377.2$^{FRTm3/FRTm3}$	Phleo Hyg	2 gene deletion
SG200Δ01796^{FRT}Δ11377.2$^{FRTm4/FRTm4}$	Phleo Hyg	2 gene deletion
SG200Δ01796^{FRT}Δ02138^{FRTm2} **SG200eff1Δ1,8**	Phleo	2 gene deletion
SG200Δ03313Δ03314$^{FRTm3/FRTm3}$ **SG200eff1Δ3,4**	Phleo Hyg	2 gene deletion

SG200Δ01796^{FRT}Δ02138^{FRTm2}Δ03313Δ03314$^{FRTm3/FRTm3}$ **SG200eff1Δ1,3,4,8**	Phleo Hyg	4 gene deletion
SG200Δ01796^{FRT}Δ11377.2^{FRTm2}Δ03313Δ03314^{FRTm3} **SG200eff1Δ1,2,3,4**	Phleo	4 gene deletion
SG200Δ01796^{FRT}Δ11377.2^{FRTm2}Δ02137Δ02138Δ02139Δ02140.2^{FRTm1} **SG200eff1Δ1,2,7,8,9,10**	Phleo	6 gene deletion
SG200Δ01796^{FRT}Δ11377.2^{FRTm2}Δ03313Δ03314^{FRTm3}Δ02137Δ02138Δ02139Δ02140.2^{FRTm1} **SG200eff1Δ1,2,3,4,7,8,9,10**	Phleo	8 gene deletion
SG200Δ01796^{FRT}Δ11377.2^{FRTm2}Δ03313Δ03314^{FRTm3}Δ02137Δ02138Δ02139Δ02140.2Δ02141^{FRTm1} **SG200eff1Δ1,2,3,4,7,8,9,10,11**	Phleo	9 gene deletion
SG200Δ01796^{FRT}Δ11377.2^{FRTm2}Δ03313Δ03314^{FRTm3}Δ02135Δ02136Δ02137Δ02138Δ02139Δ02140.2$^{FRTm1/FRTm1}$ **SG200eff1Δ1-11**	Phleo Hyg	11 gene deletion
SG200eff1Δ1,2,3,4,7,8,9,10,11-1	Phleo cbx	Single integration of *um01796* into *ip* locus of SG200eff1Δ1,2,3,4,7,8,9,10,11
SG200eff1Δ1,2,3,4,7,8,9,10,11-8	Phleo cbx	Single integration of *um02138* into *ip* locus of SG200eff1Δ1,2,3,4,7,8,9,10,11
SG200eff1Δ1,2,3,4,7,8,9,10,11-7,8,9,10	Phleo cbx	Single integration of four clustered genes (um02137, *um02138*, *um02139 and um02140.2*) into *ip* locus of SG200eff1Δ1,2,3,4,7,8,9,10,11
SG200pYUIF-FRTm2Δum01796	Phleo hyg	1 gene deletion

* Abbreviated names are in red

4.3.4 Competent cell preparation and transformation of E. coli

Competent cell preparation and chemical transformation of *E. coli* were modified from Cohen *et al*. (1972). *E. coli* TOP10 cells were grown in 20 ml dYT medium at 37°C and 200 rpm overnight, diluted 1:200 in 1000 ml dYT medium and continually grown to a cell density with OD_{600} of about 0.6. The culture was transferred to a microcentrifuge tube, incubated on ice for 30 min and centrifuged at 4°C for 8 min at

3000 rpm. The supernatant was discarded and cells were resuspended in 1/3 culture volume (330 ml) of pre-chilled RF1-solution and incubated for 30 min at 4°C. The suspension was centrifuged at 4°C for 8 min at 3000 rpm and the supernatant was discarded. *E. coli* cells were resuspended in 1/20 culture volume (50 ml) of pre-chilled RF2-solution and incubated for 30 min on ice. Finally, 100 µl aliquots of competent cell suspension in 1.5-ml microcentrifuge tubes were kept on ice for direct use or stored at - 80°C for later use.

RF1 solution	100 mM RbCl
	50 mM $MnCl_2$ x $4H_2O$
	30 mM K-acetate
	10 mM $CaCl_2$ x $2H_2O$
	15% (v/v) glycerol
	pH was adjusted to 5.8 (NaOH)
	sterile filtered
RF2 solution	10 mM MOPS
	10mM RbCl
	75 mM $CaCl_2$ x$2H_2O$
	15% (v/v) glycerol
	pH was adjusted to 5.8 (NaOH)
	sterile filtered

To transform *E. coli* by chemical transformation, 100 µl aliquots of chemically competent *E. coli* cells were thawed on ice for 2 min. Afterwards, 10-50 ng of plasmid DNA was added, gently mixed and incubated on ice for 15-30 min. *E. coli* cells were then heat shocked at 42°C for 30 sec and immediately cooled on ice for 5 min. For the recovery of the cells, 500 µl dYT medium was added and then the cells were incubated at 200 rpm for 30 min at 37°C. Finally, the entire *E. coli* cell suspension was plated on YT-agar containing the appropriated antibiotic and incubated at 37°C overnight.

4.3.5 Protoplast preparation and transformation of U. maydis

Protoplast preparation and transformation of *U. maydis* strains was performed as described in *Schulz et al.* (1990). *U. maydis* cells were grown overnight in YEPSL

medium at 28°C and 200 rpm to a cell density of OD_{600} 0.8-1.0. Cells were harvested by centrifugation at 4°C for 5 min at 3200 rpm, washed in 25 ml SCS, and resuspended in 2 ml SCS containing 3.5 mg/ml Novozyme. Cells were incubated for about 10 min at room temperature to digest the cell wall, which was monitored under the microscope. Afterwards, *U. maydis* cells were washed three times with ice cold SCS and centrifuged at 2400 rpm for 8 min at 4°C. This was followed by an additional wash with ice cold STC and centrifugation step. Finally, protoplast pellets were resuspended in 0.5 ml of ice cold STC, and 70 µl of protoplasts were aliquoted into pre-chilled 1.5 ml microcentrifuge tubes for immediate use, or stored at -80°C for later use. For transformation of protoplasts, 1 µl heparin (1 mg/ml) and up to 10 µl of DNA (3-5 µg) was added to the protoplast aliquot and incubated for 10 min on ice. Afterwards, 500 µl STC/PEG were added to the protoplasts, mixed gently, and incubated for another 15 min on ice. The transformation mix was plated on regeneration agar plates. Transformed colonies appeared after 4-6 days and were singled out and grown on PD-agar plates containing the appropriate antibiotic. Single colonies were picked and saved on PD-plates. The regeneration agar plates were prepared by first pouring a bottom phase with 12 ml regeneration agar containing the appropriate concentration of antibiotic. Afterwards, 12 ml of regeneration agar without antibiotic was poured on top and solidified.

SCS	20 mM Na-citrate, pH 5.8 1 M Sorbitol In dH_2O, sterile filtered
STC	10 mM Tris-Cl, pH 7.5 100 mM $CaCl_2$ 1 M Sorbitol in dH_2O, sterile filtered
STC/PEG	15 ml STC 10 g PEG4000

4.3.6 FLP activity and recombination assay

To assay the efficiency of FLP-mediated recombination of wild type and mutated FRT pairs, strains were generated where the *um11377.2* gene was deleted in

SG200FLP using the *hph* resistance cassette from pHwtFRT, pHFRTm1, pHFRTm2, pHFRTm3, pHFRTm4 plasmids, respectively. In each case one transformant where the *um11377.2* gene is replaced by a hygromycin resistance cassette flanked by a pair of wild type or mutated FRT sequences was recovered. These strains were grown in CM-ara medium for 24 hours and then plated on PD plates to obtain single colonies. Colonies were replica-plated to PD and PD-hyg plates. The recombination efficiency was calculated by determining the percentage of cells that had lost hygromycin resistance.

4.3.7 Pathogenicity assays

Pathogenicity assays were performed as described (Kämper *et al.*, 2006). For maize (*Zea mays*) infections, cultures of *U. maydis* strains were grown to an OD_{600} of 0.7 – 0.8 in YEPSL, pelleted, resuspended in distilled water to an OD_{600} of 1 and injected into 7-day-old seedlings of the variety Early Golden Bantam (Olds Seeds, Madison, WI). Plants were kept in the greenhouse with a light-dark cycle of 16 (28°C) and 8 hrs (20°C). Disease symptoms were scored according to severity 14 days after inoculation (Kämper *et al.*, 2006).

4.3.8 Protein expression in E. coli

E. coli BL21 cells (Invitrogen, Karlsruhe, Germany) containing plasmids encoding GST-Um02137-GFP-His and GST-GFP-His fusion proteins (in collaboration with S. Kale, Virginia Bioinformatics Institute) were grown in 200 ml of dYT medium containing 100 µg/mL ampicillin in a 1 L baffled flask shaken at 240 rpm at 37 °C and induced with 2.5 mM of isopropyl β-D-1-thiogalactopyranoside (IPTG) when OD_{600} absorption reached 0.4-0.5. The temperature was then shifted to 16 °C and the induction was continued for ~ 20 hours. Cells were harvested by centrifugation at 4°C and then stored at -20°C. Visual confirmation of GFP expression was noted by the green color of the bacterial cell pellet. To purify the GFP-fusion proteins, cells were thawed on ice for 20 min, and then resuspended in 4-5 ml of ice-cold lysis buffer. Lysozyme (Sigma-Aldrich Deisenhofen, Germany) was added to a final concentration of 1 mg/mL, and then the suspension was incubated for 10 min on ice. Sonication (with double stepped microtip, 3 mm) was done at 300 W for 15 sec bursts three times with 15 sec cooling periods between each burst. The lysate was centrifuged at 9000 rpm for 30 min at 4°C, and then the supernatant was transferred to a fresh tube and

kept on ice until use. Protein purification via Ni-NTA affinity chromatography was performed using the QiaExpressionist protocol. 1.5 ml of 50% Ni-NTA-agarose slurry (Qiagen, Hilden, Germany) was loaded onto a 5 ml Pierce centrifuge column (Thermo Scientific, Rockford, USA). The column was washed with 10 ml of lysis buffer. The protein sample was loaded onto the column, and then the column was extensively washed twice with 10 volumes (10 ml) of wash buffer containing 20mM imidazole. The protein was eluted with 3 ml of elution buffer containing 250 mM imidazole into 1-ml fractions.

To remove the Glutathione S-Transferase (GST) moiety 500 µl of the protein fractions of concentration higher than 2 mg/ml were incubated overnight with 1 µl of thrombin at room temperature and purification according to QiaExpressionist protocol was repeated. Fractions of purified proteins were pooled and concentrated on Amicon Ultra-4 3 kDa columns (Millipore, Schwalbach, Germany) at 3000 rpm. The sample was then mixed with an equal volume of 50 mM MES buffer, pH 5.8. The protein concentration was measured at 280 nm using a nanodrop spectrophotometer (ND-1000) and adjusted to 8 mg/ml.

Lysis buffer	50 mM NaH_2PO_4 300 mM NaCl 10 mM imidazole pH 7.6
Wash buffer	50 mM NaH_2PO_4 300 mM NaCl 20 mM imidazole pH 7.6
Elution buffer	50 mM NaH_2PO_4 300 mM NaCl 250 mM imidazole pH 7.6

4.3.9 Soybean root and suspension culture protein uptake assay

Soybean seeds were germinated in vermiculite for 3-5 days. Roots were washed with water thoroughly to remove any debris. Soybean root tips were cut into lengths of between 0.5 and 1 cm and then were washed with water. Each root tip was completely submerged in 100 µl of the Um02137-GFP-His and GFP-His (used as control) protein solution (8 mg/mL in 25 mM MES, pH 5.8) in an Eppendorf tube. The samples were incubated overnight at 28°C (about 12 h). The roots were then washed in 200 ml of water for 2 h while shaken at 100 rpm on a rotary shaker. The roots were then viewed using a TCS-SP5 confocal microscopy (Leica).

4.3.10 Protein-lipid overlay assay

Lipids (Echelon, Salt Lake City, USA) were dissolved in DMSO. 1 µl of each lipid (100 pmol) was spotted onto Hybond-C-extra membranes (GE Healthcare, München, Germany) and allowed to dry at room temperature for 1 h. The membrane was blocked in 3 % (w/v) fatty acid-free BSA (Sigma A-7030) in PBST for 1 h. The membrane was then incubated overnight at 4 °C with gentle stirring in the same solution containing 20 µg/ml of the indicated protein. The membranes were washed three times over 30 min in PBST, and then incubated for 1 h with 1:10000 dilution of anti-His monoclonal antibody (Sigma-Aldrich, Deisenhofen, Germany). The membranes were washed as before, then incubated for 1 h with 1:10000 dilution of anti-mouse secondary antibody (Sigma-Aldrich, Deisenhofen, Germany). Finally, the membranes were washed four times over 40 min in PBST, and the GST-fusion protein that was bound to the membranes by virtue of its interaction with phospholipid was detected by enhanced chemiluminescence using ECL reagents (GE Healthcare, München, Germany).

PBST	10mM Tris-HCl, pH 7.2 150mM NaCl 0.1% Tween-20) In dH_2O

4.3.11 Staining and microscopy

Infected leaf tissue was harvested from maize plants 1 to 9 dpi and cleared in ethanol overnight. The next day samples were washed in water before treatment with 10% KOH at 90°C for 3-4 h. For visualizing hyphae in the plant vasculature, fungal hyphae were stained with Fluorescein WGA (Vector Laboratories). Plant membranes were visualized using Propidium Iodide (Fluka, Buchs, Switzerland). Samples were incubated in staining solution (10 µg/ml WGA, 1 µg/ml Propidium Iodide, 0.02% Tween20) for 15 min and washed in 1x PBS. Confocal images were taken using a TCS-SP5 confocal microscopy (Leica).

4.4 Molecular biological methods

Standard molecular biology methods, such as purification, precipitation, electrophoresis of DNA or molecular cloning technique, are followed protocols described in Ausubel *et al.* (1987) and Sambrook *et al.*, (1989). The concentration of nucleic acids was determined by photometry. Photometric measurements were performed using a NanoDrop ND-1000 Spectrophotometer. The purity of nucleic acids was determined by the ratio of A_{260} to A_{280}. For purified DNA and RNA samples, the A_{260} to A_{280} ratios were about 1.8.

4.4.1 Oligonucleotides

All oligonucleotides in this study were purchased from Eurofins MWG Synthesis GmbH (Ebersberg bei München, Germany). The nucleotide sequences are presented in Table 4 from the 5´-end to the 3´-end.

Table 4. Primers used in this study*

PRIMER NAME	SEQUENCE
pBShygfw	ATCGGGGCCTAGATGGCCAGAAGTTCCTATTCTCTAGAAAGTATAGGAACTTCACCATGGCGTGACAATTGCGGCCGCACTCGAGTGGCGGCA
pBShygrv	ATCGGGGCCACTCAGGCCAGAAGTTCCTATACTTTCTAGAGAATAGGAACTTCGCCTATTAATGCGGCCGCACAGCTTCGCGGCGCAGCAGCG
pHFRT1fw	ATCGGGGCCTAGATGGCCAGAAGTTCCTATTCTCGAGAAAGTATAGGAACTTCACCATGGCGTGACAATTG
pHFRT1rv	CGGGGCCACTCAGGCCAGAAGTTCCTATACTTTCTCGAGAATAGGAACTTCGCCTATTAATGCGGCCGCAC

pHFRT2 fw	ATCGGGGCCTAGATGGCCAGAAGTTCCTATTCTCAAGAAAGTATAGGAACTTCACCATGGCGTGACAATTG
pHFRT2 rv	CGGGGCCACTCAGGCCAGAAGTTCCTATACTTTCTTGAGAATAGGAACTTCGCCTATTAATGCGGCCGCAC
pHFRT3 fw	ATCGGGGCCTAGATGGCCAGAAGTTCCTATTCTCCAGAAAGTATAGGAACTTCACCATGGCGTGACAATTG
pHFRT3 rv	CGGGGCCACTCAGGCCAGAAGTTCCTATACTTTCTGGAGAATAGGAACTTCGCCTATTAATGCGGCCGCAC
pHFRT4 fw	TCGGGGCCTAGATGGCCAGAAGTTCCTATTCTCTGGAAAGTATAGGAACTTCACCATGGCGTGACAATTGC
pHFRT4 rv	TCGGGGCCACTCAGGCCAGAAGTTCCTATACTTTCCAGAGAATAGGAACTTCGCCTATTAATGCGGCCGCA
pRU11crgFLPfw	ATCGGAAGCTT ATTGTGGCAGCCGCGATTC
pRU11nosFLPrv	ATCGGAAGCTTAATACGCAAACCGCCTCTCCC
pIF1fw	ATCGGAAGCTTAGGAAGTTCCTATTCTCTAGAAAGTATAGGAACTTCTTGCATGCCTGCAGGTCGAA
pIF1rv	ATCGGAAGCTTGAAGTTCCTATACTTTCTAGAGAATAGGAACTTCTCTCATGTTTGACAGCTTAT
pYUIFfw	ATCGGGGTCACCGTTGGCCGATTCATTAATGCAGGTT
pYUIFrv	ATCGGGGTGACCTCGAATTCTCATGTTTGACAGCTTA
um01796 LBfw	ACGTGGTGAGCCAATCTGACTCGTGATTAATGATTG
um01796 LBrv	ATCGGGGCCATCTAGGCCATGTCGACAAGGATTGACGCAAATCAGCGGTA
um01796 RBfw	ATCGGGGCCTGAGTGGCCAGCTTGTTGTGGCGTACCCTACAAACGCATA
um01796 RBrv	GGGGGGTAGATGGAGCGAGAAGATGGTGGTGATCAAA
um01796 nestfw	CCAATCTGACTCGTGATTAATGATTGGACC
um01796 nestrv	TGGAGCGAGAAGATGGTGGTGATCAAAGGG
um11377 LBfw	GGCAAAGCTGACGCTCACTTTG
um11377 LBrv	ATCGGGGCCATCTAGGCCCCTGATCTCGCAGCCACAACAA
um11377 RBfw	ATCGGGGCCTGAGTGGCCTGTTCTCTGGCGTTTGGGAGCAGGCTCCAGAT
um11377 RBrv	GCCAATTCTTGACAGCTCATATGAGCCCGT
um11377 nestfw	TTGTGTCCACTTACAGTGTACTCTCTGGTTTCATTTGTGC
um11377 nestrv	GCGAGAGGAGCTGTTTGTGTTGATGGCGTCTGCTATCGG
um03313 LBfw	AGGCGAGTCCTGTTACGTCGAT
um03313 LBrv	ATCGGGGCCATCTAGGCCCTGACAGAGCCAGGCTACCGTTGA
um03314 RBfw	ATCGGGGCCTGAGTGGCCCCTGTCAAGCTTCCAAGTATTGC

um03314 RBrv	CTTAGGACATAAACGGAAGAGCAG
um03313 nestfw	AGCACGACGATGCCAATATGGTTT
um03314 nestrv	TCGCTTGTGCCAAAGATGGGCGAG
um02137 LBfw	CAGAATCTATCCGAACCCGCGG
um02137 LBrv	ATCGGGGCCATCTAGGCCAAATCTCGAATCCTCGTTCGCGG
um02141 RBfw	ATCGGGGCCTGAGTGGCCGCCAAGTTTCAGATCACTGTTG
um02141 RBrv	TTGTCCCCGGATGGAAGCGTCTG
um02137 nestfw	CGTGCACGACATGAATTAAA
um02141 nestrv	GCATCTGGACTATGAATGTTGAC
um02140 RBfw	ATCGGGGCCTGAGTGGCCATTGGCGGAAATGAAGAACATTG
um02140 RBrv	CTTGGCTCCGATGTACGCAGAG
um02140 nestrv	GTATTTGGAGGGCGGCTGAA
um02141 LBfw	GACGGAGAGGGCTGAATGTCAGGC
um02141 LBrv	ATCGGGGCCATCTAGGCCGCGATGTTCGACGAGAGGGCTCTT
um02141 nestfw	CCTCCCCAGTAATGGGGGCTGT
um02135 LBfw	AACGGAGGCGAAATTGACATTATG
um02135 LBrv	ATCGGGGCCATCTAGGCCACCTGAGATAACGGCGCACTGATGC
um02135 nestfw	CCTGCCTTCTGGACTGTCACTGAG
um01796 comfw	TGCTGGCAAAAAGTTGATGTAGTT
um01796 comrv	ATCGGGCGGCCGCCTAGGCATGCATCCAAGTTGCTT
um02138 comfw	ATCGGGGATCCCGCCATGCAGATGTGCTGCTTCACT
um02138 comrv	ATCGGCATATGAGAGGCAGCCAGGGATCATTTGTA
cbxfw1	ATCGGTTAATTAAAGCCGAACGACCGAGCGCAGCGAGTCA
cbxrv1	ATCGGTTAATTAACTCACTCAAAGGCGGTAATACGGTTAT
um02137 comfw	ATCGGTTAATTAACTAGATGTGCACTCGAGACCCTTCGGT
um02140 comrv	ATCGGTTAATTAAGGCGATGTTCGACGAGAGGGCTCTTTA
um11377 - FRTassay-rv	GACAAGAACTTCGTACAGACGAT
Primers used for quantitative real-time PCR	
PRIMER NAME	**SEQUENCE**
01796rtfw1	CGGAGGAGTCTCATGAATCAC

01796rtrv1	TACGCCACAACAAGCTAGG
11377rtfw1	AGATTCTGGTGGTCCTCTAC
11377rtrv1	TAAGCATCGGGTTCCTTG
03313rtfw1	CGTCAGAAACGTGCTAAC
03313rtrv1	TCAGTGGCTCCACATAAG
03314rtfw1	CAGTGCGATCTCAGGTCAG
03314rtrv1	CCCACACCTCCTCGATTAC
02137rtfw1	GCCTCCTTTCTCTGAGAC
02137rtrv1	AACTACGGAACGGGATA
02138rtfw1	GTAGCTTGCCAGCAAATACC
02138rtrv1	GGATCATCGCCATGTTTACG
02139rtfw1	GCTAGAACGCCAAGTGTTTGTC
02139rtrv1	TCGCAAGCAACCAGAAAGTCTC
02140rtfw1	GCGAAAGATGCTGGTCAAC
02140rtrv1	GGTGTACCCACGACTCTAAAG
02141rtfw1	GCGAAAGATGCTGGTCAAC
02141rtrv1	AAGGCCACAAACCTGTAGACC
02135rtfw1	TCCAGGATGGAACGATGTC
02135rtrv1	CGCTTTGGTCTCCCATATTG
02136rtfw1	CTTGTGCATGCGACGAAC
02136rtrv1	TTGCAGGACAAGGCAGAC
rt-ppi-fw	ACATCGTCAAGGCTATCG
rt-ppi-rv	AAAGAACACCGGACTTGG
Primers used for synthesis of FLP	
PRIMER NAME	**SEQUENCE**
FLP a+1	CATATGCCGCAGTTCGACATCCTCTGCAAGACGCCGCCCAAGG
FLP a+2	TGCTGGTGCGTCAGTTTGTCGAGCGCTTCGAGCGTCCCTC
FLP a+3	GGGCGAGAAGATCGCTCTCTGCGCCGCCGAGCTCACCTAC
FLP a+4	CTCTGCTGGATGATCACCCACAACGGCACCGCCATCAAGC
FLP a+5	GTGCCACCTTCATGTCGTACAACACCATCATCTCGAACTC
FLP a+6	GCTCTCGCTCGACATCGTCAACAAGTCGCTCCAGTTCAAG
FLP a+7	TACAAGACGCAGAAGGCCACCATCCTCGAGGCCTCGCTCA
FLP a-1	GACAAACTGACGCACCAGCACCTTGGGCGGCGTCTTGCAG
FLP a-2	AGAGAGCGATCTTCTCGCCCGAGGGACGCTCGAAGCGCTC
FLP a-3	TGGGTGATCATCCAGCAGAGGTAGGTGAGCTCGGCGGCGC
FLP a-4	GTACGACATGAAGGTGGCACGCTTGATGGCGGTGCCGTTG
FLP a-5	TGACGATGTCGAGCGAGAGCGAGTTCGAGATGATGGTGTT

FLP a-6	GTGGCCTTCTGCGTCTTGTACTTGAACTGGAGCGACTTGT
FLP a-7	CCAGGCGGGGATGAGCTTCTTGAGCGAGGCCTCGAGGATG
FLP b+1	CATCCTCGAGGCCTCGCTCAAGAAGCTCATCCCCGCCTGG
FLP b+2	GAGTTCACCATCATCCCCTACTACGGTCAGAAGCACCAGT
FLP b+3	CGGACATCACCGACATCGTCTCGTCGCTCCAGCTCCAGTT
FLP b+4	CGAGTCGTCGGAAGAGGCCGACAAGGGCAACTCGCACAGC
FLP b+5	AAGAAGATGCTCAAGGCGCTGCTCTCGGAAGGCGAGTCGA
FLP b+6	TCTGGGAGATCACCGAGAAGATCCTCAACTCGTTCGAGTA
FLP b+7	CACCTCGCGCTTCACCAAGACCAAGACGCTCTACCAGTTC
FLP b+8	CTCTTCCTCGCCACCTTCATCAACTGCGGTCGCTTCTCGG
FLP b+9	ACATCAAGAACGTCGACCCCAAGTCGTTCAAGCTCGTCCA
FLP b+10	GAACAAGTACCTCGGCGTCATCATCCAGTGCCTCGTCACC
FLP b+11	GAGACCAAGACCTCGGTCTCGCGCCACATCTACTTTTTCT
FLP b+12	CGGCGCGCGGTCGCATCGACCCGCTCGTCTACCTCGACGA
FLP b+13	GTTCCTGCGCAACTCGGAACCCGTGCTCAAGCGTGTCAAC
FLP b-1	TAGGGGATGATGGTGAACTCCCAGGCGGGGATGAGCTTCT
FLP b-2	GACGATGTCGGTGATGTCCGACTGGTGCTTCTGACCGTAG
FLP b-3	CGGCCTCTTCCGACGACTCGAACTGGAGCTGGAGCGACGA
FLP b-4	AGCGCCTTGAGCATCTTCTTGCTGTGCGAGTTGCCCTTGT
FLP b-5	CTTCTCGGTGATCTCCCAGATCGACTCGCCTTCCGAGAGC
FLP b-6	TCTTGGTGAAGCGCGAGGTGTACTCGAACGAGTTGAGGAT
FLP b-7	ATGAAGGTGGCGAGGAAGAGGAACTGGTAGAGCGTCTTGG
FLP b-8	GGGGTCGACGTTCTTGATGTCCGAGAAGCGACCGCAGTTG
FLP b-9	TGACGCCGAGGTACTTGTTCTGGACGAGCTTGAACGACTT
FLP b-10	GAGACCGAGGTCTTGGTCTCGGTGACGAGGCACTGGATGA
FLP b-11	GTCGATGCGACCGCGCGCCGAGAAAAAGTAGATGTGGCGC
FLP b-12	GTTCCGAGTTGCGCAGGAACTCGTCGAGGTAGACGAGCGG
FLP b-13	GACGACGAGTTACCGGTGCGGTTGACACGCTTGAGCACGG
FLP c+1	CGCACCGGTAACTCGTCGTCGAACAAGCAGGAGTACCAGC
FLP c+2	TGCTCAAGGACAACCTGGTGCGCAGCTACAACAAGGCGCT
FLP c+3	CAAGAAGAACGCTCCCTACTCGATCTTTGCCATCAAGAAC
FLP c+4	GGTCCCAAGTCGCACATCGGTCGTCACCTCATGACCTCGT
FLP c+5	TCCTCTCGATGAAGGGTCTCACCGAGCTCACCAACGTCGT
FLP c+6	CGGCAACTGGTCGGACAAGCGTGCCTCGGCCGTCGCTCGC
FLP c+7	ACCACCTACACCCACCAGATCACCGCCATCCCCGACCACT
FLP c+8	ACTTTGCGCTCGTCTCGCGCTACTACGCCTACGACCCCAT
FLP c+9	CAGCAAGGAGATGATCGCTCTCAAGGACGAGACCAACCCC
FLP c+10	ATCGAGGAGTGGCAGCACATCGAGCAGCTCAAGGGCTCGG
FLP c+11	CCGAGGGCTCGATCCGCTACCCCGCCTGGAACGGCATCAT
FLP c+12	CTCGCAGGAGGTGCTCGACTACCTCTCGTCGTACATCAAC
FLP c-1	CACCAGGTTGTCCTTGAGCAGCTGGTACTCCTGCTTGTTC
FLP c-2	AGTAGGGAGCGTTCTTCTTGAGCGCCTTGTTGTAGCTGCG
FLP c-3	CCGATGTGCGACTTGGGACCGTTCTTGATGGCAAAGATCG
FLP c-4	GAGACCCTTCATCGAGAGGAACGAGGTCATGAGGTGACGA
FLP c-5	GCTTGTCCGACCAGTTGCCGACGACGTTGGTGAGCTCGGT
FLP c-6	ATCTGGTGGGTGTAGGTGGTGCGAGCGACGGCCGAGGCAC
FLP c-7	GCGCGAGACGAGCGCAAAGTAGTGGTCGGGGATGGCGGTG
FLP c-8	GAGCGATCATCTCCTTGCTGATGGGGTCGTAGGCGTAGTA
FLP c-9	ATGTGCTGCCACTCCTCGATGGGGTTGGTCTCGTCCTTGA
FLP c-10	GTAGCGGATCGAGCCCTCGGCCGAGCCCTTGAGCTGCTCG
FLP c-11	AGTCGAGCACCTCCTGCGAGATGATGCCGTTCCAGGCGGG
FLP c-12	GCGGCCGCGATGCGACGGTTGATGTACGACGAGAGGT

* Restriction site sequences are underlined and FRT sequences are shown in blue.

4.4.2 Plasmids and strain constructions

Plasmid **pHwtFRT** contains a *hph* gene whose expression is driven by the *U. maydis hsp70* promoter and a *nos* terminator flanked by directly repeated FTR sites and *Sfi*I sites at both ends. This construct was generated by PCR using primers pBShygfw and pBShygrv (Table 4) and pBS-hhn (Kämper *et al.*, 1995) as template. pBShygfw introduces an *Sfi*I site, 34 nucleotides of the wild type FRT sequence, and 41 nucleotides homologous to the region upstream of the *hsp70* promoter. pBShygrv introduces an *Sfi*I site, 34 nucleotides from the wild type FRT sequence, followed by 40 nucleotides homologous to the 3´ end of the *nos*-terminator. The resulting PCR fragment was cloned into pCRII-TOPO (Invitrogen, Karlsruhe, Germany).

Plasmids **pHFRTm1**, **pHFRTm2**, **pHFRTm3**, and **pHFRTm4** are derivatives of pHwtFRT and were constructed like pHwtFRT utilizing primers containing different mutations in the FRT core sequence (Fig. 9). The corresponding pairs of primers used are shown in Table S1. The *hph* cassette bordered by respective FRT sites was then excised from these plasmids by digestion with *Sfi*I and ligated to 1 kb regions flanking the gene of interest using the protocol for generation of gene replacement mutants in *U. maydis* (Kämper *et al.*, 1995).

pAflpI: The codon-optimized 1272 bp FLP-recombinase gene (Fig. 5) was generated by single step assembly as described (Stemmer *et al*., 1995, Hale and Thompson, 1998). The FLP-recombinase gene including stop codon was generated via ligation of three subfragments, synthesised by PCR from a set of 64 overlapping 40-mer oligonucleotides (except the terminal primers) coding for the plus and minus strands of the synthetic gene, respectively. The FLP recombinase gene was cloned into pCRII-TOPO vector (Invitrogen, Karlsruhe, Germany) yielding pCR-TOPO-FLP and sequenced. The FLP gene was excised as *Nde*I-*Not*I fragment and inserted into pRU11 (Brachmann *et al*., 2001), replacing the *Nde*I-*Not*I fragment harboring the green fluorescent protein gene *gfp*. In the resulting pAflpI plasmid the FLP-recombinase gene is flanked by the *crg1* promoter and the *nos* terminator.

pFLPexpC: From pAflpI, FLP including the *crg1* promoter and the *nos* terminator was amplified by PCR using primers pRU11crgFLPfw and pRU11nosFLPrv (Table 4). Via *Hin*dIII sites introduced with the primers the cassette was excised and cloned into the *Hin*dIII site of the self-replicating plasmid pNEBUC (Weinzierl *et al.*, 2002).

The autonomously replicating recombination reporter plasmid **pIF1** was generated by cloning, a 2.0 kb fragment from p123 (Aichinger *et al.*, 2003) to which wild type FRT sites flanked by *Hind*III sites were added by PCR amplification (using pIF1fw and pIF1rv primers) (see Table 4). This fragment was cloned into the *Hin*dIII restriction site of pNEBUH (Weinzierl *et al.*, 2002), a plasmid harbouring enhanced green fluorescent protein gene *egfp* flanked by the constitutive *o2tef* promoter and the *nos* terminator.

To generate **SG200FLP**, plasmid pAflpI was linearized with *Ssp*I and transformed into *U. maydis* SG200. Carboxin-resistant clones were recovered and single integrations of pAflpI in the carboxin locus were identified by southern blot analysis.

To generate **pYUIF-FRTm2** a 5.2 kb fragment comprising the FLP gene including the *crg1* promoter and *nos* terminator was amplified by PCR from pAflpI using pYUIF-FRTfw/pYUIF-FRTrv primer combination. After digestion with *Bst*EII this fragment was cloned into the *Bst*EII site of pHFRTm2.

To generate **SG200FLPΔ*um01796*$^{\mathbf{FRT/FRT}}$** a 1.0 kb fragment comprising the 5´ flank and a 1.0 kb fragment comprising the 3´ flank of the *um01796* gene were generated by PCR on *U. maydis* SG200 genomic DNA with primer combinations um01796LBfw/um01796LBrv and um01796RBfw/um01796RBrv, respectively (Table 4). The resulting PCR products were digested with *Sfi*I and ligated to the 2.8 kb *Sfi*I hygromycin-resistance cassette carrying wild type *FRT* sites from pHwtFRT. The ligation product was cloned into pCRII-TOPO to yield pΔum01796-hygwtFRT. This plasmid was subsequently used as template to amplify the *um01796* deletion construct with primers um01796nestfw/um01796nestrv (Table 4). The PCR product was transformed into *U. maydis* SG200FLP. Replacement of *um01796* was verified by southern analysis.

To generate **SG200Δ*um01796*$^{\mathbf{FRT/FRT}}$** the *um01796* deletion construct was amplified by PCR with primers um01796nestfw/um01796nestrv (Table 4) using pΔum01796-

hygwtFRT as template. The PCR product was transformed into SG200 and deletion of the *um01796* gene was shown by southern analysis.

To generate strains **SG200Δum11377$^{FRT/FRT}$**, **SG200Δum11377$^{FRTm1/FRTm1}$**, **SG200Δum11377$^{FRTm2/FRTm2}$**, **SG200Δum11377$^{FRTm3/FRTm3}$** and **SG200Δum11377$^{FRTm4/FRTm4}$** 1.0 kb left and right borders flanking the *um11377* gene were amplified by PCR on *U. maydis* SG200 genomic DNA with primer combinations um11377LBfw/um11377LBrv and um11377RBfw/um11377RBrv respectively (Table 4). The resulting PCR products were *Sfi*I digested and ligated to the 2.8 kb *Sfi*I hygromycin-resistance cassettes carrying *FRT* sites from pHwtFRT, pHFRTm1, pHFRTm2, pHFRTm3, and pHFRTm4, respectively. Respective ligation products were cloned into pCRII-TOPO giving rise to pΔum11377-hygwtFRT, pΔum11377-hygFRTm1, pΔum11377-hygFRTm2, pΔum11377-hygFRTm3, and pΔum11377-hygFRTm4 plasmids. Deletion constructs from these plasmids were amplified by PCR, using um11377nestfw/um11377nestrv primers (Table 4) and were transformed into SG200. The deletion of *um11377* was demonstrated by southern blot. The same deletion constructs were transformed into SG200Δum01796^{FRT} giving rise to SG200Δum01796^{FRT}Δum11377$^{FRT/FRT}$, SG200Δum01796^{FRT}Δum11377$^{FRTm1/FRTm1}$, SG200Δum01796^{FRT}Δum11377$^{FRTm2/FRTm2}$, SG200Δum01796^{FRT}Δum11377$^{FRTm3/FRTm3}$, and SG200Δum01796^{FRT}Δum11377$^{FRTm4/FRTm4}$, respectively. Gene replacement was shown by southern analysis.

To generate **SG200Δ01796^{FRT}Δ11377^{FRTm2}Δ03313Δ03314$^{FRTm3/FRTm3}$** a 1.0 kb fragment comprising the left border of *um03313* and a 1.0 kb fragment comprising the right border of the *um03314* gene were generated by PCR on *U. maydis* SG200 genomic DNA with primer combinations um03313LBfw/um03313LBrv and um03314RBfw/um03314RBrv respectively (Table 4). The resulting PCR products were *Sfi*I digested and ligated to the 2.8 kb *Sfi*I hygromycin-resistance cassette carrying mutated FRT sites from pHFRTm3. The ligation product was cloned into pCRII-TOPO to obtain pΔum03313-14-hygFRTm3. This plasmid was subsequently used as a template to amplify the *um03313-um03314* deletion construct with primers

um03313nestfw/um03314nestrv (Table 4). The PCR product was introduced into SG200Δum01796^{FRT}Δum11377^{FRTm2} and homologous recombination was checked by southern analysis.

To generate **SG200Δ01796^{FRT}Δ11377^{FRTm2}Δ03313Δ03314^{FRTm3}Δ02137Δ02138Δ02139Δ02140Δ02141$^{FRTm1/FRTm1}$** a 1.0 kb fragment comprising the left border of the *um02137* and a 1.0 kb fragment comprising right border of the *um02141* gene were generated by PCR on *U. maydis* SG200 genomic DNA with primer combinations um02137LBfw/um02137LBrv and um02141RBfw/um02141RBrv, respectively (Table 4). The resulting PCR products were cut wih *Sfi*I and ligated to the 2.8 kb *Sfi*I hygromycin-resistance cassette carrying mutated FRT sites from pHFRTm1. The ligation product was cloned into pCRII-TOPO to give a rise to pΔum02137-41-hygFRTm1. This plasmid was subsequently used as a template to amplify the *um02137-um02141* deletion construct with primers um02137nestfw/um02141nestrv (Table 4). The PCR product was transformed into SG200Δ01796^{FRT}Δ11377^{FRTm2}Δ03313Δ03314^{FRTm3}. The deletion of the *um02137-um02141* genes was demonstrated by southern analysis.

To generate **SG200Δum01796^{FRT}Δum11377^{FRTm2}Δum02137Δum02138Δum02139Δum02140$^{FRTm1/FRTm1}$** a 1.0 kb fragment comprising the left border of *um02137* and a 1.0 kb fragment comprising the right border of the *um02140* gene were amplified by PCR on *U. maydis* SG200 genomic DNA with primer combinations um02137LBfw/um02137LBrv and um02140RBfw/um02140RBrv, respectively (Table 4). The resulting PCR products were digested with *Sfi*I and ligated to the 2.8 kb *Sfi*I hygromycin-resistance cassette carrying mutated FRT sites from pHFRTm1. The ligation product was cloned into pCRII-TOPO to yield to pΔ02137-40-hygFRTm1. This plasmid was subsequently used as a template to amplify the *um02137-um02140* deletion construct with primers um02137nestfw/um02140nestrv (Table 4). The PCR product was transformed into SG200Δ01796^{FRT}Δ11377^{FRTm2}. Homologous recombination was verified by southern analysis.

To generate **SG200Δum01796^{FRT} Δum11377^{FRTm2}Δum03313Δum03314^{FRTm3}Δum02137Δum02138Δum02139Δum02140$^{FRTm1/FRTm1}$** a 1.0 kb fragment comprising the left border of the *um02137* and a 1.0 kb fragment comprising right border of the *um02140* gene were generated by PCR on *U. maydis* SG200 genomic DNA with primer combinations um02137LBfw/um02137LBrv and um02140RBfw/um02140RBrv, respectively (Table 4). The resulting PCR products were cut wih *Sfi*I and ligated to the 2.8 kb *Sfi*I hygromycin-resistance cassette carrying mutated FRT sites from pHFRTm1. The ligation product was cloned into pCRII-TOPO to give a rise to pΔum02137-40-hygFRTm1. This plasmid was subsequently used as a template to amplify the *um02137-um02140* deletion construct with primers um02137nestfw/um02140nestrv (Table 4). The PCR product was transformed into SG200Δ01796^{FRT}Δ11377^{FRTm2}Δ03313Δ03314^{FRTm3}. The deletion of the *um02137-um02140* genes was demonstrated by southern analysis.

To generate **SG200Δum01796^{FRT}Δum11377^{FRTm2}Δum03313Δum03314^{FRTm3}Δum02135Δum02136Δum02137Δum02138Δum02139Δum02140Δum02141^{FRTm1}** a 1.0 kb fragment comprising the left border of *um02135* and a 1.0 kb fragment comprising the right border of the *um02141* gene were generated by PCR on *U. maydis* SG200 genomic DNA with primer combinations um02135LBfw/um02135LBrv and um02141RBfw/um02141RBrv, respectively (Table 4). The resulting PCR products were cut with *Sfi*I and ligated to the 2.8 kb *Sfi*I hygromycin-resistance cassette carrying mutated FRT sites from pHFRTm1. The ligation product was cloned into pCRII-TOPO to give a rise to pΔ02135-41-hygFRTm4. This plasmid was subsequently used as a template to amplify the *um02135-41* deletion construct with primers um02135nestfw/um02141nestrv (Table 4). The resulting PCR fragment was then used for transformation of SG200Δum01796^{FRT} Δum11377^{FRTm2}Δum03313Δum03314^{FRTm3}Δum02137Δum02138Δum02139Δum02140^{FRTm1} Replacement of the whole cluster was shown by southern analysis.

To generate **SG200pYUIF-FRTm2Δ*um01796*** a 1.0 kb fragment comprising the 5´ flank and a 1.0 kb fragment comprising the 3´ flank of the *um01796* gene were

generated by PCR on *U. maydis* SG200 genomic DNA with primer combinations um01796LBfw/um01796LBrv and um01796RBfw/um01796RBrv, respectively (Table 4). The resulting PCR products were digested with *Sfi*I and ligated to the 8 kb *Sfi*I hygromycin-resistance cassette carrying FRTm2 sites from pYUIF-FRTm2. The ligation product was cloned into pCRII-TOPO to yield pΔum01796-pYUIF-FRTm2. This plasmid was subsequently used as template to amplify the *um01796* deletion construct with primers um01796nestfw/um01796nestrv (Table 4). The PCR product was transformed into *U. maydis* SG200. Replacement of *um01796* was verified by southern analysis.

For complementation analysis, plasmid p01796com was constructed by replacing the 1.8 kb *Nde*I-*Not*I *o2tef-egfp* fragment of p123 with a 2.7 kb *Nde*I-*Not*I fragment comprising the *um01796* gene together with 1.3 kb region located upstream of the start codon. This fragment was amplified by PCR from SG200 DNA with um01796comfw and um01796comrv primers (Table 4) and digested with *NdeI* and *NotI*. p01794com was linearized by *Ssp*I and transformed into SG200Δ01796Δ11377^{FRTm2}Δ03313Δ03314^{FRTm3}Δ02137Δ02138Δ02139Δ02140Δ02141$^{FRTm1/FRTm1}$. Carboxin-resistant clones were recovered, and integration of the *um01796* gene into the *ip* locus (Loubradou *et al.*, 2001) was shown by southern analysis. Strain **SG200eff1Δ1,2,3,4,7,8,9,10,11-1** contains a single copy integration of *um01796* in the *ip* locus.

To obtain plasmid p02138com, a 2.1 kb *Nde*I-*Bam*HI fragment comprising the *um02138* gene and 0.7 kb sequence upstream of the start codon was ligated into the respective sites of p123. This fragment was generated by PCR using um02138comfw and um02138comrv primers (Table 4) and *U. maydis* SG200 genomic DNA. p02138com was linearized by *Ssp*I and transformed into SG200Δ9. Carboxin-resistant clones were recovered, and integration of the *um02138* into the *ip* locus was verified by southern analysis. Strain **SG200eff1Δ1,2,3,4,7,8,9,10,11-8** bears a single copy integration of the *um02138* gene.

For construction of the p02137-02140com plasmid 4.8 kb from pBScbx(-) (Keon *et al.*, 1991) was amplified by PCR with cbxfw1/cbxrv1 primers (Table 4), which introduced *Pac*I restriction sites at both ends of the PCR fragment. After digestion

with *Pac*I, this fragment was ligated with a 8.0 kb *Pac*I digested PCR product comprising the four genes *um02137*, *um02138*, *um02139*, *um02140* together with 0.6 kb region upstream of the *um02140* start codon. This fragment was generated by PCR using um02137comfw and um02140comrv primers (Table 4) and *U. maydis* SG200 genomic DNA. The complementation strain **SG200eff1Δ1,2,3,4,7,8,9,10,11-7,8,9,10** was generated by transforming SG200Δ9 with *Ssp*I-linearized p02137-02140com. Carboxin-resistant clones were recovered, and single integration of the *um02137* – *um02140* genes into the *ip* locus was demonstrated by southern analysis.

4.4.3 Isolation of nucleic acids

4.4.3.1 Isolation of E. coli plasmid DNA

E. coli plasmid minipreparation was performed via "lysis by boiling" as previously described in Sambrook *et al*. (1989). *E. coli* culture grown at 37°C and 180 rpm overnight was transferred to a 1.5-ml microcentrifuge tube and centrifuged for 1 min at 13,000 rpm. The supernatant was discarded and the cell pellet was resuspended in 300 µl of STET and 20 µl of lysozyme solution using a Vibrax-VXR shaker (IKA), and incubated for 1 min at 95°C. To pellet the cell debris, the *E. coli* lysate was centrifuged for 15 min at 13,000 rpm, and cell debris was removed using a sterile tooth stick. To precipitate plasmid DNA, 40 µl of 3 M sodium acetate (pH 4.8) and 400 µl of isopropanol were added. The mixture was incubated at room temperature for 5 min followed by centrifugation for 5 min at 13,000 rpm. The supernatant was discarded, the DNA pellet was washed with 70% ethanol and air dried for 5 min. The DNA pellet was dissolved in 100 µl TE buffer containing 20 µg/ml RNase A, and incubated in a heating block at 50°C with gentle shaking for 20 min.

STET	50 mM Tris-Cl, pH 8.0 50 mM Na_2-EDTA 8% (w/v) Sucrose 5% (v/v) Triton X-100 in dH_2O
Lysozyme solution	10 mg/ml Lysozyme 10mM Tris-Cl, pH 8.0 in dH_2O

4.4.3.2 Isolation of genomic DNA from U. maydis

U. maydis cultures grown in YEPSL at 28°C and 200 rpm overnight were transferred to 2-ml microcentrifuge tubes containing 300 mg glass beads, and centrifuged for 2 min at 13,000 rpm. The supernatant was discarded and 400 µl of *Ustilago*-lysis buffer and 500 µl of TE-phenol/chloroform was added and shaken for 10-15 min on a Vibrax-VXR shaker (IKA) set to 1,400. Next, samples were centrifuged for 15 min at 13,000 rpm, and 400 µl of the aqueous phase was transferred to a new 1.5-ml microcentrifuge tube. Afterwards, 1 ml of ethanol was added and mixed by inverting 2 - 3 times, and incubated at the room temperature for about 5 min. Subsequently the mixtures were centrifuged for 15 min at 13,000 rpm. The DNA pellets were washed once with 70% ethanol and air dried for 5 - 10 min. Finally, DNA pellets were dissolved in 50 µl TE buffer containing 20 µg/ml RNase A, and incubated in a heating block at 50°C with gentle shaking for 20 min. Genomic DNA was stored at - 20°C.

***Ustilago*-lysis buffer**	50 mM Tris-Cl, pH 7.5 50 mM Na_2-EDTA 1% (w/v) SDS in dH_2O
TE-phenol/chloroform	Mixture of phenol (in TE-buffer) and chloroform in an 1:1 ratio

4.4.3.3 U. maydis total RNA isolation from axenic culture

Trizol reagent (Invitrogen, Karlsruhe, Germany) was used for total RNA isolation as described by the manufacturer. 50 ml of *U. maydis* overnight culture having a cell density of OD_{600} 0.8 - 1.0 was harvested by centrifugation at 3,200 rpm for 5 min. The pellet was resuspended in 1.0 ml Trizol reagent and transferred to 2-ml microcentrifuge tube containing 300 mg of glass beads and homogenized with a cell mill (Retsch MM200) for 5 min. Then samples were incubated for 5 min at room temperature. After 200 µl of chloroform was added to the samples they were shaken for 15 sec and incubated for an additional 2-3 min. Samples were centrifuged at 4°C for 15 min at 11,500 rpm. The upper aqueous phase (500 µl) was transferred to a 1.5-ml RNase free microcentrifuge tube. RNA was precipitated by addition of 500 µl isopropanol and incubated for 10 min at room temperature. After centrifugation at

4°C for 10 min at 11,500 rpm the pellets were washed once with 1 ml of 70% ethanol, centrifuged at 7,500g for 5 min and air dried. Finally, the RNA pellet was dissolved in 50 µl RNase free water and incubated in a heating block at 55°C with gentle shaking for 20 min.

4.4.3.4 Total RNA isolation from infected plant material

For the isolation of total RNA from *U. maydis* infected plant tissue, tested strains were inoculated into the corn variety Early Golden Bantam as described in the section entitled "Plant infection assay". Infected leaf tissue was harvested at 3, 5, and 8 dpi as well as uninfected plant tissue was harvested at 12 dpi. In all cases, three independently conducted experiments (biological replicates) were carried out for RNA isolation. Infected leaf tissue were removed from plants, stored in 50 ml Falcon tubes, flash frozen in liquid nitrogen, and directly used for RNA isolation or stored at -80°C for later use. Total RNA was extracted from frozen homogenized infected plant tissue using Trizol reagent (Invitrogen, Karlsruhe, Germany) as described in the previous section "*U. maydis* total RNA isolation from axenic culture".

4.4.4 Nucleic acid blotting and hybridization (DIG-labeling)

4.4.4.1 DNA blotting and hybridization (Southern analysis)

A total of 20-30 µg of genomic DNA was digested using 5-10 U of the respective restriction enzyme/s in a total volume of 20 µl overnight. Digestions were separated on a 1X TAE 0.8% agarose gel for 14 - 16 h at 19V. The gel was incubated in 0.25 M HCl for 20-30 min, and then placed in 0.25 M NaOH for 20-30 min. Labeling reactions were carried out as described in the DIG-High Prime protocol (Roche, Mannhein, Germany). The nucleic acid fragments were transferred to a positively charged nylon membrane (Hybond-N+, GE Healthcare München, Germany) by capillary blotting overnight with 0.25 M NaOH. In a parallel experiment, 1.5 µg of DIG-labeled DNA fragments (in a total volume of 10 µl) were denatured at 99°C for 10 min, briefly centrifuged and put on ice. Next, the transfer membrane was prehybridized with 40 ml of Southern-hybridization buffer at 65°C in a hybridization oven for 15-30 min. After the prehybridization solution was discarded 10 µl of labeled probe in 20 ml of Southern hybridization buffer was added to the membrane followed by incubation at 65°C overnight in a hybridization oven. Next, the probe was discarded and the membrane was washed twice for 5 min with 20 ml DIG-Wash

buffer (0.3% (v/v) of Tween-20 in DIG1) at 25°C. The following steps were carried out at 25°C: incubation for 30 min with 25 ml of DIG2 (10x blocking solution in DIG1 (1:10)), incubation for 30 min with 10 ml of Anti-DIG antibody solution (1:5000 in DIG2), two incubations for 15 min with DIG-Wash, and finally incubation for 5 min with 40 ml of DIG3 followed by incubation for 5 min with 10 ml of CDP-Star solution (100 µl CDP-Star in 10 ml DIG3 (1:100)). The membrane was sealed in a plastic bag and incubated at 37 °C for 15 min. It was exposed to the Kodak XAR-5 film.

Southern hybridization buffer	500 mM Na-phosphate buffer, pH 7.0 7% (w/v) SDS in dH_2O
Southern wash buffer	0.1 M Na-phosphate buffer, pH 7.0 1% (w/v) SDS in dH_2O
1 M Na-phosphate buffer, pH 7.0	Solution 1: 1 M Na_2HPO_4 Solution 2: 1 M $NaH_2PO_4xH_2O$ Add Solution 2 to Solution 1 until pH will reach 7.0 In dH_2O
DIG1 (1x)	0.1 M maleic acid 0.15 M NaCl in dH_2O, adjust pH to 7.5 (NaOH)
DIG2 (1x)	1% (w/v) milk powder in DIG1
DIG3 (1x)	0.1 M maleic acid 0.1 M NaCl 0.05 M $MgCl_2x6H_2O$ in dH_2O, adjust pH to 9.5 (Tris-HCl)

CDP-Star Solution	100 µl of CDP-Star (Roche) in 10 ml DIG3

4.4.4.2 RNA blotting and hybridization (northern analysis)

To determine the expression level of the codon-optimized FLP gene, RNA blotting and hybridization was performed. For the induction of the *crg1* promoter cells were grown in CM-glu medium to an OD_{600} of 0.7, washed twice with distilled water, resuspended in CM medium containing 1% arabinose as sole carbon source (CM-ara) and incubated for the times indicated. Total RNA was denatured in 1x MOPS, 0.8 M glyoxal, 50% (v/v) DMSO, incubated at 50°C for 1 h and separated by electrophoresis in a 1x MOPS 1% agarose gel for 3 h at 80V at circulated buffer reservoir. The RNA gel was saturated in 20x SSC buffer for 1 h and blotted to a Hybond-NX membrane (Amersham Biosciences). The hybridization and further steps were similarly performed as described in "DNA-blotting and hybridization", with the exception of Northern hybridization and Northern wash buffers replacing the Southern hybridization and Southern wash buffers. To detect FLP, a 1.3 kb fragment was generated by PCR, using a combination of M13fw and M13rv primers (Invitrogen, Karlsruhe, Germany) and pCR-TOPO-FLP as a template.

10x MOPS buffer	200 mM MOPS 80 mM Na-acetate 10 mM Na2-EDTA x2H_2O in dH_2O, adjust to pH 7.0 (5M NaOH)
20x SSC buffer	3 M NaCl 0.3 M Na-citrate x2H_2O in dH_2O, adjust to pH 7.0 (HCl)
Northern wash buffer	5% (v/v) 20x SSC 25% (v/v) 20% SDS in dH_2O

Northern hybridization buffer	5% (v/v) 1 M Na-phosphate buffer, pH 7.0 5% (v/v) 1 M PIPES 2% (v/v) 5 M NaCl 25% (v/v) 20% SDS 0.2% (v/v) 0.5 M EDTA, in dH_2O pH 8.0

4.4.5 PCR techniques

4.4.5.1 Polymerase Chain Reaction (PCR)

This method is modified from Innis *et al*. (1990). A standard PCR reaction (25 µl of a total volume) consists of about 10 ng of a template DNA, a pair of primers (1 µM), dNTPs (200 µM), and 1-2 U of polymerase. All PCR reactions were performed using a Thermocycler PTC-100 or PTC-200 (MJ Research). PCR reactions with Phusion High-Fidelity DNA Polymerase (Finnzymes, Frankfurt am Main, Germany) and KOD Extreme Polymerase (Merck, Darmstadt, Germany) were performed according to the manufacturer´s protocol. All PCR products were purified using the QiaQuick PCR Purification kit (Qiagen, Hilden, Germany). The strategy for the PCR assembly of the codon-optimized FLP-recombinase gene followed Stemmer *et al.* (1995) and Hale & Thompson (1998). Primers used to synthesize FLP gene are shown in Table 4.

4.4.5.2 Quantitative Real-Time-PCR

To determine the expression patterns of *eff1* genes by quantitative PCR, cells of SG200 were grown in axenic culture and harvested at an OD_{600} of 0.8 after incubation in YEPSL for 12 – 14 h in three independently conducted experiments. Cells were flash frozen in liquid nitrogen and stored at -80°C until use. To analyze expression levels of family *eff1* genes during different biotrophic stages, 7 day old maize seedlings were infected with SG200. Samples of the infected tissue (about 1000 mg) were collected in three independently performed experiments 1 day post infection (dpi) as well as 3, 5 and 8 dpi and directly frozen in liquid nitrogen. To test the expression of the *eff1* genes in uninfected maize plant material from 12 days old plants was used for the RNA preparation. Total RNA was prepared following the TRIZOL reagent protocol (Invitrogen, Karlsruhe, Germany). To remove traces of DNA, RNA samples were treated with Turbo DNA-free kit (Ambion/Applied Biosystems, Darmstadt, Germany) according to the manufacturer´s protocol. RNA

was purified using an RNeasy kit (Qiagen, Hilden, Germany). Purity and quantity of RNA samples were measured using the NanoDrop ND-1000 spectrophotometer (NanoDrop Technologies, Wilmington, DE, USA). Synthesis of cDNA was performed by random hexamer priming employing the SuperScript III first-strand synthesis SuperMix kit (Invitrogen, Karlsruhe, Germany) as outlined in the manufacturer´s protocol. The reaction was performed with 1.0 µg of total RNA. Quantitative Real-Time-PCR was performed on a Bio-Rad iCycler using the Platinum SYBR Green qPCR SuperMix-UDG (Invitrogen, Karlsruhe, Germany). The cycling conditions were: 2 min 95°C, followed by 45 cycles of 30 sec 95°C / 30 sec 62°C / 30 sec 72°C. Sequences of primers used for Real-Time-PCR are shown in Table S1. All Real-Time-PCR quantifications were performed using Bio-Rad iCycler iQ system (BioRad, Hercules, USA). A fluorescence threshold value (Ct) was calculated for each sample using the iCycle iQ system software. The levels of each gene expression were standardized to the ppi housekeeping genes (Table 4).

4.5 Bioinformatics

Multiple alignments of *eff1* genes were made in MACAW (Schuler *et al.*, 1991) and signal sequences were predicted with SignalP at www.cbs.dtu.dk/services/SignalP (Bendtsen *et al*., 2004). Sequence logos were generated using a Hidden Markov Model based program named multiple em for motif elucidation (MEME) version 4.3.0. Several bioinformatic analyses were performed within the MPI Bioinformatics Toolkit at http://toolkit.tuebingen.mpg.de/ (Biegert *et al*., 2006). Searches for members of the Eff1 protein family were made by comparison of profile Hidden Markov Models (HMMs) in HHpred (Söding *et al*., 2005). To this end, HMMs were generated for all ORFs of the *U. maydis* genome and are made publicly available for searching at http://toolkit.tuebingen.mpg.de/HHpred/. The cluster analysis was made with CLANS (Frickey & Lupas, 2004).

4.6 Statistical analysis

All results are representative of triplicate experiments. For Real-Time-PCR results, infection data, as well as the FLP-mediated recombination assay on differentially mutated FRT sites Mean ± sd (standard deviation) has been calculated. Student´s t-test was used to assess statistical significance for expression values of *eff1* genes and

infection symptoms caused by the strains tested. Asterisks (*, **, and ***) indicate significant differences at a P value < 0.05, 0.01, 0,001, respectively.

Aichinger C, Hansson K, Eichhorn H, Lessing F, Mannhaupt G, Mewes W, Kahmann R. 2003. Identification of plant-regulated genes in *Ustilago maydis* by enhancer-trapping mutagenesis. *Mol Genet Genomics* **270**(4): 303-314.

Andrews BJ, McLeod M, Broach J, Sadowski PD. 1986. Interaction of the FLP recombinase of the *Saccharomyces cerevisiae* 2 micron plasmid with mutated target sequences. *Mol Cell Biol* **6**(7): 2482-2489.

Angot A, Peeters N, Lechner E, Vailleau F, Baud C, Gentzbittel L, Sartorel E, Genschik P, Boucher C, Genin S. 2006. *Ralstonia solanacearum* requires F-box-like domain-containing type III effectors to promote disease on several host plants. *Proc Natl Acad Sci U S A* **103**(39): 14620-14625.

Ausubel MA, Brent R, Kingston RE, Moore DD, Seidmann JG, Smith JA. 1987. Current protocols in molecular biology. (John & Sons, Inc.).

Babineau D, Vetter D, Andrews BJ, Gronostajski RM, Proteau GA, Beatty LG, Sadowski PD. 1985. The FLP protein of the 2-micron plasmid of yeast. Purification of the protein from Escherichia coli cells expressing the cloned FLP gene. *J Biol Chem* **260**(22): 12313-12319.

Baker B, Zambryski P, Staskawicz B, Dinesh-Kumar SP. 1997. Signaling in plant-microbe interactions. *Science* **276**(5313): 726-733.

Banuett F, Herskowitz I. 2002. Bud morphogenesis and the actin and microtubule cytoskeletons during budding in the corn smut fungus, *Ustilago maydis*. *Fungal Genet Biol* **37**(2): 149-170.

Barekzi N, Beinlich K, Hoang TT, Pham XQ, Karkhoff-Schweizer R, Schweizer HP. 2000. High-frequency flp recombinase-mediated inversions of the oriC-containing region of the *Pseudomonas aeruginosa* genome. *J Bacteriol* **182**(24): 7070-7074.

Barrett AR, Kang Y, Inamasu KS, Son MS, Vukovich JM, Hoang TT. 2008. Genetic tools for allelic replacement in *Burkholderia* species. *Appl Environ Microbiol* **74**(14): 4498-4508.

Bent AF, Mackey D. 2007. Elicitors, effectors, and R genes: the new paradigm and a lifetime supply of questions. *Annu Rev Phytopathol* **45**: 399-436.

Birch PR, Armstrong M, Bos J, Boevink P, Gilroy EM, Taylor RM, Wawra S, Pritchard L, Conti L, Ewan R, Whisson SC, van West P, Sadanandom A, Kamoun S. 2009. Towards understanding the virulence functions of RXLR effectors of the oomycete plant pathogen *Phytophthora infestans*. *J Exp Bot* **60**(4): 1133-1140.

Birch PR, Boevink PC, Gilroy EM, Hein I, Pritchard L, Whisson SC. 2008. Oomycete RXLR effectors: delivery, functional redundancy and durable disease resistance. *Curr Opin Plant Biol* **11**(4): 373-379.

Birch PR, Rehmany AP, Pritchard L, Kamoun S, Beynon JL. 2006. Trafficking arms: oomycete effectors enter host plant cells. *Trends Microbiol* **14**(1): 8-11.

Birling MC, Gofflot F, Warot X. 2009. Site-specific recombinases for manipulation of the mouse genome. *Methods Mol Biol* **561**: 245-263.

Bischof J, Basler K. 2008. Recombinases and their use in gene activation, gene inactivation, and transgenesis. *Methods Mol Biol* **420**: 175-195.

Boller T, Felix G. 2009. A renaissance of elicitors: perception of microbe-associated molecular patterns and danger signals by pattern-recognition receptors. *Annu Rev Plant Biol* **60**: 379-406.

Boller T, He SY. 2009. Innate immunity in plants: an arms race between pattern recognition receptors in plants and effectors in microbial pathogens. *Science* **324**(5928): 742-744.

Bolton MD, van Esse HP, Vossen JH, de Jonge R, Stergiopoulos I, Stulemeijer IJ, van den Berg GC, Borras-Hidalgo O, Dekker HL, de Koster CG, de Wit PJ, Joosten MH, Thomma BP. 2008. The novel *Cladosporium fulvum* lysin motif effector Ecp6 is a virulence factor with orthologues in other fungal species. *Mol Microbiol* **69**(1): 119-136.

Brachmann A, Konig J, Julius C, Feldbrugge M. 2004. A reverse genetic approach for generating gene replacement mutants *in Ustilago maydis*. *Mol Genet Genomics* **272**(2): 216-226.

Brachmann A, Weinzierl G, Kamper J, Kahmann R. 2001. Identification of genes in the bW/bE regulatory cascade in *Ustilago maydis*. *Mol Microbiol* **42**(4): 1047-1063.

Branda CS, Dymecki SM. 2004. Talking about a revolution: The impact of site-specific recombinases on genetic analyses in mice. *Dev Cell* **6**(1): 7-28.

Brefort T, Doehlemann G, Mendoza-Mendoza A, Reissmann S, Djamei A, Kahmann R. 2009. *Ustilago maydis* as a Pathogen. *Annu Rev Phytopathol* **47**: 423-445.

Buchholz F, Ringrose L, Angrand PO, Rossi F, Stewart AF. 1996. Different thermostabilities of FLP and Cre recombinases: implications for applied site-specific recombination. *Nucleic Acids Res* **24**(21): 4256-4262.

Bucholtz F. 2008. Principles of site-specific recombinase (SSR) technology. *J Vis Exp*(15).

Calderone TL, Stevens RD, Oas TG. 1996. High-level misincorporation of lysine for arginine at AGA codons in a fusion protein expressed in *Escherichia coli*. *J Mol Biol* **262**(4): 407-412.

Catanzariti AM, Dodds PN, Lawrence GJ, Ayliffe MA, Ellis JG. 2006. Haustorially expressed secreted proteins from flax rust are highly enriched for avirulence elicitors. *Plant Cell* **18**(1): 243-256.

Chen Y, Rice PA. 2003. New insight into site-specific recombination from Flp recombinase-DNA structures. *Annu Rev Biophys Biomol Struct* **32**: 135-159.

Chisholm ST, Coaker G, Day B, Staskawicz BJ. 2006. Host-microbe interactions: shaping the evolution of the plant immune response. *Cell* **124**(4): 803-814.

Conant GC, Wolfe KH. 2008. Turning a hobby into a job: how duplicated genes find new functions. *Nat Rev Genet* **9**(12): 938-950.

Dangl JL, Jones JD. 2001. Plant pathogens and integrated defence responses to infection. *Nature* **411**(6839): 826-833.

Datsenko KA, Wanner BL. 2000. One-step inactivation of chromosomal genes in *Escherichia coli* K-12 using PCR products. *Proc Natl Acad Sci U S A* **97**(12): 6640-6645.

Davis RP, Costa M, Grandela C, Holland AM, Hatzistavrou T, Micallef SJ, Li X, Goulburn AL, Azzola L, Elefanty AG, Stanley EG. 2008. A protocol for removal of antibiotic resistance cassettes from human embryonic stem cells genetically modified by homologous recombination or transgenesis. *Nat Protoc* **3**(10): 1550-1558.

de Jonge R, Thomma BP. 2009. Fungal LysM effectors: extinguishers of host immunity? *Trends Microbiol* **17**(4): 151-157.

Di Paolo G, De Camilli P. 2006. Phosphoinositides in cell regulation and membrane dynamics. *Nature* **443**(7112): 651-657.

Doehlemann G, van der Linde K, Assmann D, Schwammbach D, Hof A, Mohanty A, Jackson D, Kahmann R. 2009. Pep1, a secreted effector protein

of *Ustilago maydis*, is required for successful invasion of plant cells. *PLoS Pathog* **5**(2): e1000290.

Doehlemann G, Wahl R, Horst RJ, Voll LM, Usadel B, Poree F, Stitt M, Pons-Kuhnemann J, Sonnewald U, Kahmann R, Kamper J. 2008. Reprogramming a maize plant: transcriptional and metabolic changes induced by the fungal biotroph *Ustilago maydis*. *Plant J* **56**(2): 181-195.

Dou D, Kale SD, Wang X, Chen Y, Wang Q, Jiang RH, Arredondo FD, Anderson RG, Thakur PB, McDowell JM, Wang Y, Tyler BM. 2008. Conserved C-terminal motifs required for avirulence and suppression of cell death by *Phytophthora sojae* effector Avr1b. *Plant Cell* **20**(4): 1118-1133.

Doublet B, Douard G, Targant H, Meunier D, Madec JY, Cloeckaert A. 2008. Antibiotic marker modifications of lambda Red and FLP helper plasmids, pKD46 and pCP20, for inactivation of chromosomal genes using PCR products in multidrug-resistant strains. *J Microbiol Methods* **75**(2): 359-361.

Drobak BK, Ferguson IB, Dawson AP, Irvine RF. 1988. Inositol-Containing Lipids in Suspension-Cultured Plant Cells: An Isotopic Study. *Plant Physiol* **87**(1): 217-222.

Drobak BK, Franklin-Tong VE, Staiger CJ. 2005. The role of the actin cytoskeleton in plant cell signaling. *New Phytol* **163**: 13-30.

Ellis JG, Rafiqi M, Gan P, Chakrabarti A, Dodds PN. 2009. Recent progress in discovery and functional analysis of effector proteins of fungal and oomycete plant pathogens. *Curr Opin Plant Biol* **12**(4): 399-405.

Fladung M, Becker D. 2010. Targeted integration and removal of transgenes in hybrid aspen (*Populus tremula* L. x *P. tremuloides* Michx.) using site-specific recombination systems. *Plant Biol (Stuttg)* **12**(2): 334-340.

Fladung M, Schenk TMH, Polak O, Becker D. 2009. Elimination of marker genes and targeted integration via FLP/FRT recombination system from yeast in hybrid aspen (*Populus tremula* L. x *P. tremuloides* Michx.). *Tree Genetics & Genomes* **6**(2): 205 - 207.

Flor HH. 1942. Inheritance of pathogenicity in *Melampsora lini*. *Phytopathology* **32**: 653-669.

Forment JV, Ramon D, MacCabe AP. 2006. Consecutive gene deletions in *Aspergillus nidulans*: application of the Cre/loxP system. *Curr Genet* **50**(3): 217-224.

Glazebrook J. 2005. Contrasting mechanisms of defense against biotrophic and necrotrophic pathogens. *Annu Rev Phytopathol* **43**: 205-227.

Göhre V, Robatzek S. 2008. Breaking the barriers: microbial effector molecules subvert plant immunity. *Annu Rev Phytopathol* **46**: 189-215.

Gold SE, Bakkeren G, Davies JE, Kronstad JW. 1994. Three selectable markers for transformation of *Ustilago maydis*. *Gene* **142**(2): 225-230.

Grant MR, Jones JD. 2009. Hormone (dis)harmony moulds plant health and disease. *Science* **324**(5928): 750-752.

Greenberg JT, Yao N. 2004. The role and regulation of programmed cell death in plant-pathogen interactions. *Cell Microbiol* **6**(3): 201-211.

Gronostajski RM, Sadowski PD. 1985. The FLP recombinase of the *Saccharomyces cerevisiae* 2 microns plasmid attaches covalently to DNA via a phosphotyrosyl linkage. *Mol Cell Biol* **5**(11): 3274-3279.

Haas BJ, Kamoun S, Zody MC, Jiang RH, Handsaker RE, Cano LM, Grabherr M, Kodira CD, Raffaele S, Torto-Alalibo T, Bozkurt TO, Ah-Fong AM, Alvarado L, Anderson VL, Armstrong MR, Avrova A, Baxter L, Beynon

J, Boevink PC, Bollmann SR, Bos JI, Bulone V, Cai G, Cakir C, Carrington JC, Chawner M, Conti L, Costanzo S, Ewan R, Fahlgren N, Fischbach MA, Fugelstad J, Gilroy EM, Gnerre S, Green PJ, Grenville-Briggs LJ, Griffith J, Grunwald NJ, Horn K, Horner NR, Hu CH, Huitema E, Jeong DH, Jones AM, Jones JD, Jones RW, Karlsson EK, Kunjeti SG, Lamour K, Liu Z, Ma L, Maclean D, Chibucos MC, McDonald H, McWalters J, Meijer HJ, Morgan W, Morris PF, Munro CA, O'Neill K, Ospina-Giraldo M, Pinzon A, Pritchard L, Ramsahoye B, Ren Q, Restrepo S, Roy S, Sadanandom A, Savidor A, Schornack S, Schwartz DC, Schumann UD, Schwessinger B, Seyer L, Sharpe T, Silvar C, Song J, Studholme DJ, Sykes S, Thines M, van de Vondervoort PJ, Phuntumart V, Wawra S, Weide R, Win J, Young C, Zhou S, Fry W, Meyers BC, van West P, Ristaino J, Govers F, Birch PR, Whisson SC, Judelson HS, Nusbaum C. 2009. Genome sequence and analysis of the Irish potato famine pathogen *Phytophthora infestans*. *Nature* **461**(7262): 393-398.

Hacking DF. 2008. 'Knock, and it shall be opened': knocking out and knocking in to reveal mechanisms of disease and novel therapies. *Early Hum Dev* **84**(12): 821-827.

Hahn M, Neef U, Struck C, Gottfert M, Mendgen K. 1997. A putative amino acid transporter is specifically expressed in haustoria of the rust fungus *Uromyces fabae*. *Mol Plant Microbe Interact* **10**(4): 438-445.

Hale RS, Thompson G. 1998. Codon optimization of the gene encoding a domain from human type 1 neurofibromin protein results in a threefold improvement in expression level in *Escherichia coli*. *Protein Expr Purif* **12**(2): 185-188.

Hare PD, Chua NH. 2002. Excision of selectable marker genes from transgenic plants. *Nat Biotechnol* **20**(6): 575-580.

Heath MC. 2000. Hypersensitive response-related death. *Plant Mol Biol* **44**(3): 321-334.

Hiller NL, Bhattacharjee S, van Ooij C, Liolios K, Harrison T, Lopez-Estrano C, Haldar K. 2004. A host-targeting signal in virulence proteins reveals a secretome in malarial infection. *Science* **306**(5703): 1934-1937.

Hoess R, Abremski K, Irwin S, Kendall M, Mack A. 1990. DNA specificity of the Cre recombinase resides in the 25 kDa carboxyl domain of the protein. *J Mol Biol* **216**(4): 873-882.

Hoffman CS, Winston F. 1987. A ten-minute DNA preparation from yeast efficiently releases autonomous plasmids for transformation of *Escherichia coli*. *Gene* **57**(2-3): 267-272.

Holliday R. 1964. The Induction of Mitotic Recombination by Mitomycin C in *Ustilago* and *Saccharomyces*. *Genetics* **50**: 323-335.

Holliday R. 1974. *Ustilago maydis*. *Handbook of genetics edited by R. C. King* **1**: 575 - 595.

Hu Q, Nelson K, Luo H. 2006. FLP-mediated site-specific recombination for genome modification in turfgrass. *Biotechnol Lett* **28**(22): 1793-1804.

James TY, Kauff F, Schoch CL, Matheny PB, Hofstetter V, Cox CJ, Celio G, Gueidan C, Fraker E, Miadlikowska J, Lumbsch HT, Rauhut A, Reeb V, Arnold AE, Amtoft A, Stajich JE, Hosaka K, Sung GH, Johnson D, O'Rourke B, Crockett M, Binder M, Curtis JM, Slot JC, Wang Z, Wilson AW, Schussler A, Longcore JE, O'Donnell K, Mozley-Standridge S, Porter D, Letcher PM, Powell MJ, Taylor JW, White MM, Griffith GW, Davies DR, Humber RA, Morton JB, Sugiyama J, Rossman AY, Rogers

JD, Pfister DH, Hewitt D, Hansen K, Hambleton S, Shoemaker RA, Kohlmeyer J, Volkmann-Kohlmeyer B, Spotts RA, Serdani M, Crous PW, Hughes KW, Matsuura K, Langer E, Langer G, Untereiner WA, Lucking R, Budel B, Geiser DM, Aptroot A, Diederich P, Schmitt I, Schultz M, Yahr R, Hibbett DS, Lutzoni F, McLaughlin DJ, Spatafora JW, Vilgalys R. 2006. Reconstructing the early evolution of Fungi using a six-gene phylogeny. *Nature* **443**(7113): 818-822.

Jia Y, McAdams SA, Bryan GT, Hershey HP, Valent B. 2000. Direct interaction of resistance gene and avirulence gene products confers rice blast resistance. *Embo J* **19**(15): 4004-4014.

Jiang RH, Tripathy S, Govers F, Tyler BM. 2008. RXLR effector reservoir in two *Phytophthora* species is dominated by a single rapidly evolving superfamily with more than 700 members. *Proc Natl Acad Sci U S A* **105**(12): 4874-4879.

Jones JD, Dangl JL. 2006. The plant immune system. *Nature* **444**(7117): 323-329.

Kahmann R, Rudt F, Koch C, Mertens G. 1985. G inversion in bacteriophage Mu DNA is stimulated by a site within the invertase gene and a host factor. *Cell* **41**(3): 771-780.

Kahmann R, Steinberg G, Basse CW, Feldbrügge M, Kämper J. 2000. *Ustilago maydis*, the causative agent of corn smut disease. *Fungal Pathology Kluwer Academic Publishers. Dodrecht. The Netherlands. Kronstad, J. W. (ed.) 347-371*

Kale SD, Gu B, Capelluto DGS, Dou D, Feldman E, Rumore A, Arredonado FD, Hanlon R, Fudal I, Rouxel T, Lawrence CB, Shan W, Tyler BM. 2010. *External lipid PI-3-P mediates entry of eukaryotic effectors into plant and animal host cells. Cell.* In press.

Kaku H, Nishizawa Y, Ishii-Minami N, Akimoto-Tomiyama C, Dohmae N, Takio K, Minami E, Shibuya N. 2006. Plant cells recognize chitin fragments for defense signaling through a plasma membrane receptor. *Proc Natl Acad Sci U S A* **103**(29): 11086-11091.

Kamoun S. 2006. A catalogue of the effector secretome of plant pathogenic oomycetes. *Annu Rev Phytopathol* **44**: 41-60.

Kamoun S. 2007. Groovy times: filamentous pathogen effectors revealed. *Curr Opin Plant Biol* **10**(4): 358-365.

Kamoun S, Goodwin SB. 2007. Fungal and oomycete genes galore. *New Phytol* **174**(4): 713-717.

Kämper J. 2004. A PCR-based system for highly efficient generation of gene replacement mutants in *Ustilago maydis*. *Mol Genet Genomics* **271**(1): 103-110.

Kämper J, Kahmann R, Bolker M, Ma LJ, Brefort T, Saville BJ, Banuett F, Kronstad JW, Gold SE, Muller O, Perlin MH, Wosten HA, de Vries R, Ruiz-Herrera J, Reynaga-Pena CG, Snetselaar K, McCann M, Perez-Martin J, Feldbrugge M, Basse CW, Steinberg G, Ibeas JI, Holloman W, Guzman P, Farman M, Stajich JE, Sentandreu R, Gonzalez-Prieto JM, Kennell JC, Molina L, Schirawski J, Mendoza-Mendoza A, Greilinger D, Munch K, Rossel N, Scherer M, Vranes M, Ladendorf O, Vincon V, Fuchs U, Sandrock B, Meng S, Ho EC, Cahill MJ, Boyce KJ, Klose J, Klosterman SJ, Deelstra HJ, Ortiz-Castellanos L, Li W, Sanchez-Alonso P, Schreier PH, Hauser-Hahn I, Vaupel M, Koopmann E, Friedrich G, Voss H, Schluter T, Margolis J, Platt D, Swimmer C, Gnirke A, Chen F, Vysotskaia V, Mannhaupt G, Guldener U, Munsterkotter M, Haase D,

Oesterheld M, Mewes HW, Mauceli EW, DeCaprio D, Wade CM, Butler J, Young S, Jaffe DB, Calvo S, Nusbaum C, Galagan J, Birren BW. 2006. Insights from the genome of the biotrophic fungal plant pathogen *Ustilago maydis*. *Nature* **444**(7115): 97-101.

Kämper J, Reichmann M, Romeis T, Bolker M, Kahmann R. 1995. Multiallelic recognition: nonself-dependent dimerization of the bE and bW homeodomain proteins in Ustilago maydis. *Cell* **81**(1): 73-83.

Kane JF. 1995. Effects of rare codon clusters on high-level expression of heterologous proteins in *Escherichia coli*. *Curr Opin Biotechnol* **6**(5): 494-500.

Kay S, Hahn S, Marois E, Hause G, Bonas U. 2007. A bacterial effector acts as a plant transcription factor and induces a cell size regulator. *Science* **318**(5850): 648-651.

Keen NT. 1990. Gene-for-gene complementarity in plant-pathogen interactions. *Annu Rev Genet* **24**: 447-463.

Kemen E, Kemen AC, Rafiqi M, Hempel U, Mendgen K, Hahn M, Voegele RT. 2005. Identification of a protein from rust fungi transferred from haustoria into infected plant cells. *Mol Plant Microbe Interact* **18**(11): 1130-1139.

Keon JP, White GA, Hargreaves JA. 1991. Isolation, characterization and sequence of a gene conferring resistance to the systemic fungicide carboxin from the maize smut pathogen, *Ustilago maydis*. *Curr Genet* **19**(6): 475-481.

Kerbach S, Lorz H, Becker D. 2005. Site-specific recombination in *Zea mays*. *Theor Appl Genet* **111**(8): 1608-1616.

Kondo S, Takahashi Y, Shiozawa S, Ichise H, Yoshida N, Kanegae Y, Saito I. 2006. Efficient sequential gene regulation via FLP-and Cre-recombinase using adenovirus vector in mammalian cells including mouse ES cells. *Microbiol Immunol* **50**(10): 831-843.

Koornneef A, Pieterse CM. 2008. Cross talk in defense signaling. *Plant Physiol* **146**(3): 839-844.

Kvitko BH, Park DH, Velasquez AC, Wei CF, Russell AB, Martin GB, Schneider DJ, Collmer A. 2009. Deletions in the repertoire of *Pseudomonas syringae* pv. tomato DC3000 type III secretion effector genes reveal functional overlap among effectors. *PLoS Pathog* **5**(4): e1000388.

Ladendorf O. 2003. Transposition and heterologous gene expression in *Ustilago maydis*. *Ph. D. Thesis* **Phillips University of Marburg. Marburg**.

Loonstra A, Vooijs M, Beverloo HB, Allak BA, van Drunen E, Kanaar R, Berns A, Jonkers J. 2001. Growth inhibition and DNA damage induced by Cre recombinase in mammalian cells. *Proc Natl Acad Sci U S A* **98**(16): 9209-9214.

Loubradou G, Brachmann A, Feldbrugge M, Kahmann R. 2001. A homologue of the transcriptional repressor Ssn6p antagonizes cAMP signalling in *Ustilago maydis*. *Mol Microbiol* **40**(3): 719-730.

Luo H, Kausch AP. 2002. Application of FLP/FRT site-specific DNA recombination system in plants. *Genet Eng (N Y)* **24**: 1-16.

Lyznik LA, Rao KV, Hodges TK. 1996. FLP-mediated recombination of FRT sites in the maize genome. *Nucleic Acids Res* **24**(19): 3784-3789.

Marti M, Good RT, Rug M, Knuepfer E, Cowman AF. 2004. Targeting malaria virulence and remodeling proteins to the host erythrocyte. *Science* **306**(5703): 1930-1933.

Matsuzaki H, Nakajima R, Nishiyama J, Araki H, Oshima Y. 1990. Chromosome engineering in *Saccharomyces cerevisiae* by using a site-specific recombination system of a yeast plasmid. *J Bacteriol* **172**(2): 610-618.

McLeod M, Craft S, Broach JR. 1986. Identification of the crossover site during FLP-mediated recombination in the *Saccharomyces cerevisiae* plasmid 2 microns circle. *Mol Cell Biol* **6**(10): 3357-3367.

Mendoza-Mendoza A, Berndt P, Djamei A, Weise C, Linne U, Marahiel M, Vranes M, Kamper J, Kahmann R. 2009. Physical-chemical plant-derived signals induce differentiation in *Ustilago maydis*. *Mol Microbiol* **71**(4): 895-911.

Michielse CB, van Wijk R, Reijnen L, Manders EM, Boas S, Olivain C, Alabouvette C, Rep M. 2009. The nuclear protein Sge1 of *Fusarium oxysporum* is required for parasitic growth. *PLoS Pathog* **5**(10): e1000637.

Misas-Villamil JC, van der Hoorn RA. 2008. Enzyme-inhibitor interactions at the plant-pathogen interface. *Curr Opin Plant Biol* **11**(4): 380-388.

Miya A, Albert P, Shinya T, Desaki Y, Ichimura K, Shirasu K, Narusaka Y, Kawakami N, Kaku H, Shibuya N. 2007. CERK1, a LysM receptor kinase, is essential for chitin elicitor signaling in *Arabidopsis*. *Proc Natl Acad Sci U S A* **104**(49): 19613-19618.

Molina L, Kahmann R. 2007. An Ustilago maydis gene involved in H2O2 detoxification is required for virulence. *Plant Cell* **19**(7): 2293-2309.

Morschhauser J, Michel S, Staib P. 1999. Sequential gene disruption in *Candida albicans* by FLP-mediated site-specific recombination. *Mol Microbiol* **32**(3): 547-556.

Mueller O, Kahmann R, Aguilar G, Trejo-Aguilar B, Wu A, de Vries RP. 2008. The secretome of the maize pathogen *Ustilago maydis*. *Fungal Genet Biol* **45 Suppl 1**: S63-70.

Munnik T, Irvine RF, Musgrave A. 1998. Phospholipid signalling in plants. *Biochim Biophys Acta* **1389**(3): 222-272.

Nunes-Düby SE, Kwon HJ, Tirumalai RS, Ellenberger T, Landy A. 1998. Similarities and differences among 105 members of the Int family of site-specific recombinases. *Nucleic Acids Res* **26**(2): 391-406.

Nürnberger T, Brunner F, Kemmerling B, Piater L. 2004. Innate immunity in plants and animals: striking similarities and obvious differences. *Immunol Rev* **198**: 249-266.

O'Gorman S, Fox DT, Wahl GM. 1991. Recombinase-mediated gene activation and site-specific integration in mammalian cells. *Science* **251**(4999): 1351-1355.

Oh SK, Young C, Lee M, Oliva R, Bozkurt TO, Cano LM, Win J, Bos JI, Liu HY, van Damme M, Morgan W, Choi D, Van der Vossen EA, Vleeshouwers VG, Kamoun S. 2009. In planta expression screens of *Phytophthora infestans* RXLR effectors reveal diverse phenotypes, including activation of the Solanum bulbocastanum disease resistance protein Rpi-blb2. *Plant Cell* **21**(9): 2928-2947.

Oliva R, Win J, Raffaele S, Boutemy L, Bozkurt TO, Chaparro-Garcia A, Segretin ME, Stam R, Schornack S, Cano LM, van Damme M, Huitema E, Thines M, Banfield MJ, Kamoun S. 2010. Recent developments in effector biology of filamentous plant pathogens. *Cell Microbiol*.

Orbach MJ, Farrall L, Sweigard JA, Chumley FG, Valent B. 2000. A telomeric avirulence gene determines efficacy for the rice blast resistance gene Pi-ta. *Plant Cell* **12**(11): 2019-2032.

Patel RD, Lodge JK, Baker LG. 2010. Going green in *Cryptococcus neoformans*: the recycling of a selectable drug marker. *Fungal Genet Biol* **47**(3): 191-198.

Perez-Martin J, Castillo-Lluva S, Sgarlata C, Flor-Parra I, Mielnichuk N, Torreblanca J, Carbo N. 2006. Pathocycles: *Ustilago maydis* as a model to study the relationships between cell cycle and virulence in pathogenic fungi. *Mol Genet Genomics* **276**(3): 211-229.

Radhakrishnan P, Srivastava V. 2005. Utility of the FLP-FRT recombination system for genetic manipulation of rice. *Plant Cell Rep* **23**(10-11): 721-726.

Reuss O, Vik A, Kolter R, Morschhauser J. 2004. The SAT1 flipper, an optimized tool for gene disruption in *Candida albicans*. *Gene* **341**: 119-127.

Sacristan S, Garcia-Arenal F. 2008. The evolution of virulence and pathogenicity in plant pathogen populations. *Mol Plant Pathol* **9**(3): 369-384.

Sacristan S, Vigouroux M, Pedersen C, Skamnioti P, Thordal-Christensen H, Micali C, Brown JK, Ridout CJ. 2009. Coevolution between a family of parasite virulence effectors and a class of LINE-1 retrotransposons. *PLoS One* **4**(10): e7463.

Salmeron JM, Oldroyd GE, Rommens CM, Scofield SR, Kim HS, Lavelle DT, Dahlbeck D, Staskawicz BJ. 1996. Tomato Prf is a member of the leucine-rich repeat class of plant disease resistance genes and lies embedded within the Pto kinase gene cluster. *Cell* **86**(1): 123-133.

Sambrook J, Fritsch EF, Maniatis T. 1989. Molecular Cloning: a laboratory manual. *2-nd Edition. New York. Cold Spring Harbor laboratory. Cold Spring Harbor Press.*

Schipper K. 2009. Characterisation of a *Ustilago maydis* gene cluster that encodes three novel secreted proteins

Ph. D. Thesis(Phillips University of Marburg. Marburg).

Schmidt EE, Taylor DS, Prigge JR, Barnett S, Capecchi MR. 2000. Illegitimate Cre-dependent chromosome rearrangements in transgenic mouse spermatids. *Proc Natl Acad Sci U S A* **97**(25): 13702-13707.

Schulz B, Banuett F, Dahl M, Schlesinger R, Schafer W, Martin T, Herskowitz I, Kahmann R. 1990. The b alleles of *U. maydis*, whose combinations program pathogenic development, code for polypeptides containing a homeodomain-related motif. *Cell* **60**(2): 295-306.

Schweizer HP. 2003. Applications of the Saccharomyces cerevisiae Flp-FRT system in bacterial genetics. *J Mol Microbiol Biotechnol* **5**(2): 67-77.

Senecoff JF, Bruckner RC, Cox MM. 1985. The FLP recombinase of the yeast 2-micron plasmid: characterization of its recombination site. *Proc Natl Acad Sci U S A* **82**(21): 7270-7274.

Senecoff JF, Rossmeissl PJ, Cox MM. 1988. DNA recognition by the FLP recombinase of the yeast 2 mu plasmid. A mutational analysis of the FLP binding site. *J Mol Biol* **201**(2): 405-421.

Shen QH, Saijo Y, Mauch S, Biskup C, Bieri S, Keller B, Seki H, Ulker B, Somssich IE, Schulze-Lefert P. 2007. Nuclear activity of MLA immune receptors links isolate-specific and basal disease-resistance responses. *Science* **315**(5815): 1098-1103.

Silver DP, Livingston DM. 2001. Self-excising retroviral vectors encoding the Cre recombinase overcome Cre-mediated cellular toxicity. *Mol Cell* **8**(1): 233-243.

Skibbe DS, Doehlemann G, Fernandes J, Walbot V. 2010. Maize tumors caused by Ustilago maydis require organ-specific genes in host and pathogen. *Science* **328**(5974): 89-92.

Snetselaar KM, Mims CW. 1993. Infection of maize by *Ustilago maydis*: light and electron microscopy. *Phytopathology* **83**: 843-850.

Soanes DM, Alam I, Cornell M, Wong HM, Hedeler C, Paton NW, Rattray M, Hubbard SJ, Oliver SG, Talbot NJ. 2008. Comparative genome analysis of filamentous fungi reveals gene family expansions associated with fungal pathogenesis. *PLoS One* **3**(6): e2300.

Song H, Niederweis M. 2007. Functional expression of the Flp recombinase in *Mycobacterium bovis* BCG. *Gene* **399**(2): 112-119.

Staats M, van Baarlen P, Schouten A, van Kan JA, Bakker FT. 2007. Positive selection in phytotoxic protein-encoding genes of *Botrytis* species. *Fungal Genet Biol* **44**(1): 52-63.

Stemmer WP, Crameri A, Ha KD, Brennan TM, Heyneker HL. 1995. Single-step assembly of a gene and entire plasmid from large numbers of oligodeoxyribonucleotides. *Gene* **164**(1): 49-53.

Stergiopoulos I, de Wit PJ. 2009. Fungal effector proteins. *Annu Rev Phytopathol* **47**: 233-263.

Stergiopoulos I, van den Burg HA, Okmen B, Beenen HG, van Liere S, Kema GH, de Wit PJ. 2010. Tomato Cf resistance proteins mediate recognition of cognate homologous effectors from fungi pathogenic on dicots and monocots. *Proc Natl Acad Sci U S A* **107**(16): 7610-7615.

Storici F, Coglievina M, Bruschi CV. 1999. A 2-microm DNA-based marker recycling system for multiple gene disruption in the yeast *Saccharomyces cerevisiae*. *Yeast* **15**(4): 271-283.

Stukenbrock EH, McDonald BA. 2009. Population genetics of fungal and oomycete effectors involved in gene-for-gene interactions. *Mol Plant Microbe Interact* **22**(4): 371-380.

Sugio A, Yang B, Zhu T, White FF. 2007. Two type III effector genes of *Xanthomonas oryzae* pv. *oryzae* control the induction of the host genes OsTFIIAgamma1 and OsTFX1 during bacterial blight of rice. *Proc Natl Acad Sci U S A* **104**(25): 10720-10725.

Symington L. 1997. What's hot for recombination. *Trends Genet* **13**(11): 431.

Takken FL, Tameling WI. 2009. To nibble at plant resistance proteins. *Science* **324**(5928): 744-746.

Tang X, Frederick RD, Zhou J, Halterman DA, Jia Y, Martin GB. 1996. Initiation of Plant Disease Resistance by Physical Interaction of AvrPto and Pto Kinase. *Science* **274**(5295): 2060-2063.

Thompson JD, Higgins DG, Gibson TJ. 1994. CLUSTAL W: improving the sensitivity of progressive multiple sequence alignment through sequence weighting, position-specific gap penalties and weight matrix choice. *Nucleic Acids Res* **22**(22): 4673-4680.

Tyler BM. 2009. Entering and breaking: virulence effector proteins of oomycete plant pathogens. *Cell Microbiol* **11**(1): 13-20.

Tyler BM, Tripathy S, Zhang X, Dehal P, Jiang RH, Aerts A, Arredondo FD, Baxter L, Bensasson D, Beynon JL, Chapman J, Damasceno CM, Dorrance AE, Dou D, Dickerman AW, Dubchak IL, Garbelotto M, Gijzen M, Gordon SG, Govers F, Grunwald NJ, Huang W, Ivors KL, Jones RW, Kamoun S, Krampis K, Lamour KH, Lee MK, McDonald WH, Medina M, Meijer HJ, Nordberg EK, Maclean DJ, Ospina-Giraldo MD, Morris PF, Phuntumart V, Putnam NH, Rash S, Rose JK, Sakihama Y, Salamov AA, Savidor A, Scheuring CF, Smith BM, Sobral BW, Terry A, Torto-

Alalibo TA, Win J, Xu Z, Zhang H, Grigoriev IV, Rokhsar DS, Boore JL. 2006. *Phytophthora* genome sequences uncover evolutionary origins and mechanisms of pathogenesis. *Science* **313**(5791): 1261-1266.

Van den Ackerveken G, Bonas U. 1997. Bacterial avirulence proteins as triggers of plant disease resistance. *Trends Microbiol* **5**(10): 394-398.

van der Hoorn RA, Kamoun S. 2008. From Guard to Decoy: a new model for perception of plant pathogen effectors. *Plant Cell* **20**(8): 2009-2017.

Vetter D, Andrews BJ, Roberts-Beatty L, Sadowski PD. 1983. Site-specific recombination of yeast 2-micron DNA in vitro. *Proc Natl Acad Sci U S A* **80**(23): 7284-7288.

Walbot V, Skibbe DS. 2010. Maize host requirements for *Ustilago maydis* tumor induction. *Sex Plant Reprod* **23**(1): 1-13.

Wang D, Pajerowska-Mukhtar K, Culler AH, Dong X. 2007. Salicylic acid inhibits pathogen growth in plants through repression of the auxin signaling pathway. *Curr Biol* **17**(20): 1784-1790.

Wang J, Holden DW, Leong SA. 1988. Gene transfer system for the phytopathogenic fungus *Ustilago maydis*. *Proc Natl Acad Sci U S A* **85**(3): 865-869.

Weinzierl G, Leveleki L, Hassel A, Kost G, Wanner G, Bolker M. 2002. Regulation of cell separation in the dimorphic fungus *Ustilago maydis*. *Mol Microbiol* **45**(1): 219-231.

Welti R, Wang X. 2004. Lipid species profiling: a high-throughput approach to identify lipid compositional changes and determine the function of genes involved in lipid metabolism and signaling. *Curr Opin Plant Biol* **7**(3): 337-344.

Whisson SC, Boevink PC, Moleleki L, Avrova AO, Morales JG, Gilroy EM, Armstrong MR, Grouffaud S, van West P, Chapman S, Hein I, Toth IK, Pritchard L, Birch PR. 2007. A translocation signal for delivery of oomycete effector proteins into host plant cells. *Nature* **450**(7166): 115-118.

Whiteson KL, Rice PA. 2008. Binding and catalytic contributions to site recognition by flp recombinase. *J Biol Chem* **283**(17): 11414-11423.

Wirsching S, Michel S, Morschhäuser J. 2000. Targeted gene disruption in *Candida albicans* wild-type strains: the role of the MDR1 gene in fluconazole resistance of clinical *Candida albicans* isolates. *Mol Microbiol* **36**(4): 856-865.

Wirth D, Gama-Norton L, Riemer P, Sandhu U, Schucht R, Hauser H. 2007. Road to precision: recombinase-based targeting technologies for genome engineering. *Curr Opin Biotechnol* **18**(5): 411-419.

Wu S, Ying G, Wu Q, Capecchi MR. 2008. A protocol for constructing gene targeting vectors: generating knockout mice for the cadherin family and beyond. *Nat Protoc* **3**(6): 1056-1076.

Xiang T, Zong N, Zou Y, Wu Y, Zhang J, Xing W, Li Y, Tang X, Zhu L, Chai J, Zhou JM. 2008. Pseudomonas syringae effector AvrPto blocks innate immunity by targeting receptor kinases. *Curr Biol* **18**(1): 74-80.

Xing W, Zou Y, Liu Q, Liu J, Luo X, Huang Q, Chen S, Zhu L, Bi R, Hao Q, Wu JW, Zhou JM, Chai J. 2007. The structural basis for activation of plant immunity by bacterial effector protein AvrPto. *Nature* **449**(7159): 243-247.

Zarnack K, Maurer S, Kaffarnik F, Ladendorf O, Brachmann A, Kamper J, Feldbrugge M. 2006. Tetracycline-regulated gene expression in the pathogen *Ustilago maydis*. *Fungal Genet Biol* **43**(11): 727-738.

Zheng Y, Kief J, Auffarth K, Farfsing JW, Mahlert M, Nieto F, Basse CW. 2008. The *Ustilago maydis* Cys2His2-type zinc finger transcription factor Mzr1 regulates fungal gene expression during the biotrophic growth stage. *Mol Microbiol* **68**(6): 1450-1470.

Zhong R, Ye ZH. 2003. The SAC domain-containing protein gene family in Arabidopsis. *Plant Physiol* **132**(2): 544-555.

Zipfel C. 2008. Pattern-recognition receptors in plant innate immunity. *Curr Opin Immunol* **20**(1): 10-16.

I would like to express my sincere gratitude to my supervisor, Prof. Dr. Regine Kahmann not only for her guidance and advice throughout my research, but above all for her constructive criticism prompting my academic advancement. I would also like to thank you for all of the support and encouragement you have provided me throughout the past few years. I am heartily thankful to my thesis and defense committee members, Prof. Dr. Michael Bölker, Prof. Dr. Martin Thanbichler, Prof. Dr. Uwe Maier, Prof. MD, PhD Lotte Søgaard-Andersen, Prof. Dr. Gerhard Kost for their time and valuable suggestions from which I have benefited. Especially I would like to thank Prof. Dr. Michael Bölker for his time in reviewing this work and for all the fruitful discussions during my research.

I am very much grateful to International Max Planck Research School for Environmental, Cellular and Molecular Microbiology for providing financial support during my studies. I would like to extend my thanks to Dr. Ronald Brudler, Susanne Rommel and Christian Bengelsdorff for taking care of all the documents and helping so much during my stay in Marburg.

My sincere thanks go to Karin Münch, Dr. Thomas Brefort, Dr. Gunther Döhlemann, Dr. Maurizio Di Stasio, Dr. Artemio Mendoza-Mendoza, Dr. Lazaro Molina for helpful discussions, support and great atmosphere during my stay here. I am especially indebted to the people in our lab who gave so much assistance and enjoyable time during my stay.

In a special way I would like to thank all my friends, particularly Iryna, Andrea, Jörg, Stefan and Christian for their understanding, support and all the great laughs we shared together. I would also like to take this opportunity to thank my parents for their endless love and faith in me. Finally I would like to thank my fiancée Igor for all the enormous support, love, encouragements and laughter. You have been the source of my energy and self-confidence during all this time.

CURRICULUM VITAE

Yuliya Khrunyk

PERSONAL INFORMATION

Date of birth **22.12.1979**

Place of birth **Lviv, Ukraine**

EDUCATION

Phillips-University Marburg, Marburg, Germany
Dissertation at the faculty in Biology: October 2010
Supervisor: Prof. Dr. Regine Kahmann
Thesis: "The use of FLP-mediated recombination for the functional analysis of an effector gene family in the biotrophic smut fungus *Ustilago maydis*"

University of Alaska Fairbanks, Fairbanks, Alaska
Master of Science Degree: May 2005
Major: Environmental Management
Thesis: "Uptake of C14-atrazine by prairie grasses in a phytoremediation setting"

I. Franko Lviv National University, Lviv, Ukraine
Master of Science Degree: June 2003
Majors: Biology & Physiology
Thesis: "The influence of plant growth regulators zeastimulin and ivin on the early stages of maize seedlings development"
Diploma of Master with Distinction

Lviv Ukrainian Private Gymnasium, Lviv, Ukraine
1991 – 1995

Elementary School N 29, Lviv-Vynnyky, Ukraine
1986 - 1991